



JOHANNES GUTENBERG
UNIVERSITÄT MAINZ

**The physiological role of APP in the activation of
neuroprotective signaling mechanisms**

Dissertation
zur Erlangung des Grades
Doktor der Naturwissenschaften
(Dr. rer. nat.)

am Fachbereich Biologie
der Johannes-Gutenberg-Universität Mainz

Nelli Milosch,
geboren am 26.07.1985
in Berlin

Mainz, 2014

Dekan:

Erster Gutachter:

[Die Namen von Dekan und Gutachtern sind gelöscht.]

Zweiter Gutachter:

Tag der mündlichen Prüfung:

18.05.2015

Die Ergebnisse dieser Arbeit wurden bereits teilweise in folgender Publikation veröffentlicht:

Holo-APP and G-protein-mediated signaling are required for sAPP α -induced activation of the Akt survival pathway

Nelli Milosch, Gaye Tanriöver, Arpita Kundu, Abdelhaq Rami, Jean-Christophe François, Frederik Baumkötter, Sascha W. Weyer, Ayan Samanta, Andres Jäschke, Florian Brod, Christian J. Buchholz, Stefan Kins, Christian Behl, Ulrike C. Müller, Donat Kögel

Cell Death & Disease, published online 28 August 2014

Summary

Accumulating evidence indicates that loss of physiological amyloid precursor protein (APP) function leads to enhanced susceptibility of neurons to cellular stress during brain aging. This study investigated the neuroprotective function of the soluble APP ectodomain sAPP α . Recombinant sAPP α protected primary hippocampal neurons and neuroblastoma cells from cell death induced by trophic factor deprivation. This protective effect was abrogated in APP-depleted neurons, but not in APLP1-, APLP2- or IGF1-R-deficient cells, indicating that expression of holo-APP is required for sAPP α -dependent neuroprotection. Strikingly, recombinant sAPP α , APP-E1 domain and the copper-binding growth factor-like domain (GFLD) of APP were able to stimulate PI3K/Akt survival signaling in different wildtype cell models, but failed in APP-deficient cells. An ADAM10 inhibitor blocking endogenous sAPP α secretion exacerbated neuron death in organotypic hippocampal slices subjected to metabolic stress, which could be rescued by exogenous sAPP α . Interestingly, sAPP α -dependent neuroprotection was unaffected in neurons of APP- Δ CT15 mice which lack the intracellular C-terminal YENPTY motif of APP. In contrast, sAPP α -dependent Akt signaling was completely abolished in APP mutant cells lacking the C-terminal G-protein interaction motif and by specifically blocking G_{i/o}-dependent signaling with pertussis toxin. Collectively, the present thesis provides new mechanistic insights into the physiological role of APP: the data suggest that cell surface APP mediates sAPP α -induced neuroprotection via G_o-protein-coupled activation of the Akt pathway.

Zusammenfassung

Eine zunehmende Zahl an Studien zeigt, dass der Verlust der physiologischen Funktion des Amyloid-Vorläufer-Proteins (APP) entscheidend zur erhöhten Sensitivität von Neuronen gegenüber Stressbedingungen während der Hirnalterung beitragen kann. Für diese Arbeit wurde die neuroprotektive Funktion der löslichen APP-Ektodomäne sAPP α untersucht. Es konnte gezeigt werden, dass rekombinantes sAPP α dem durch Entzug tropher Faktoren induzierten Zelltod in primären hippocampalen Neuronen sowie in Neuroblastomzellen entgegenwirkt. Dieser protektive Effekt war im Gegensatz zu APLP1-, APLP2- oder IGF1-R-defizienten Modellen in APP-knockout-Zellen nicht festzustellen, was für die Notwendigkeit einer Expression von holo-APP für die sAPP α -abhängige Neuroprotektion spricht. Rekombinantes sAPP α , APP-E1 und die kupferbindende growth factor-like domain (GFLD) von APP konnten den PI3K/Akt-Überlebenssignalweg in verschiedenen Wildtyp-Zellmodellen stimulieren, wohingegen in APP-defizienten Zellen keine Aktivierung zu beobachten war. Ein ADAM10-Inhibitor, der die Sekretion von endogenem sAPP α inhibiert, steigerte den neuronalen Zelltod in organotypischen hippocampalen Schnittkulturen, die metabolischem Stress ausgesetzt waren. Dieser Effekt konnte durch die Gabe von exogenem sAPP α rückgängig gemacht werden. Die sAPP α -vermittelte Neuroprotektion war in Neuronen aus APP- Δ CT15-Mäusen, denen das C-terminale YENPTY-Motiv von APP fehlte, unverändert. Dagegen wurde der sAPP α -abhängige Akt-Signalweg in APP-mutierten Zellen ohne das C-terminale G-Protein-Interaktionsmotiv oder durch Blockierung der G_{i/o}-abhängigen Signalweiterleitung mit Pertussistoxin vollständig unterdrückt. Zusammenfassend bietet diese Arbeit neue mechanistische Erkenntnisse zur physiologischen Rolle von APP: Die Daten legen nahe, dass membranständiges APP die sAPP α -induzierte Neuroprotektion durch G_o-Protein-gekoppelte Aktivierung des Akt-Signalwegs vermittelt.

Table of Contents

Summary.....	i
Zusammenfassung.....	ii
Table of Contents	3
1 Introduction.....	6
1.1 Pathology of Alzheimer's Disease	6
1.2 Amyloid Cascade Hypothesis vs. Tau Theory vs. Inflammation.....	8
1.3 Amyloid Precursor Protein.....	10
1.3.1 The APP Family.....	10
1.3.2 APP Structure and Processing.....	11
1.3.3 APP Function.....	13
1.4 Cell Death.....	14
1.4.1 Apoptosis.....	14
1.4.2 Necrosis.....	16
1.4.3 Autophagy.....	17
1.4.4 Cell Death Mechanisms in AD.....	17
1.5 The Role of APP in Survival/Stress Signaling	19
1.6 Aim of this Thesis.....	21
2 Materials	23
2.1 Chemicals	23
2.2 Buffers and Solutions	23
2.3 Cell Biology.....	25
2.3.1 Media.....	25
2.3.2 Cell Lines.....	27
2.3.3 Animals.....	27
2.4 Molecular Biology.....	28
2.4.1 Kits	28
2.4.2 Primary Antibodies	28
2.4.3 Secondary Antibodies.....	29
2.4.4 Viral Vectors and Plasmids	29
2.4.5 Bacteria Strain.....	30
2.5 Software.....	30
2.6 Plastic- and Glassware	30
2.7 Equipment and Other Instruments	31
3 Methods.....	34

3.1	Cell Culture	34
3.2	Determination of Cell Number and Seeding of Cells	34
3.3	Freezing and Thawing of Cells	34
3.4	Preparation of Hippocampal Neurons	35
3.5	Preparation and Maintenance of Hippocampal Slice Cultures	36
3.6	Transfection of Plasmids	37
3.7	Production of Lentiviral Particles	37
3.8	Generation of Stable Knockdown Cell Lines	38
3.9	Cytotoxic Stress Stimuli and Treatments	39
3.10	Cell Viability and Cell Death Assays	40
3.10.1	Caspase Assay	40
3.10.2	Bioluminescence ATP Assay	41
3.10.3	PI/Hoechst Staining	41
3.10.4	FACS Analysis	41
3.10.5	Live-dead Assay	42
3.11	Protein Analysis	43
3.11.1	Cell Harvest and Protein Concentration	43
3.11.2	Akt Kinase Assay	43
3.11.3	SDS-PAGE	44
3.11.4	Western Blot	44
3.11.5	Immunodetection	45
3.11.6	Immunostaining/In-cell-western	45
3.11.7	On-cell-western	46
3.12	Purification of sAPP α /E1 from Yeast	47
3.13	Plasmid Preparation from <i>E. coli</i>	48
3.13.1	Transformation of <i>E. coli</i>	48
3.13.2	Bacterial Culture and Plasmid Preparation	49
3.13.3	Determination of DNA Concentration	49
3.14	Microscopy	49
3.15	Data Analysis	50
4	Results	51
4.1	Yeast-derived sAPP α and E1 Have Neuroprotective Properties	51
4.2	Recombinant sAPP α and E1 Promote Cell Survival Only in the Presence of Holo-APP	53
4.3	Recombinant sAPP α and APP-E1 Domain Activate the PI3K/Akt Survival Pathway, which Requires the Expression of Holo-APP	59

4.4	PI3K/Akt Survival Signaling Mediated by sAPP α and APP-E1 Domain Does Not Depend on the Expression of APLP1 or APLP2	63
4.5	The AICD but Not the YENPTY Motif Is Required for sAPP α -mediated Akt Signaling....	65
4.6	Activation of the PI3K/Akt Pathway by sAPP α /E1 Is Mediated by G-protein-dependent Signaling.....	68
4.7	IGF1-R Expression Is Not Required for sAPP α -dependent Survival Signaling	72
4.8	The Growth Factor-like Domain (GFLD) of APP Is Protective, but Not the Mutated Copper Binding Domain	73
5	Discussion.....	75
5.1	Yeast-derived sAPP α and E1 Have Neuroprotective Properties.....	76
5.2	Recombinant sAPP α and E1 Antagonize Stress Induced by Trophic Factor Deprivation and Proteasomal Inhibition	77
5.3	APP Fragments Promote Cell Survival Only in the Presence of Holo-APP.....	79
5.4	APP-dependent Cell Survival Involves Activation of the PI3K/Akt Pathway	80
5.5	Cytoprotection Depends on the AICD and G-Protein Signaling.....	83
5.6	Copper Binding Abilities of the Growth Factor-like Domain of APP Are Required for Activation of Survival Signaling	85
5.7	Conclusion and Outlook.....	86
6	References	90
7	Appendix.....	110
7.1	Abbreviations.....	110
7.2	Tables.....	112
7.3	Images	112
8	Declaration/Erklärung.....	114
9	Acknowledgments.....	115
10	Curriculum Vitae.....	116

1 Introduction

1.1 Pathology of Alzheimer's Disease

Alzheimer's Disease (AD) is the most common neurodegenerative disorder and currently affects over 35 million people worldwide with dramatically increasing numbers due to a higher life expectancy in the aging population (Alzheimer's Society UK, Facts and Figures 2014; Brookmeyer et al., 2007). This mostly age-related and currently incurable form of dementia involves a progressive decline of cognitive abilities, mood and behavioral changes. Early indicators include short-term memory loss, but symptoms eventually worsen until bodily functions become impaired leading to the death of the patient due to secondary diseases (Förstl and Kurz, 1999; Shankar and Walsh, 2009). AD was first described in 1906 by German psychiatrist Alois Alzheimer treating a 51-year old patient, Auguste Deter, who showed a severe form of dementia, confusion and disorientation. Neuropathological hallmarks of the disease that Alzheimer found in his patient's brain after her death included massive brain atrophy, neurofibrillary structures and protein plaques (Figure 1; Allsop, 2000).

To this day, the disease is characterized by a progressive loss of neurons and synapses, extracellular (senile) plaques consisting of accumulated amyloid beta peptides ($A\beta$) and intracellular aggregation of neurofibrillary tangles (NFTs) composed of paired helical filaments (PHFs, for review see Goedert and Spillantini, 2006). PHFs contain aggregated, abnormally phosphorylated microtubule-associated protein (MAP) tau. Under physiological conditions, tau interacts with tubulin to stimulate microtubule assembly and stability which is controlled by its phosphorylation state (Mandelkow and Mandelkow, 2012; Weingarten et al., 1975). In AD, tau is hyperphosphorylated and accumulates in NFTs, thereby disrupting axonal transport which leads to neurodegeneration (Garcia and Cleveland, 2001). Senile plaques, on the other hand, mainly consist of $A\beta$ which is cleaved from the amyloid precursor protein (APP). The soluble peptide finally aggregates into insoluble extracellular plaques that have toxic effects on the surrounding tissue possibly through inflammation and proteasomal inhibition (Glenner and Wong, 2012; Hardy and Selkoe, 2002). Brain regions with high rates of life-long plasticity are usually affected very early during AD. These include the entorhinal cortex and the hippocampus, which justifies some of the initial symptoms of AD (Braak and Braak, 1991; Fjell et al., 2014). The hippocampus plays a pivotal role in learning and memory consolidation (Hempel et al., 2008) with diminished synaptic density and function accounting for memory loss and learning impairment (Arendt, 2009).

In most cases, AD occurs as the age-associated, sporadic, late-onset form of the disease (LOAD) that normally sets in after the age of 65. However, risk factors for developing LOAD were reported

to be certain diseases such as diabetes (Toro et al., 2009), environmental factors and the apolipoprotein E4 (APOE4) (Kamboh, 2004; Roses, 1996). The hereditary or familial form of the disease (FAD) and early-onset AD (EOAD) make up only 10 % of AD cases and may cause symptoms from age 30. EOAD was linked to different autosomal mutations in the amyloid precursor protein (APP) known as the Swedish, Arctic or London mutation (Guo et al., 2010). Moreover, mutations in the presenilin genes PS1 and PS2 also represent a major risk factor for EOAD (Goate, 2006; Haass and De Strooper, 1999; Steiner et al., 1999). Nevertheless, the phenotypes of both sporadic AD and FAD are nearly identical and similar signaling pathways are most likely involved (Lee et al., 2013).

AD is usually diagnosed based on neuropsychological tests, the patient's history and behavior. It is known today that pathological changes occur two to three decades before the onset of cognitive symptoms (Lee et al., 2013). Medical imaging techniques like magnetic resonance imaging (MRI) or positron emission tomography (PET) and neurological examinations may aid the differential diagnosis and exclude other brain pathologies (Desikan et al., 2009; Schroeter et al., 2009). Biochemical analysis of the cerebrospinal fluid to identify early biomarkers of AD, such as A β peptides and hyperphosphorylated tau proteins, is intensely discussed. While significantly higher levels of these proteins may substantiate the diagnosis in most patients (Marksteiner et al., 2007), other longitudinal studies yielded contradictory results (cf. The Nun Study of Aging and Alzheimer's Disease, SantaCruz et al., 2011; Snowden and Nun Study, 2003). Eventually, a certain confirmation of the disease can still only be achieved by post-mortem histological analysis of brain material (Nagele et al., 2011).

Despite intensive research, there is currently no cure for AD. However, a balanced diet, mental and physical exercise were suggested to prevent or delay the onset of cognitive symptoms (Intlekofer and Cotman, 2013; Solfrizzi et al., 2011). The few available medications on the market aim at symptomatic relief, but fail to delay or modify the progression of the disease (for review, see Corbett et al., 2012). Acetylcholinesterase inhibitors are utilized to increase the amount of free acetylcholine in the brain of AD patients, which showed little efficacy in mild to moderate AD (Birks and Harvey, 2006; Pohanka, 2011). The noncompetitive NMDA receptor antagonist Memantine acts through inhibition of excitotoxic glutamate, but also failed to show a major clinical effect (Areosa Sastre et al., 2004). Hundreds of pharmaceutical substances are currently being investigated in clinical trials. Many of them focus on the reduction of or even vaccination against A β , but also tau represents a pharmacological target. However, most of these promising compounds failed late phases in clinical testing and many trials were discontinued early (Schneider et al., 2014).

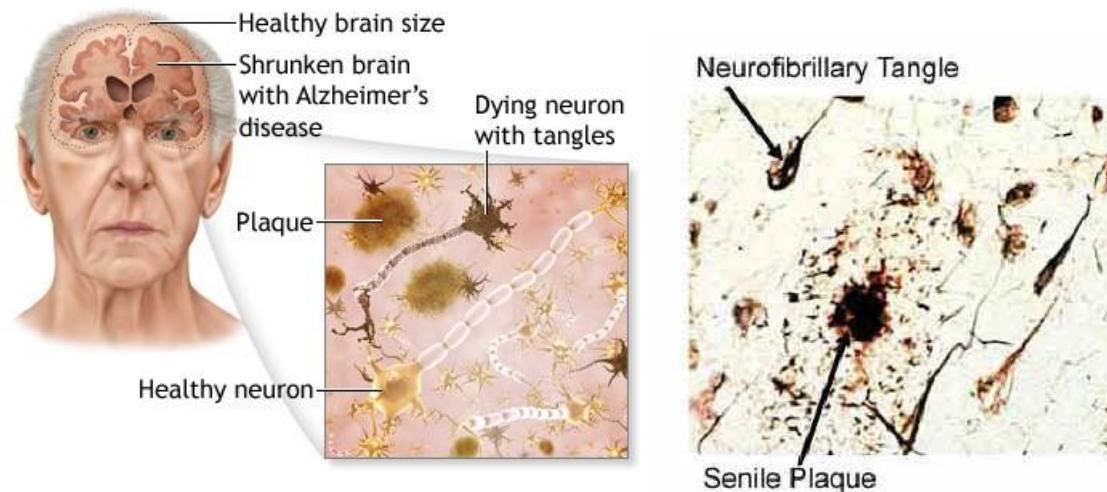


Figure 1. Hallmarks of Alzheimer's Disease. Patients suffering from AD exhibit cortical atrophy and enlarged ventricles due to progressive loss of neurons, extracellular amyloid (senile) plaques and intracellular abnormally phosphorylated tau proteins that aggregate in neurofibrillary tangles. Image on the right shows silver stained tangles and plaques. Taken from: http://www.stemcelltreatments.in/alzheimers_disease and <http://www.all-creatures.org/health/alzheimers.html>.

1.2 Amyloid Cascade Hypothesis vs. Tau Theory vs. Inflammation

The “amyloid cascade hypothesis” has dominated AD research for the past decades (Karran et al., 2011; Mudher and Lovestone, 2002). Supporters assume that the increased generation of soluble, but aggregate-prone, neurotoxic oligomeric A β mediates synapto- and neurotoxicity possibly by disruption of calcium ion homeostasis (Kawahara, 2010). According to this hypothesis, a series of events initiated by the deposition of A β ultimately causes the pathological symptoms of AD. All other hallmarks of AD are a mere consequence of this first critical step (reviewed in Karran et al., 2011; Krstic and Knuesel, 2013). Evidence for a crucial role of A β is given by a vast amount of studies, e. g. it was revealed that a mutation in APP (A673T) as observed in 1795 Icelanders protects against cognitive decline and AD by reducing the formation of A β by 40 % (Jonsson et al., 2012). Additionally, any mutations or genetic aberrations leading to an enhanced A β secretion, e. g. by increased APP gene copy numbers as seen in patients with Down Syndrome or the familiar Swedish mutation of APP, triggered an early-onset of the disease (Karran et al., 2011; Nistor et al., 2007). The finding that autosomal dominant mutations in presenilin 1 and 2 (PS1/2) represent a major risk factor further substantiated the hypothesis as these two homologous proteins are components of γ -secretase cleaving off A β (Karran et al., 2011; Sherrington et al., 1995; Zheng and Koo, 2006). Even though plaques consisting of insoluble aggregated A β fibrils are found in AD and amyloid fibrils were shown to kill neurons in culture, many studies have reported that the amount of plaque formation does not correlate with the degree of cognitive dysfunction. Soluble A β oligomers preceding fibril formation, however, do (Swomley et al., 2014). This led to the

assumption that soluble A β might rather be the neurotoxic species underlying synaptic dysfunction and neuronal death (Lacor et al., 2007; Nhan et al., 2014; Shankar et al., 2008; Walsh and Selkoe, 2004). Accordingly, soluble A β oligomers were found to activate stress responsive kinases (e. g. GSK3 β) and increase APP dimerization initiating caspase activation (Crews and Masliah, 2010; Nhan et al., 2014). Furthermore, A β was shown to aggregate in mitochondria in AD brain inhibiting metabolic and enzyme function (Chen and Yan, 2006). Consistently, many reports emphasize the causal relationship of oxidative stress with A β pathology arguing that A β oligomers perturb mitochondrial function leading to oxidative stress and an increase in reactive oxygen species (ROS) generation (Thathiah and De Strooper, 2011). In turn, free radical damage by ROS may lead to protein oxidation and lipid peroxidation subsequently causing neuronal degeneration and AD pathology (Swomley et al., 2014).

In summary, the amyloid cascade hypothesis places tau pathology downstream of A β and is postulated as the concept that aggregation of toxic A β accelerates tau pathology possibly by disrupting proteasomal degradation (Karran et al., 2011; Mandelkow, 1999). Consequently, A β plaques induce tau hyperphosphorylation that eventually leads to neuronal loss and dementia by the formation of neurofibrillary tangles and PHFs (Busciglio et al., 1995; Karran et al., 2011). The exact mechanisms of A β toxicity and AD pathology, however, remain poorly defined and chemical compounds designed to reduce A β burden have failed (Huang and Mucke, 2012).

The tau hypothesis suggests a neurotoxic and disease-initiating role of tau itself, as the loss of microtubule-stabilization leads to the degradation of the cytoskeleton (Gray et al., 1987; Morris et al., 2011) and drugs targeting A β did not show efficacy. The theory is also based on the observation that amyloid plaque burden does not correlate well with neuron loss (Schmitz et al., 2004; Swomley et al., 2014) and was further supported by reports on tau mutations that cause neuronal loss in the absence of A β (Hutton et al., 1998; Karran et al., 2011). Reduction of tau levels show improvement of A β -mediated deficits (Roberson et al., 2007) and other tauopathies causing similar symptoms as seen in AD prove that misfolded tau directly mediates neurodegeneration independent of A β (Chesser et al., 2013; Williams, 2006). A characteristic pattern of neurofibrillary tangle formation could be differentiated between six different stages of AD rendering amyloid plaque depositions of rather limited significance (Ahmed et al., 2014; Braak and Braak, 1991).

More recent findings have led to the proposition of the inflammation theory of AD or “inflammaging” (termed by Franceschi et al., 2007). The discovery of abundant inflammatory mediators in brain areas and plasma of AD patients suggests that neuroinflammation may play a key role in the development of the disease (Cribbs et al., 2012; Swardfager et al., 2010). Combining results from a multitude of studies pointing into the same direction, Krstic and Knuesel (2013) suggest that the sequence of neuropathological events in AD starts with alterations in the innate

immune system and inflammatory stress. They argue that certain anti-inflammatory drugs were shown to decrease the risk of AD while high-pathology (plaque) control groups without cognitive symptoms exhibited no neuroinflammation (cf. the Nun study, SantaCruz, 2011). Mice with repeated immune challenges showed AD-like phenotypes (Krstic et al., 2012). Moreover, the cognitive status in AD patients proved inversely correlated with microglial activation, but not A β load, which argues for a stringent neuroinflammatory activity in AD (Yokokura et al., 2011). Krstic and Knuesel further propose that repeated or chronic inflammation (e. g. by infection or inflammatory diseases during the lifetime of a patient) may lead to tau missorting due to hyperphosphorylation and increased APP production (Krstic and Knuesel, 2013). Consequently, axonal swellings will impair axonal transport and energy metabolism which induces synaptic loss and neuronal death. In the following, accumulated APP may leak out and form extracellular neurotoxic plaques due to closer proximity to A β cleaving proteases. Hence, degenerating neurites might rather be a cause than a consequence of A β plaques (Sergeant et al., 2003; Xiao et al., 2011). At the same time, intracellular PHFs are formed as a response to axonopathy (as described by Iijima-Ando et al., 2012; Xiao et al., 2011). As an innate immune response of the brain, microglia become hyperactive and “primed” and build toxic pro-inflammatory hot-spots (Püntener et al., 2012). Taken together, Krstic and Knuesel (2013) suggest that the impaired clearance of apoptotic neurons and damaged proteins exacerbate the neurotoxic environment and lead to neurodegeneration during brain aging and AD.

1.3 Amyloid Precursor Protein

1.3.1 The APP Family

The amyloid precursor protein (APP) and its family members are highly conserved type 1 transmembrane proteins. The APP family consists of APP and the mammalian paralogues APP-like proteins 1 and 2 (APLP1 and APLP2) as well as APL-1 in *C. elegans* and APPL in *Drosophila*. Most of the sequence motifs are shared by all members, except the A β domain, which is unique to APP (Figure 2; reviewed in Coulson et al., 2000; Muller and Zheng, 2012). Mammalian APP and APLP2 are expressed ubiquitously, while APPL (*Drosophila*) and APLP1 are expressed in neurons only (Lorent et al., 1995; Martin-Morris and White, 1990; Muller and Zheng, 2012). Single APP or APLP knockout mice are viable and reveal only mild phenotypes such as impaired long-term potentiation, reduced body weight and minor memory loss (Heber et al., 2000; Ring et al., 2007). However, APP/APLP2 and APLP1/APLP2 double knockouts as well as APP/APLP1/APLP2 triple knockouts are lethal, while at the same time APP/APLP1 double knockout mice are viable (Korte et al., 2012). These findings indicate that different APP family members can compensate for each other.

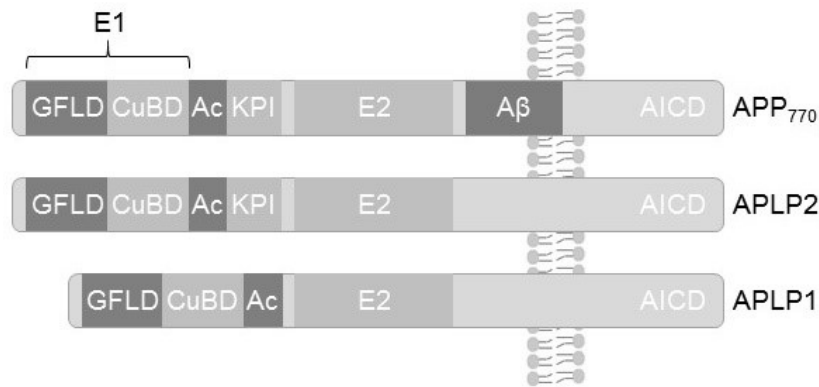


Figure 2. APP family members. Domain structures of the three mammalian APP family members share the E1 and E2 domains, the acidic region (Ac) and the APP intracellular domain (AICD) of the carboxyl terminus. The E1 domain contains a heparin binding or growth factor-like domain (GFLD) and the copper binding domain (CuBD). Aβ is unique for APP; KPI, Kunitz-type protease inhibitor domain. Adapted and modified from Muller and Zheng (2012).

1.3.2 APP Structure and Processing

The human APP gene is located on chromosome 21 and encodes several alternative splicing isoforms from 365 to 770 amino acids. The isoforms that AD research mainly focuses on are APP695, APP751 and APP770 as they encode Aβ. However, only APP695 is expressed in neurons (Sandbrink et al., 1994; Zheng and Koo, 2006). The extracellular ectodomain of APP contains the E1 and E2 domains, which are linked by an acidic region (Figure 2, Ac) and a Kunitz-type protease inhibitor domain (Figure 2, KPI). E1 includes the N-terminal growth factor-like domain (Figure 2, GFLD) binding heparin and collagen followed by a metal (copper and zinc) binding motif (Figure 2, CuBD). The intracellular C-terminal domain of APP is much shorter (Aydin et al., 2012; Reinhard et al., 2005).

APP is proteolytically processed by at least three secretases (α , β , γ) and undergoes post-translational modifications such as glycosylation and phosphorylation (Haass et al., 2012; De Strooper and Annaert, 2000). There are two major pathways of APP processing (cf. Figure 3). Under physiological conditions, the majority of APP is cleaved by α -secretase along the non-amyloidogenic pathway, which releases the membrane-bound carboxyterminal fragment (CTF) C83 and the neuroprotective soluble ectodomain sAPP α (reviewed in Endres and Fahrenholz, 2012). Subsequent proteolysis of C83 by γ -secretase, an enzyme complex consisting of presenilins, produces the 3 kD product p3 and the APP intracellular domain (AICD; Kögel et al., 2012a; Müller et al., 2008). APP processing along the amyloidogenic pathway by β -secretase cleaves off the extracellular domain releasing sAPP β and CTF C99. Additional proteolysis by γ -secretase at the carboxyl-terminus of Aβ within the transmembrane region liberates the AICD and Aβ_{40/42} or other Aβ species depending on the exact cleavage position (Zheng and Koo, 2006; Winkler et al., 2012; Wagner et al., 2014). In addition, sAPP β is assumed to be further processed

by a currently unknown secretase to produce the aminoterminal fragment N-APP that was proposed to bind death receptor 6 (DR6), activate caspases and trigger degeneration (Kim and Tsai, 2009; Nikolaev et al., 2009). The neuronal β -secretase BACE1 (β -site APP cleaving enzyme 1) is a transmembrane aspartyl protease (Vassar et al., 2014), while ADAM9/10/17 (a disintegrin and metalloproteinase) and other α -secretases are zinc metalloproteinases. The latter cleave APP within the A β domain, thereby inhibiting the formation of intact A β and liberating neuroprotective sAPP α instead (Kögel et al., 2012b). ADAM10 and ADAM17 are considered the main α -secretases involved in the physiological cleavage of APP, but at the same time are known to process at least 40 other substrates (Endres and Fahrenholz, 2012; Del Turco et al., 2014). A moderately increased expression of ADAM10 was observed to yield higher sAPP α levels, stimulated synaptogenesis and lowered A β plaque burden (Postina, 2008). Cleavage with BACE1 and γ -secretase produces different A β species and even though A β 42 is produced at much lower levels than A β 40, it is proposed to be the more toxic fragment. This may be due to the fact that A β 42 was found to aggregate faster by building fibrils due to its hydrophobic properties (Hardy and Selkoe, 2002; Shi et al., 2014). Yet, as mentioned earlier, other groups refer to soluble A β as the toxic species (Swomley et al., 2014).

APLP1 and APLP2 undergo cleavage comparable to APP and produce soluble ectodomains sAPLP1 and sAPLP2 after ADAM10, ADAM17 or BACE1 processing. After cleavage by γ -secretase, the APP-like intracellular domain (ALICD) and a fragment similar to A β is formed that is, however, not toxic and incapable of aggregating (Eggert et al., 2004; Minogue et al., 2009).

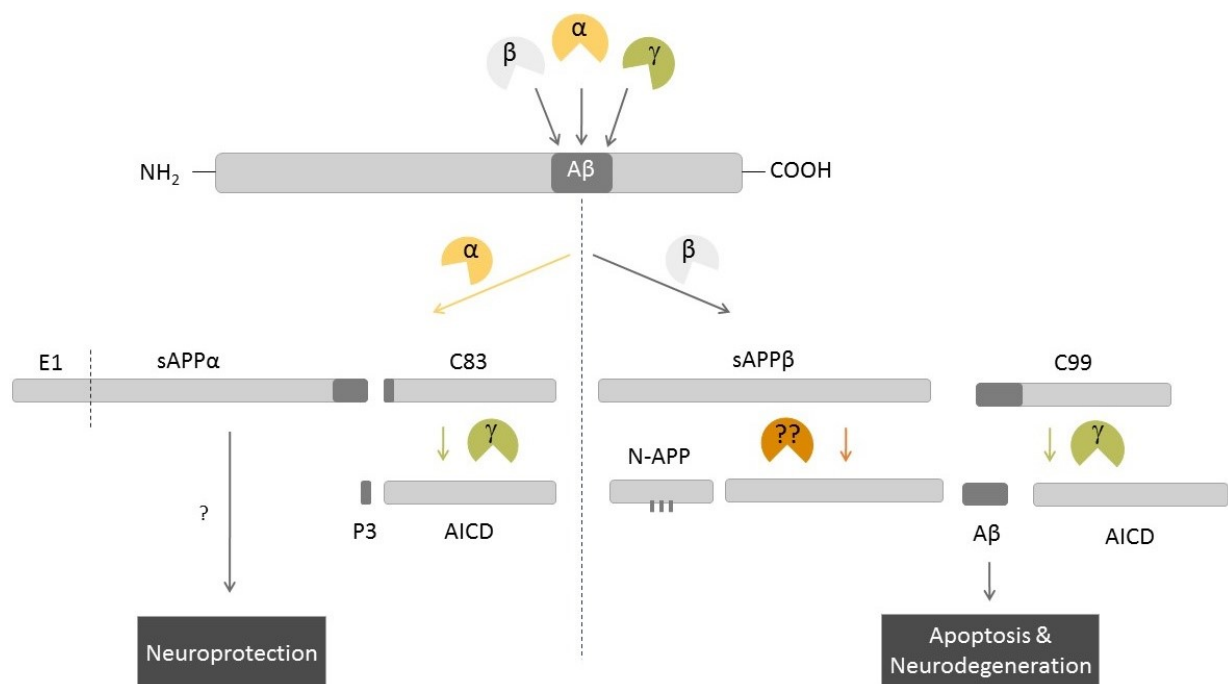


Figure 3. APP processing. The amyloid precursor protein is processed by three secretases (α , β , γ). Cleavage along the non-amyloidogenic pathway (left) by α -secretase yields C83 and the soluble ectodomain sAPP α with its subdomain E1 that was shown to have neuroprotective abilities. Proteolysis by β -secretase

along the amyloidogenic pathway (right) releases sAPP β and C99. Upon further cleavage of C99 by γ -secretase the APP intracellular domain (AICD) and the toxic A β fragment are liberated. If C83 is cleaved by γ -secretase the AICD and a tiny fragment, P3, are released. Processing of sAPP β by a yet unknown secretase produces N-APP.

1.3.3 APP Function

Although APP is mainly associated with the generation of the insoluble A β peptide that leads to the formation of amyloid plaques in the brains of patients suffering from AD, there is plenty of evidence for its crucial physiological functions. These, however, remain poorly understood (Dawkins and Small, 2014). Several studies point to a pivotal role in synaptic and neural plasticity, neurite outgrowth as well as cell-cell/cell-surface adhesion, cell signaling and cell survival (Müller and Zheng, 2012; Nicolas and Hassan, 2014; Weyer et al., 2011). APP also facilitates the anterograde neuronal transport by interaction with the motor protein kinesin (Chiba et al., 2014; Satpute-Krishnan et al., 2006).

APP expression was shown to be upregulated during neuronal differentiation and after ischemic/traumatic brain damage (Blennow et al., 2012; Van den Heuvel et al., 1999; Murakami et al., 1998; Nicolas and Hassan, 2014). This upregulation argues for a stress-induced role of APP as a protein of damage response similar to other proteins also known to be upregulated after brain injury, including heat shock proteins and c-Jun (Dewji and Do, 1996; Kim et al., 2012; Zheng et al., 2014). Furthermore, APP and its cleavage product sAPP α were found to exert neuroprotective effects *in vitro* in various studies (reviewed in Kögel et al., 2012b). While several other groups confirmed these neuroprotective abilities of APP and especially sAPP α following brain injury (Corrigan et al., 2014; Masliah et al., 1997; Ring et al., 2007; Smith-Swintosky et al., 1994; Weyer et al., 2014), decreased levels of soluble APP fragments were detected in the brains of AD patients (Fahrenholz, 2007). Moreover, sAPP α was proposed to act as a neurotrophic growth factor stimulating cell proliferation, axonal growth, synaptogenesis and synaptic plasticity with positive effects on long-term potentiation (LTP) and memory consolidation (reviewed in Chasseigneaux and Allinquant, 2012).

Mattson and colleagues were able to show that sAPP α -mediated neuroprotection was associated with rapid effects on ion channel function, thereby modulating ion homeostasis (Hoe et al., 2012; Mattson et al., 1997). Consistently, APP and soluble APPs were proposed to affect the inhibition of Ca²⁺ accumulation by suppressing NMDA currents and activating potassium channels, thus protecting neurons against excitotoxic stress (Camandola and Mattson, 2011; Furukawa and Mattson, 1998; LaFerla, 2002). This neuroprotective effect, however, was only detectable after incubation with sAPP α over several hours, suggesting that a persistent activation

of cell survival signaling pathways may be necessary for sAPP α -mediated protection (Kögel et al., 2012b).

Several studies support the notion that APP acts as a (membrane-bound) cell surface receptor or adhesion molecule for various interaction partners. Among others, binding with F-spondin (Ho and Südhof, 2004) and the Nogo-66 receptor (Park et al., 2006) was shown to regulate A β production and downstream signaling. APP interaction with the adaptor protein Fe65 led to decreased internalization of APP, enhanced sAPP α production and reduced formation of A β (Haass et al., 2012). Other studies propose that APP and APLPs form hetero- and homodimers, which promotes cell-cell adhesion via transdimerization (Baumkötter et al., 2012+2014; Soba et al., 2005). Recently, Gralle et al. suggested that enforced APP dimerization by APP N-terminal antibody 22C11 induces apoptosis unless disrupted by sAPP α as a competitive inhibitor rendering holo-APP expression necessary for sAPP α -mediated neuroprotection (Gralle et al., 2009).

In consequence to the findings outlined above, loss of the various functions of APP may reduce neuronal signaling and plasticity and render cells more prone to cellular stress during brain aging (loss-of-function theory). However, despite extensive research, it remains undetermined whether these diverse functions of APP are mediated by its membrane-bound form or its soluble ectodomains and which intracellular downstream targets are involved (Kögel et al., 2012b).

1.4 Cell Death

For the development and longevity of multi-cellular organisms, a perfectly balanced waste management and regulated cell death is essential. Tissues and cells are removed during differentiation (e. g. fingers and toes in human embryos); damaged or abnormally altered, mutated or otherwise degenerated cells have to be eliminated to prevent toxic effects on the organism. There are different forms of cell death (apoptotic, necrotic, autophagic or cell death associated with failed mitosis) that are discriminated according to their biochemical mechanisms and morphology (Galluzzi et al., 2007, 2012; Peter, 2011; Surova and Zhivotovsky, 2013).

1.4.1 Apoptosis

Apoptosis (type 1 cell death) is the highly regulated, active form of programmed cell death that requires energy/ATP (Skulachev, 2006). Diminished or excessive apoptosis rates are held responsible for several pathological conditions such as autoimmune diseases and cancer, e. g. if autoreactive or mutated cells are not removed efficiently (Galluzzi et al., 2007). Morphologically, cells are found to be rounded, nuclear and cellular volumes shrink, the plasma membrane starts blebbing, chromatin condensates and the nucleus eventually becomes fragmented (Galluzzi et al., 2012; Kerr et al., 1972). An early apoptotic event is the exposition of phosphatidylserine (PS) as

it is flipped from the inner cell membrane (cytosolic side) to the outer surface of the cell (Galluzzi et al., 2012; Verhoven et al., 1995). The surrounding tissue is usually protected from inflammatory processes, since no cellular contents leak out but are rather stored in apoptotic bodies during exocytosis of membranous vesicles that will be engulfed by phagocytic macrophages (Akers et al., 2013; Kroemer et al., 2005).

Several regulatory proteins control apoptotic intracellular signaling. Caspases, cysteine-dependent proteases, are the major executors of classic apoptosis and are classified into initiator and effector caspases (Orrenius et al., 2011). Their respective precursor molecules, pro-caspases, are widely distributed within the cell and can be activated by proteolytic cleavage (Würstle et al., 2012). Caspase activation is controlled by “inhibitor of apoptosis proteins” (IAPs), which are, in turn, inhibited by mitochondrial proteins Smac/DIABLO (Fuchs and Steller, 2011; Gottfried et al., 2004). The activation of initiator caspases can be triggered by an extrinsic (type 1) and intrinsic (mitochondrial, type 2) pathway which eventually leads to the activation of effector caspases that induce apoptosis (Figure 4).

In the intrinsic pathway, genotoxic stimuli, cytokines or growth factor deprivation activate intracellular stress signaling proteins that directly target mitochondria. This leads to mitochondrial swelling and membrane permeabilization. In consequence, the so-called apoptosome is formed upon leakage of cytochrome c and its binding to the pro-caspase-activating protein Apaf1 and other caspase-activating proteins (Bao and Shi, 2007). In turn, the apoptosome activates effector caspase-3 and -7 by cleaving pro-caspase-9. Both effector caspases start the caspase cascade and cleave cytosolic and nuclear proteins, which finally leads to the intranucleosomal degradation of DNA (Figure 4; de Almagro and Vucic, 2012; Kim et al., 2006). The most important regulators of the intrinsic pathway are Bcl-2 protein family members that can have pro- (e.g. PUMA, Bax/Bak, Bim, Bad) or anti-apoptotic (e.g. Bcl-2, Bcl-w, Bcl-xL, Mcl-1) abilities (Kögel et al., 2010).

In the extrinsic pathway, receptor-mediated direct signal transduction leads to apoptotic mechanisms. Upon activation by stress-inducing ligands death receptors of the TNF/NGF super family expressed on the cell surface, such as TRAIL, Fas, TNF-R1, assemble and form death domains (de Almagro and Vucic, 2012; Gupta, 2001). Initiator pro-caspase-8 binds to the respective adaptor proteins to build the death-inducing signal complex DISC. In consequence, caspase-8 is activated within DISC and activates effector caspase-3 and -7 and other pro-apoptotic proteins of the Bcl-2 family (Figure 4; Galluzzi et al., 2012; Lavrik et al., 2005a).

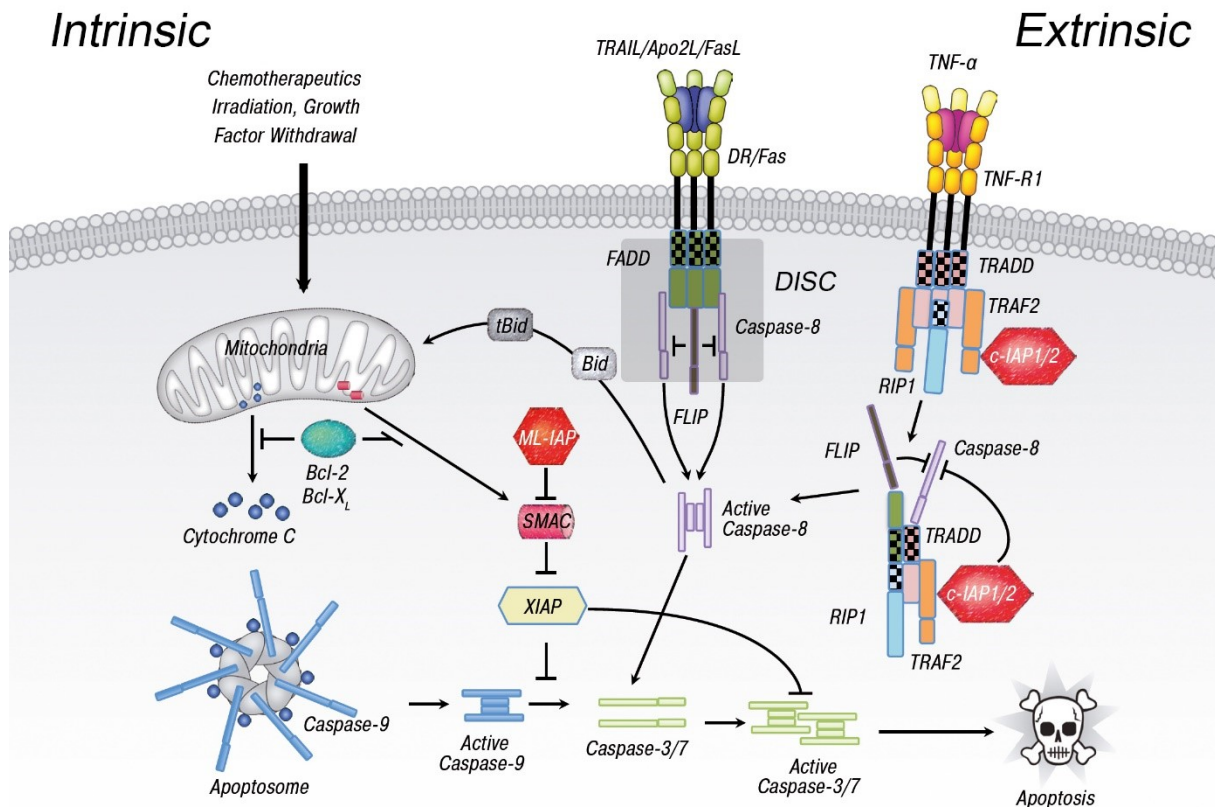


Figure 4. Intrinsic and extrinsic pathway of apoptosis. Apoptosis that is triggered by external stress stimuli is activated by ligand (TRAIL, Apo2L, FasL, TNF- α) binding to transmembrane death receptors (DR, Fas, TNF-R1). The intrinsic pathway is activated by apoptotic stress signals (e. g. irradiation, growth factor withdrawal) that permeabilize mitochondrial membranes which leads to cytochrome c release. Upon activation of pro-caspase-9, the cytochrome c-bound complex (apoptosome) activates caspase-9. This may be regulated by pro- (Bid) or anti-apoptotic (Bcl-2, Bcl-xL) proteins and leads to the activation of caspase-3 and -7 and the induction of the caspase cascade triggering apoptotic cell death. In the extrinsic pathway, the stimulated cell surface receptors build DISC by recruiting endogenous adaptor protein FADD and binding of pro-caspase-8. In turn, active caspase-8 initiates the caspase cascade by activating effector caspase-3/-7 and activates other pro-apoptotic proteins. Crosstalk between both pathways may include activation of Bid, which is a potent inducer of the intrinsic pathway. Caspase activation is controlled by “inhibitor of apoptosis proteins” (IAPs), which are, in turn, inhibited by mitochondrial proteins such as Smac. Abbreviations: Apo2L, apoptosis ligand 2; Bcl-2, B-cell lymphoma 2; Bcl-xL, Bcl-x long; Bid, BH3 interacting domain death agonist; cIAP1/2, cellular inhibitor of apoptosis 1; DISC, death-inducing signal complex; DR, death receptor; FADD, Fas (TNFRSF6)-associated via death domain; FasL, Fas ligand; FLIP, FLICE-like inhibitory protein; ML-IAP, melanoma inhibitor of apoptosis; RIP1, receptor-interacting protein 1; Smac, second mitochondrial activator of caspases; tBid, truncated Bid; TNF- α , tumor necrosis factor alpha; TNF-R1, tumor necrosis factor receptor 1; TRADD, TNF receptor-associated death domain; TRAF2, tumor necrosis factor receptor-associated factor 2; TRAIL, TNF-related apoptosis-inducing ligand; XIAP, X-linked inhibitor of apoptosis. Modified from de Almagro (2012).

1.4.2 Necrosis

Necrosis is the passive, non-physiological form of cell death that usually occurs due to external factors, hypoxia, after traumatic injury or infection. In contrast to apoptosis, different receptors are activated, which results in cell swelling and eventually rupture of plasma membranes

(Proskuryakov et al., 2003; Vanden Berghe et al., 2010). In consequence, leakage of cytoplasm and cell organelles into the surrounding extracellular space triggers local inflammation hot spots, which was found to ameliorate tumor growth. Makrophages eliminating the debris further exacerbate inflammation by producing pro-inflammatory factors such as TNF α , which in turn trigger apoptosis (Khandelwal et al., 2011; Vakkila and Lotze, 2004).

A regulated and programmed form of necrosis, termed necroptosis, was suggested an alternative to apoptosis, when signaling is disrupted by mutations or exogenous factors. This form of cell death is controlled by RIP1 and RIP3 kinases and may play an important role in neurodegenerative diseases and viral infections (Dunai et al., 2011; Kaczmarek et al., 2013).

1.4.3 Autophagy

Autophagy (type 2 or caspase-independent cell death) is the catabolic mechanism of cellular self-digestion and lysosomal degradation as well as recycling of cellular components. It has cytoprotective housekeeping functions, especially during periods of cell stress and starvation as it removes misfolded or aggregated proteins, intracellular pathogens and damages organelles (Lin et al., 2013). Autophagy regulates homeostasis by balancing energy sources during development and in response to nutrient stress (Deng et al., 2012). However, excessive and prolonged autophagy is also linked to pathological events (e. g. survival of starved tumor cells), cell death and aging (Cuervo et al., 2005; Patel et al., 2012).

1.4.4 Cell Death Mechanisms in AD

Changes in synaptic plasticity and neural circuits are being observed very early during brain aging and the development of AD and often before most other pathological events become evident (Karran et al., 2011). This suggests that inspite of detecting abundant neuronal cell death in the “late phase” of the disease synaptic dysfunction and dendritic spine loss may already suffice for AD pathology. As described earlier, a combination of A β aggregation and its hampered clearance might impair mitochondrial function provoking these changes in synaptic plasticity (Cavallucci et al., 2012). Consistently, D’Amelio and colleagues review on several groups that show cell death-independent activation of caspase-3 questioning its traditional role in apoptosis (D’Amelio et al., 2012). They further suggest that neurons may tolerate a certain level of caspase activity without undergoing immediate cell death, but caspase activation and caspase-dependent protein cleavage might promote an apoptotic program (de Calignon et al., 2010; D’Amelio et al., 2011, 2012).

It is controversially discussed whether the final step in AD leading to neuronal cell loss is caused primarily by apoptosis or if other mechanisms are involved. Some studies present findings of typical apoptosis-like morphological changes in AD (Hyman and Yuan, 2012; Loo et al., 1993), while others claim that only very few cells display apoptotic features and rather appear necrotic

(Lassmann et al., 1995; Troncoso et al., 1996). An important role of apoptosis during brain aging and in the development and onset of AD is supported by the observation of DNA fragmentation with increased levels of c-Jun, Bax and several caspases (reviewed in Behl, 2000). It was further reported that soluble A β impairs mitochondrial function and leads to a build-up of free radicals, which triggers apoptotic stress but also necrosis (Manczak et al., 2006). The peptide was also shown to indirectly stimulate death receptors, caspase-3 activation and nuclear fragmentation along with increased levels of endoplasmic reticulum (ER) stress and pro-apoptotic proteins (Behl, 2000; Ghavami et al., 2014). A few studies revealed that apoptotic activity of cells was increased after overexpression of AD-associated mutant PS1/PS2 or A β (Ghavami et al., 2014; Guo et al., 1996). In agreement, TUNEL-positive neurons and upregulated initiating and executioner caspases were detected in AD brains by various groups (reviewed in Hyman and Yuan, 2012).

On the other hand, Zhu and colleagues challenge the traditional view of apoptosis as the leading cause considering that apoptosis is a relatively rapid process leading to cell deterioration within hours rather than decades as is the case in AD (Zhu et al., 2006). Their reasoning is supported by groups describing non-apoptotic caspase activity in an AD model suggesting that caspase activation may promote neurodegeneration by removing neurons with accumulated protein aggregates (e. g. tau) (Cavallucci et al., 2012; D'Amelio et al., 2012).

Both cell death pathways may overlap and the exact distinction between necrosis and apoptosis may not always be possible. Behl is suggesting that an initial response to protein aggregates in AD may first lead to necrosis, which in turn triggers an exaggerated apoptotic reaction due to leaking necrotic cells (Behl, 2000).

In addition to apoptosis and necrosis, the autophagy process was also reported to function abnormally in AD. Efficiency is described to decline during normal aging, whereas macroautophagy was shown to be transcriptionally upregulated in AD (Lipinski et al., 2010). Even though autophagy is considered beneficial, excessive formation of autophagosomes and autolysosomes as observed in AD brains is thought to hamper effective degradation of protein aggregates and increase γ -secretase activity (Lee et al., 2013; Ohta et al., 2010). Furthermore, maturation of autophagosomes was observed to be impaired (Yu et al., 2005). On the one hand, inducers of autophagy facilitated tau clearance, reduced tau aggregates and improved cognitive performance in AD (Berger et al., 2006; Congdon et al., 2012). On the other hand, substantial evidence points to a more crucial role of the ubiquitin-proteasome-system (UPS) in tau degradation, physiological brain aging and AD (protein quality control). The UPS regulates intracellular protein levels by conjugating misfolded or otherwise damaged proteins and substrates with ubiquitin, that targets them to 26S proteasomes for proteolysis (Glickman and Ciechanover, 2002). Inhibition of the proteasome, e. g. by MG132 (a potent reversible inhibitor of the 26S complex) treatment in this work, therefore mimics similar stress conditions as seen in the

aging brain leading to an accumulation of damaged proteins, which causes the activation of stress pathways and cell death. Levels of ubiquitin were significantly increased in AD (Kudo et al., 1994; Song and Jung, 2004) and dysfunction of the UPS was shown to facilitate tau aggregation and increase neurodegeneration (Krstic and Knuesel, 2013; Mandelkow, 1999; Lee et al., 2013). Lee and colleagues further propose that both degradation systems, UPS and autophagy, may be closely linked during AD. In the beginning, soluble tau and other Alzheimer-relevant proteins may be actively cleared by the UPS, but aggregates rather seem to be degraded via autophagy when the proteasome becomes impaired due to oxidative stress and accumulated substrates (Lee et al., 2013). In turn, reduced UPS activity is seen to hamper normal autophagic processes exacerbating AD phenotypes (Korolchuk et al., 2009; Lee et al., 2013).

1.5 The Role of APP in Survival/Stress Signaling

As described earlier, abundant experimental evidence points to a crucial physiological and neuroprotective function of APP despite its role in A β plaque formation. It is associated with synaptic and neural plasticity, neuronal survival and cell signaling (Müller and Zheng, 2012; Nicolas and Hassan, 2014).

The PI3K/Akt pathway is a central survival pathway that can be activated by several neurotrophins and members of the insulin-like growth factor family such as insulin-like growth factor 1 (IGF1). Upon binding of stimulant ligands to their respective receptors, the lipid kinase phosphoinositide 3 (PI3) is activated and the serine-threonine protein kinase Akt (or alternatively protein kinase B, PKB) is stimulated downstream, which in turn indirectly activates mammalian target of rapamycin (mTOR; Manning and Cantley, 2007). Different proteins are phosphorylated and thereby activated or inhibited, e. g. pro-apoptotic glycogen synthase kinase-3 (GSK3), Bad and FOXO that are inhibited (Maurer et al., 2014; Song et al., 2005). This causes a number of downstream effects, which leads to the promotion of cell survival and the inhibition of apoptosis. At the same time, protein synthesis, transcription, cell growth and proliferation are initiated (Hay and Sonenberg, 2004; Maurer et al., 2014). The PI3K/Akt pathway also plays an important role in cancer by reducing apoptosis and ameliorating cell proliferation (De Luca et al., 2012).

An important target of Akt, the stress kinase GSK3, was found to be relevant in AD pathology by promoting A β production and tangle formation (Jope et al., 2007). Furthermore, the AICD of APP was shown to induce p53-mediated apoptosis (Ozaki et al., 2006) and activate neurotoxic GSK3 β transcription (Trazzi et al., 2014). The two isoforms of GSK3, GSK3 α and GSK3 β , are phosphorylated at tyrosine-216/279 and serine-21/9 which leads to their inactivation. In the non-phosphorylated form, GSK3 was shown to influence over 40 proteins and several different signaling pathways, i. a. Wnt pathway (Hers et al., 2011; Jope and Johnson, 2004).

The c-Jun/N-terminal kinase (JNK) or stress-activated phospho-kinase (SAPK) pathway is a major stress signaling pathway and modulator of both the extrinsic and intrinsic pathway of apoptosis implicated in brain aging and AD pathology (Kögel et al., 2012b; Putcha et al., 2003). Several stimuli, such as UV radiation and interleukins, but also physiological processes and aging were shown to activate JNKs that belong to the family of mitogen-activated protein kinases (MAPK; Moriguchi et al., 1997; Plotnikov et al., 2011). After their activation by MAPK kinases (MAPKK) JNKs relocate to the nucleus and phosphorylate transcription factors such as c-Jun (Plotnikov et al., 2011). In consequence, other proteins are phosphorylated and inhibited or activated, e. g. anti-apoptotic Bcl-2 and pro-apoptotic Bax, which trigger apoptosis (Waetzig and Herdegen, 2005).

Kögel et al. (2012b) suggest that the activation of survival pathways by APP/sAPP α may interfere with pro-apoptotic stress pathways, e. g. by antagonizing the c-Jun/JNK pathway. In an earlier study, members from the Kögel lab could show that transcriptional repression of c-Jun and JNK activity was dependent on APP and the application of sAPP α reduced JNK signaling and apoptosis (Copanaki et al., 2010; Kögel et al., 2005). This would propose an important physiological function of APP/sAPP α in the control of stress signaling and apoptosis due to cytotoxic stress. Additionally, Jimenez et al. (2011) and other groups suggested that sAPP α inhibits GSK3 β by activation of the PI3K/Akt survival pathway, supposedly through activation of IGF1/insulin receptors (Copanaki et al., 2010; Eckert et al., 2011; Jimenez et al., 2011). This cytoprotective function of APP/sAPP α by activation of survival pathways was further substantiated by making use of selective inhibitors against PI3K or p42 (ERK1) and p44 (ERK2) MAP kinases (Cheng et al., 2002). Furthermore, sAPP α -mediated survival may also include the activation of pro-survival genes with simultaneous suppression of pro-apoptotic genes (e. g. c-Jun) most likely involved in stress responses and neuronal survival such as manganese superoxide dismutase (MnSOD), peroxiredoxins, catalase, insulin-like growth factor 2 (IGF2; Kögel et al., 2005; Stein et al., 2004). Kögel et al. also propose certain crosstalk between survival and stress pathways as upstream JNK kinases such as mixed lineage kinase 3 (MLK3) and apoptosis signal-regulating kinase-1 (ASK1) were shown to be inhibited by Akt (Kögel et al. 2012b).

Consequently, the exact mechanisms of APP/sAPP α -mediated neuroprotection and signaling are not fully understood. Especially the putative receptors and/or interactors require stringent experimental proof to shed light on the complex interplay between stress and survival pathways affected by APP (Figure 5).

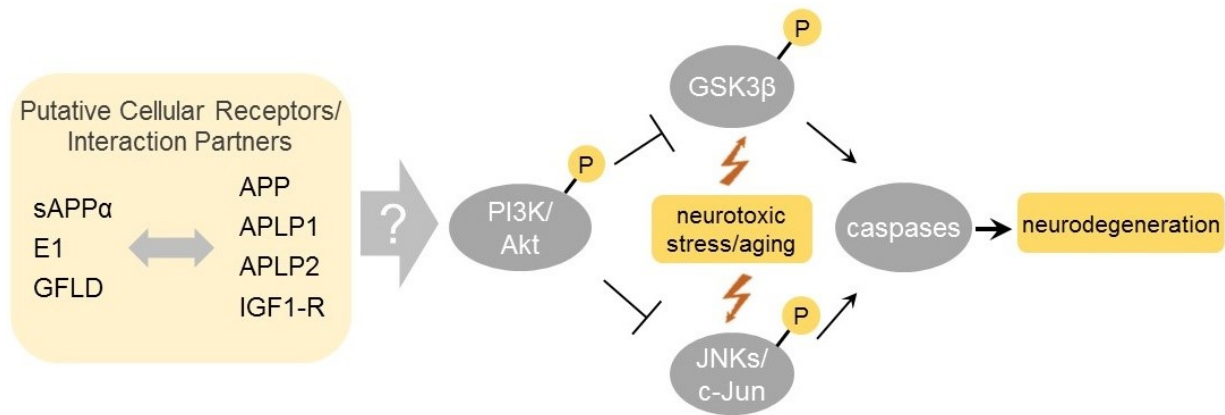


Figure 5. Modulation of survival/stress signaling by APP and its putative interactors. It is currently not developed whether holo-APP or other interactors/co-receptors mediate sAPP α -induced survival signaling. However, earlier studies suggest that APP, APP family members APLP1 and APLP2 and putative cell surface receptors such as IGF1-R might interact with each other and/or soluble APP ectodomains sAPP α , E1 and GFLD (cf. Figure 2), which may, in turn, modulate stress and survival pathways. It is established that PI3K is activated via stimulation of IGF1-R, I-R and other receptors of the IGF family. In a similar fashion, APP interaction/binding may stimulate PI3K, which consequently activates Akt by phosphorylation to trigger survival. To this end, activated Akt inhibits GSK3 β , JNKs/c-Jun and other stress-induced downstream targets by phosphorylation to prevent stimulation of caspases that trigger apoptosis. Stress-induced proteins were shown to be upregulated and activated during aging and by neurotoxic stimuli.

1.6 Aim of this Thesis

Under physiological conditions, APP is cleaved by α -secretase along the non-amyloidogenic pathway to yield a large soluble fragment, sAPP α . Earlier results from this and other groups point to a pivotal role of APP and sAPP α in neuronal plasticity, axonal growth, synaptogenesis and neuroprotection (Zheng and Koo, 2011). In consequence, loss of these physiological functions and diminished sAPP α secretion during aging renders neurons susceptible to cellular stress as found in AD. However, the exact mechanisms of sAPP α /APP-mediated neuroprotection are still poorly understood and most likely involve a complex interplay between survival/stress pathways and interaction with surface receptors and other targets (Figure 5).

It is established that APP and APLPs are integral transmembrane proteins which may function as membrane-bound signaling receptors and/or adhesion molecules (Baumkötter et al., 2012; Soba et al., 2005). In this context, it was proposed that sAPP α may act as a competitive inhibitor disrupting membrane-bound APP homodimers, thereby inducing cell survival (Gralle et al., 2009). Another study postulated that the *Drosophila* orthologue of sAPP α , sAPPL, only exhibited protective abilities in the presence of membrane-bound APPL (Wentzell et al., 2012). These findings speak for an important function of APP in neuroprotective signaling - possibly as a receptor. However, it remains unclear, whether these functions are primarily mediated by holo-

APP or by secreted sAPP α . Also, the cellular receptors and downstream signaling targets are yet to be identified. Previous results from this lab on the inhibitory influence of sAPP α on the c-Jun/JNK stress pathway suggest a complicated signaling network involved in neuroprotection (Kögel et al., 2003, 2005). Likewise, several groups postulate that the PI3K/Akt signaling pathway is involved in sAPP α -mediated cytoprotection (Cheng et al., 2002; Copanaki et al., 2010; Eckert et al., 2011; Jimenez et al., 2011). However, most of the experimental evidence is solely based on indirect approaches and pharmacological inhibitors of the putatively involved pathways, which often exhibit a limited specificity. Consequently, the exact relevance of survival signaling for sAPP α -mediated neuroprotection and the molecular mechanisms underlying their activation are currently not well understood and need to be further investigated. This work aims at contributing mechanistic insights into the physiological function of APP and sAPP α -mediated survival signaling in limiting neuronal damage and cell death due to neurotoxic stress conditions and brain aging (Figure 5).

During the work on this thesis, the principal molecular mechanisms of APP/sAPP α -induced neuroprotection were to be analyzed. To this end, purification of recombinant APP fragments, sAPP α and its subdomain E1, is established in a yeast model (*Pichia pastoris*). Their neuroprotective abilities are tested in a combination of different cell and tissue models including SH-SY5Y cells, MEFs and hippocampal slices under stress conditions by serum and/or glucose deprivation. Additionally, to further investigate the role of holo-APP and other APP family members, different knockdown (KD) and knockout (KO) models of APP/APLPs as well as APP mutants were to be utilized. To this end, a varied set of techniques is employed, which includes cell death and viability assays, kinase assays and protein analysis. To address the contribution of sAPP α -dependent signaling pathways and to support experimental results from knockout studies, pharmacological intervention with inhibitors completes the approach.

2 Materials

2.1 Chemicals

Unless stated otherwise, all chemicals were provided in analytical grade purity from the following companies:

AppliChem GmbH, Darmstadt, Germany
 Biozym Scientific GmbH, Hessisches Oldendorf, Germany
 Carl Roth GmbH & Co. KG, Karlsruhe, Germany
 Fluka Chemie AG, Buchs, Switzerland
 Invitrogen (Gibco), Karlsruhe, Germany
 Merck KgaA, Darmstadt, Germany
 Qiagen GmbH, Hilden, Germany
 Serva Feinbiochemica, Heidelberg, Germany
 Sigma-Aldrich Laborchemikalien GmbH, Seelze, Germany

2.2 Buffers and Solutions

Table 1. Buffers and Solutions

Buffer or Solution	Composition
10-12 % separation gel (for SDS-PAGE)	10-12 % acrylamide/bis solution 375 mM Tris/HCl (1 M, pH 8.8) % SDS (10%) % APS (10 %) 0.05 % TEMED
10x biotin (for yeast culture)	20 mg biotin ddH ₂ O ad 100 ml
10x glycerol (for yeast culture)	10 ml glycerol ddH ₂ O ad 100 ml filter-sterilized
10x LEW buffer (for protein isolation from yeast)	500 mM NaH ₂ PO ₄ 3 M NaCl ddH ₂ O ad 1 l filter-sterilized, pH 8.0 (with NaOH)
10x methanol (for yeast culture)	5 ml methanol ddH ₂ O ad 100 ml filter-sterilized, stored at 4 °C
10x PBS	95.5 g PBS powder ddH ₂ O ad 1000 ml
10x YNB (for yeast culture)	134 g yeast nitrogen base (YNB, Invitrogen) with ammonium sulphate/without amino acids

	ddH ₂ O ad 1000 ml filter-sterilized, stored at 4 °C
1x electrophoresis running buffer (for SDS-PAGE)	25 mM Tris 192 mM glycine 0.1 % SDS
1x electrophoresis transfer buffer (for SDS-PAGE)	25 mM Tris 192 mM glycine 10-20 % methanol
1x TBS	50 mM Tris 150 mM NaCl ddH ₂ O ad 1000 ml pH 7.5
5 % stacking gel (for SDS-PAGE)	5 % acrylamide/bis solution 120 mM Tris/HCl (1 M, pH 6.8) % SDS (10%) 0.1 % APS (10 %) 0.05 % TEMED
5x SDS loading buffer	250 mM Tris/HCl, pH 6.8 10 % SDS 30 % glycerol 5 % β-mercaptoethanol 0.02 % bromophenol blue
ampicillin stock solution	100 mg/ml in ddH ₂ O (Sigma-Aldrich, Seelze) filter-sterilized, stored at -20 °C
blocking solution (for immunodetection)	5 % skim milk powder in 1x TBS-Tween
CA lysis buffer	10 mM Hepes, pH 7.4 42 mM KCl 5 mM MgCl ₂ 0.1 mM EDTA 0.1 mM EGTA 0.5 % Chaps added freshly: 1 mM DTT 5 µg/ml aprotinin 1 µg/ml leupeptin 1 µg/ml pepstatin 1 mM PMSF
CA reaction buffer	25 mM Hepes, pH 7.5 1 mM EDTA 0.1 % Chaps 10 % sucrose added freshly: 3 µg/ml DTT 10 µM Caspase-3 substrate (DEDV)
Coomassie stain	Imperial Protein Stain (Thermo Scientific, Schwerte, Germany)

fixing solution	4 % paraformaldehyde dissolved in PBS at 70 °C
Fungizone solution	antimycotic (Gibco)
HEPES buffer (for FACS)	10 mM HEPES 140 mM NaCl 5 mM CaCl ₂ ddH ₂ O ad 500 ml
imidazole (for protein isolation from yeast)	2 M imidazole in ddH ₂ O filter-sterilized, stored at 4 °C
Ni-sepharose beads	Ni sepharose 6 Fast Flow (GE Healthcare, Little Chalfont, UK)
penicillin, streptomycin (pen/strep)	antibiotics, 10000 µg/ml (Gibco)
potassium phosphate buffer (for yeast culture)	132 ml K ₂ HPO ₄ (1 M) 868 ml KH ₂ PO ₄ (1 M) autoclaved, pH 6.0 (with KOH or phosphoric acid only!)
protein marker (for SDS-PAGE)	Precision Plus Protein All Blue Standards (10-250 kD, Bio-Rad, Munich, Germany)
SDS lysis buffer	2 % SDS 68.5 mM Tris/HCl 10 % glycerin 1 mM protease/phosphatase inhibitor cocktail
TBS-Tween	1x TBS 0.05 % (v/v) polyethylenesorbitan monolaurate (Tween20) stored at RT, pH 7.4
Tris/HCl buffer (for protein isolation from yeast)	5 mM Tris 150 mM NaCl ddH ₂ O ad 1 l filter-sterilized, pH 8.0 (with NaOH)
Trypan blue	1x PBS 0.4 % (v/v) Trypan Blue (Sigma-Aldrich, Seelze)
Trypsin/EDTA solution	0.25 % trypsin/EDTA (1x, Gibco)

2.3 Cell Biology

2.3.1 Media

All culture media and their supplements were provided in sterile and endotoxin-free quality. Supplemented media were stored at 4 °C for up to 4 weeks, pre-warmed and pH-adjusted (medium for hippocampal slices) prior to use. Fetal calf serum (FCS) and horse serum (HS) were heat-inactivated at 56 °C for 45 min.

Table 2. Media

Cell Line/Primary Culture	Medium Composition
hippocampal slice cultures (culture medium for cell death experiments)	Neurobasal A Medium (glucose-free) supplied with: 1 % L-glutamine (200 mM) 1 % pen/strep adjusted to pH 7.2
hippocampal slice cultures (culture medium)	Minimum Essential Medium supplied with: 25 % Basal Medium Eagle 25 % horse serum (HS) 3 % glucose (20 %) 1 % L-glutamine (200 mM) 0.5 % pen/strep 0.5 % fungizone adjusted to pH 7.2
hippocampal slice cultures (dissection medium)	Minimum Essential Medium supplied with: 1 % L-glutamine (200 mM) 1 % pen/strep adjusted to pH 7.35
human embryonic kidney cells (HEK293T, culture medium)	Dulbecco's modified Eagle's medium (DMEM GlutaMAX) supplied with: 10 % FCS 1 % L-glutamine (200 mM) 1 % pen/strep
human SH-SY5Y neuroblastoma (culture medium)	Dulbecco's modified Eagle's medium (DMEM) with F-12 Nutrient Mixture (Ham) supplied with: 10 % FCS 1 % L-glutamine (200 mM) 1 % pen/strep
<i>E. coli</i> (LB medium = culture medium)	22.5 g Luria Broth Base (Miller's LB Broth Base) 900 ml ddH ₂ O autoclaved, stored at RT
mouse embryonic fibroblasts (MEFs, culture medium)	DMEM GlutaMAX supplied with: 10 % FCS 1 % L-glutamine (200 mM) 1 % pen/strep
mouse hippocampal neurons (culture medium)	Neurobasal A Medium supplied with: 2 % B27 2 % GlutaMAX 0.2 % pen/strep 1 % gentamycin
mouse hippocampal neurons (culture medium for cell death experiments)	Neurobasal A medium supplied with: 2 % GlutaMAX 0.2 % pen/strep 1 % gentamycin
<i>Pichia pastoris</i> (BMGY culture medium)	10 g yeast 20 g peptone

	ddH ₂ O ad 700 ml autoclaved added freshly: 100 ml potassium phosphate buffer (see Buffers and Solutions) 100 ml 10x YNB (see Buffers and Solutions) 20 ml 50x biotin (see Buffers and Solutions) 100 ml 10x glycerol (see Buffers and Solutions)
<i>Pichia pastoris</i> (BMMY secretion medium)	10 g yeast 20 g peptone ddH ₂ O ad 700 ml autoclaved added freshly: 100 ml potassium phosphate buffer (see Buffers and Solutions) 100 ml 10x YNB (see Buffers and Solutions) 20 ml 50x biotin (see Buffers and Solutions) 100 ml 10x methanol (see Buffers and Solutions)

2.3.2 Cell Lines

Table 3. Cell Lines

Cell Line	Description (Origin)
SH-SY5Y wt and APP-KD	human neuroblastoma cells, wt (from ATCC, Wesel, Germany) or stable lentiviral KD of APP
MEF wt and APP-KO	mouse embryonic fibroblasts prepared from wt or APP-KO mice, immortalized (from Prof. Ulrike Müller, University of Heidelberg, Germany)
MEF IGF1-R KO	mouse embryonic fibroblasts prepared from IGF1-R KO mice, mortal (from Dr. Jean-Christophe François, UPMC, Paris, France)
HEK293T	human embryonic kidney cells with SV40 T-antigen for enhanced replication of transfected plasmids (virus production, from ATCC)

2.3.3 Animals

Table 4. Animals

Animals	Description (Origin)
wildtype mouse line	<i>Mus musculus</i> , C57Bl/6 (obtained from Prof. Ulrike Müller, University of Heidelberg, Germany)

transgenic mouse lines

Mus musculus, C57Bl/6, APP-KO lack membrane-anchored full-length APP and all of its proteolytic fragments (from Prof. Ulrike Müller, University of Heidelberg, Germany, see also Aydin et al., 2012)

Mus musculus, C57Bl/6, APP APP-ΔCT15 lack the last 15 amino acids (aa) of the C-terminus of APP, which includes the YENPTY motif (from Prof. Ulrike Müller, University of Heidelberg, Germany, see also Aydin et al., 2012)

2.4 Molecular Biology

2.4.1 Kits

Table 5. Kits

Use	Name (Origin, Cat. #)
protein concentration	Pierce BCA Protein Assay (Thermo Scientific)
ECL blot developer	ECL kit (Western Lightning, PerkinElmer, Hamburg, Germany), luminol/enhancer und hydrogen peroxide/oxidizer reagents in a ratio of 1:1
bioluminescence assay	CellTiter-Glo Luminescence Assay (Promega, Mannheim, Germany, #G7571)
plasmid DNA preparation	Endofree Qiagen Plasmid Purification Maxi Kit (Qiagen)
live-dead assay	Live/Dead Cell Staining Kit II (PromoKine, Heidelberg, Germany, #PK-CA707-30002)
Akt kinase assay	Non-radioactive Akt Kinase Assay Kit for 40 assays (Cell Signaling, Frankfurt/Main, Germany, #9840S)
transfection	FuGENE Transfection Reagent (Roche Diagnostics, Mannheim, Germany)

2.4.2 Primary Antibodies

Table 6. Primary Antibodies

Name and Designated Antigen	Type and Origin, Applied Dilution (Manufacturer)
anti-pGSK3α/β (Ser 9/21, 37F11)	monoclonal rabbit, 1:1000 (Cell Signaling)
anti-pGSK3β (Ser 9) XP (D85E12)	monoclonal rabbit, 1:1000 (Cell Signaling)
anti-GSK3β	monoclonal mouse, 1:1000 (Cell Signaling)
anti-APP (22C11)	monoclonal mouse, 1:1000 (Millipore, Darmstadt, Germany)
anti-APLP1	polyclonal rabbit, 1:1000 (Millipore)
anti-APLP2	polyclonal rabbit, 1:2000 (Millipore)
anti-GAPDH	monoclonal mouse, 1:20000 (Millipore)

immobilized anti-pAkt (Ser 473, D9E)	monoclonal rabbit, bead conjugate (Cell Signaling)
anti-beta-3-tubulin (neuron-specific)	polyclonal mouse, 1:1000 (R&D, Wiesbaden, Germany)
anti-GFAP (glia-specific)	monoclonal rabbit, 1:200 (Cell Signaling)
anti-NeuN (neuron-specific)	monoclonal mouse, 1:500 (Millipore)
anti-MAP2 (neuron-specific)	monoclonal mouse, 1:500 (Millipore)

2.4.3 Secondary Antibodies

Table 7. Secondary Antibodies

Name and Designated Antigen	Origin, Applied Dilution (Manufacturer)
IRDye red 680 RD anti-rabbit	goat, 1:15000 (LI-COR Biosciences, Bad Homburg, Germany)
IRDye red 680 RD anti-mouse	goat, 1:15000 (LI-COR Biosciences)
IRDye green 800 CW anti-rabbit	goat, 1:20000 (LI-COR Biosciences)
IRDye green 800 CW anti-mouse	goat, 1:20000 (LI-COR Biosciences)
anti-rabbit IgG 488 conjugated (green)	donkey antibody DyLight, 1:5000 (BioMol, Hamburg, Germany)
anti-mouse IgG 488 conjugated (green)	donkey antibody DyLight, 1:5000 (BioMol)

2.4.4 Viral Vectors and Plasmids

Table 8. Viral Vectors and Plasmids

Vector/Plasmid	Description (Origin)
human sAPP β -PDGFR-TMD	pHAIN-CMV plasmid encoding human sAPP β with N-terminal HA and C-terminal myc tag followed by the transmembrane domain of the platelet-derived growth factor receptor (PDGFR) as provided by the pDisplay plasmid (Invitrogen, from Prof. Christian Buchholz, PEI, Langen, Germany)
APP- Δ NPTY	pCDNA3.1-APP with N-terminal myc tag lacking the YENPTY motif (aa 680-691 of APP695, from Prof. Stefan Kins, University of Kaiserslautern, Germany)
APP- Δ PEER	pCDNA3.1-APP with N-terminal myc tag lacking the G-protein interaction motif (aa 669-679 of APP695, from Prof. Stefan Kins, University of Kaiserslautern, Germany)
Mission® shRNA Plasmid DNA	APP: NM_000484.2-3202s1c1 APLP1: NM_005166.2-1711s1c1 APLP2: NM_001642.1-1582s1c1 all contain the pLKO.1-puro vector (Sigma-Aldrich)

packaging plasmid (for virus particles)	psPAX2 (Addgene, Cambridge, MA, USA)
enveloping plasmid (for virus particles)	pMD2.G (Addgene, Cambridge, MA, USA)

2.4.5 Bacteria Strain

Table 9. Bacterial Strain

Name	Description (Origin)
<i>Escherichia coli</i> DH5 α competent cells	F- ϕ 80 <i>lacZ</i> Δ M15 D(<i>lacZYA-argF</i>) U169 <i>deoR recA1 endA1 hsdR17</i> (rk-, mk+) <i>phoA</i> supE44 <i>thi-1 gyrA96 relA1</i> λ - (Invitrogen)

2.5 Software

Table 10. Software

Use	Name (Origin)
immunoblot fluorescence scanning and blot quantification	Image Studio 3.1 (LI-COR Odyssey)
image editing and cropping	Photoshop 7.0 and Illustrator 7.0 (Adobe, San Jose, USA) ImageJ (NIH, Bethesda, MD, USA)
fluorescence microscopic imaging	NIS Elements AR 3.22 (Nikon, Düsseldorf, Germany)
protein sequences, alignments and BLAST	ApE – a plasmid editor (Wayne Davis, University of Utah, USA)
statistical analysis	Excel (Microsoft Corp., Redmond, USA) SPSS (IBM, Armonk, NY, USA)

2.6 Plastic- and Glassware

Unless stated otherwise all laboratory glass- or plasticware such as pipette tips, reaction tubes and dishes were purchased from the following manufacturers:

Brand GmbH & Co KG, Wertheim, Germany
 Braun Melsungen AG, Melsungen, Germany
 Carl Roth GmbH & Co. KG, Karlsruhe, Germany
 Eppendorf AG, Hamburg, Germany
 Greiner BioOne GmbH, Frickenhausen, Germany
 Hirschmann Laborgeräte GmbH & Co KG, Eberstadt, Germany
 Nunc GmbH & Co KG, Langenselbold, Germany
 Sarstedt AG & Co, Nürnbrecht, Germany
 Schott Glas, Mainz, Germany

2.7 Equipment and Other Instruments

Table 11. Equipment and Other Instruments

Item	Name (Origin)
autoclave	Varioklav (Biomedis, Gießen, Germany)
blotter	Trans-Blot SD Semi-Dry (Bio-Rad)
centrifuge tubes (for yeast supernatant)	Centrifugal Filter Units, Amicon Ultra-15 (10 K) (Millipore)
centrifuges	<ul style="list-style-type: none"> • table centrifuge Biofuge Fresco (Heraeus, Hanau, Germany) • Biofuge stratos (Heraeus) • Minispin (Eppendorf, Hamburg, Germany) • Sigma laboratory centrifuges 4-15C (Qiagen)
cold light emitter	Macrospot 1500 (Kaiser, Buchen, Germany)
FACS cytometer	BD FACS Canto II V96100345, cell wash and cleaning solutions (BD Biosciences, Heidelberg, Germany)
filter paper	Whatman 3 MM (Whatman, Kent, UK)
fluorescence plate reader	fluorescence reader GENios (Tecan, Mainz, Germany)
hemocytometer	Neubauer Improved (Optiklabor, Friedrichsdorf, Germany), volume: 0.0025 mm ² , depth: 0.1 mm
horizontal rocker	3014 (GFL, Eppelheim, Germany)
horizontal shaker	KM-2 (Edmund Bühler AG, Hechingen, Germany)
ice machine	Scotsman AF80 (Enodis Deutschland GmbH, Herborn, Germany)
immunoblot fluorescence scanner/infrared imager	Odyssey LI-COR (LI-COR Odyssey)
incubators	<ul style="list-style-type: none"> • HeraCell (Kendro Laboratory Products GmbH, Langenselbold, Germany) • Binder (Tuttlingen, Deutschland)
liquid nitrogen tank	CBS Cryosystems 6000 series (Sanyo, Osaka, Japan)
magnetic stirrer and heat plate	Variomag Powertherm (IKA Werke GmbH & Co. KG, Staufen, Germany)
microscopes	<ul style="list-style-type: none"> • fluorescence microscope: Nikon Eclipse TE2000-S with Plan Fluor x4, x10 or x20 dry objectives, a 100 W mercury lamp and FITC (green, ex: 465-495 nm, dichroic mirror: 505 nm, em: 515-555 nm) or Texas Red (red, ex: 540-580 nm, dichroic mirror: 595 nm, em: 600-660 nm) excitation filters and a DS-5Mc cooled color digital camera (Nikon) • light microscope: Nikon Eclipse TS100 (Nikon) • stereomicroscope: Nikon SMZ645 (Nikon)
multistepper	HandyStep (Brand, Wertheim, Germany)
orbital incubator/shaker	Incubator Shaker Series 25 (New Brunswick Scientific, Edison, NJ, USA)
parafilm	(Pechiney Plastic Packaging, Menasha, WI, USA)

PD-10 columns (for protein purification from yeast)	PD-10 columns Sephadex G-25M (GE Healthcare)
pH meter	Lab850 (Schott AG)
photometer	Eppendorf Bio-Photometer (Eppendorf)
pipettes	<ul style="list-style-type: none"> • Eppendorf 2 µl, 10 µl, 100 µl, 1000 µl (Eppendorf) • Gilson 2 µl, 10 µl, 20 µl, 200 µl, 1000 µl (Gilson, Limburg an der Lahn, Germany)
pipettor	<ul style="list-style-type: none"> • Easypet (Eppendorf) • Pipetus (Hirschmann Laborgeräte, Eberstadt, Germany)
plasticizer-free reaction tubes (for virus stocks)	(Eppendorf)
power supply	Power Pac (Bio-Rad)
precision scales	TE3135-DS (Sartorius AG, Göttingen, Germany)
preparation instruments	scissors, spatulas, forceps and scalpels of different sizes (Fine Science Tools GmbH, Heidelberg, Germany)
protective gloves	Peha-soft nitrile (Hartmann, Heidenheim, Germany)
PVDF transfer membrane	Protran BA83, 0.2 µm pore size (GE Healthcare)
razor blades	single packed (Wilkinson, London, GB)
refrigerators and freezers	<ul style="list-style-type: none"> • 4 °C and -20 °C: Liebherr Comfort or Bosch economic/super (Liebherr, Biberach an der Riss, Germany; Bosch, Munich, Germany) • -80 °C: Thermo Electron HeraFreeze (Heraeus)
roller mixer	<ul style="list-style-type: none"> • SSRT9D (Stuart, Meckenheim, Germany) • RM5 (Hecht/Assistent, Sondheim, Germany)
scales	BL15000S (Sartorius)
scepter counter	Scepter Automated Cell Counter (Millipore)
SDS-PAGE running chamber and accessories	chamber, glass plates and spacers, 10-well-combs (Bio-Rad)
single-use pipettes , sterile	Costar Stripette 5 ml, 10 ml, 25 ml (Corning Life Sciences, Wiesbaden, Germany)
slice culture inserts	Millicell CM low height, pore size 0.4 µm (Millipore)
sonicator	UW/HD 2070 (Bandelin electronic GmbH & Co. KG, Berlin, Germany)
sterile benches	<ul style="list-style-type: none"> • HeraSafe laminar flow hood (Kendro Laboratories Products GmbH, Langenselbold, Germany) • 2F120-II GS (Integra Biosciences. Fernwald, Germany)
sterile filters	Steriflip (50 ml) and Steritop-GP (500 ml) 0.22 µm Express™ Membrane (Millipore)
sterilizer (for preparation tools)	Steri250 (Simon Keller AG, Burgdorf, Switzerland)
thermomixer	Eppendorf Thermomixer comfort (Eppendorf)
tissue chopper	McIlwain (Gabler, Bad Schwalbach, Germany)

UV crosslinker	CL-1000 UV crosslinker (UVP, Jena, Germany)
vacuum pump	Sonorex RK 100 H (Bandelin electronic GmbH & Co. KG, Berlin, Germany)
vortexer	Vortex-Genie 2 (Scientific Industries Inc., Bohemia, NY, USA)
water bath	<ul style="list-style-type: none">• Köttermann Labortechnik (Uetze, Germany)• GFL
water destillator	Milli-Q Q-Gard 1 (Millipore)
X-ray film developer (ECL system)	Curix 60 with rapid fixer and developer solutions (Agfa, Mortsel, Belgium)

3 Methods

3.1 Cell Culture

All cell and tissue culture works were performed under sterile laminar flow hoods to minimize the risk for contamination or biological hazard. Only sterile single-packed and/or autoclaved plastic- and glassware was used. Cells were maintained in humidified incubators at 37 °C and 5 % CO₂ in their respective media (see Materials). Cell media were changed every 2-3 days and cultures were regularly passaged to prevent overgrowing. To this aim, all medium was aspirated, the cell layer was washed with PBS (-Mg²⁺/-Ca²⁺) and detached from culture dishes with trypsin/EDTA solution. Afterwards, the appropriate amount of cells was resuspended in fresh medium to stop trypsinization. Human SH-SY5Y APP-KD cells were treated with 1.5 µg/ml puromycin to positively select for cells carrying the puromycin resistance. All lines were regularly checked for mycoplasma infection and discarded or treated according to the manufacturer's protocol with BM-Cyclin (Roche Diagnostics) if tested positive.

3.2 Determination of Cell Number and Seeding of Cells

Before cells were seeded into (multi-well) dishes for experiments, the appropriate cell number was determined with a Neubauer-type hemocytometer chamber or Merck Millipore's Scepter Automated Cell Counter. To use the Neubauer chamber, 9 µl of an appropriate cell dilution was added to the chamber assembled with a glass slide. If necessary, trypan blue (0.4 % w/v in PBS) was added before to distinguish live (transparent) from dead cells (blue) as the dye would penetrate the membranes of dead cells only. Cells were counted microscopically and the mean average of all cells counted in the four depicted squares was taken and multiplied with 10⁴ to yield the cell number per ml cell suspension. When utilizing the Scepter Automated Cell Counter, an appropriate cell suspension was diluted in PBS and precisely measured with single-use sensors yielding a detailed histogram to evaluate health and quantity of the cell suspension. Generally, cells were pelleted at 1000 rpm for 3 min and seeded into suitable cell culture dishes. Hippocampal neurons were grown on poly-D-lysine-coated plates.

3.3 Freezing and Thawing of Cells

Cryoconservation of cells allows for long-term storage of cell cultures in the vapor phase of liquid nitrogen. To prevent cell damage by ice crystals, the freezing medium contained DMSO, a potent anti-freezing agent. After pelleting, approximately 3 x 10⁶ cells were resuspended in 800 µl culture medium per aliquot. Next, 800 µl FCS supplemented with 20 % DMSO were added to each cryo

tube. Tubes were cooled down slowly in isopropanol cryo boxes (Nunc, Wiesbaden, Germany) at -80 °C for >24 h before being transferred to liquid nitrogen tanks. For thawing, cryo tubes were quickly warmed to 37 °C in a water bath. Cell suspensions were resuspended in 10 ml pre-warmed fresh medium and pelleted at 1000 rpm for 3 min to remove all remains of toxic DMSO. Afterwards, cells were transferred to culture flasks containing fresh medium and cultured for at least 5 days before initial experiments.

3.4 Preparation of Hippocampal Neurons

Hippocampal neurons are a useful tool to analyze molecular interactions and signaling mechanisms in an *ex vivo* neuronal cell model. Preparation was performed under a semi-sterile laminar flow hood using sterilized preparation instruments, surgical mask and cloths. Mice were bred, maintained and killed according to the FELASA and national Animal Experimental Ethics Committee Guidelines.

Preparations tools (Figure 6A) were disinfected in a glass beads sterilizer and rinsed with sterile ddH₂O before use. Primary hippocampal neurons were dissociated from hippocampal slices obtained from P1-3 transgenic (APP-KO or APP-ΔCT15) and non-transgenic (wildtype) littermate mouse pups (see section 2.3.3, Figure 6B). First, mice were decapitated with scissors. After disinfection of the head, the skull was opened with pointy scissors and the brain was removed (Figure 6C) and transferred to a petri dish with ice-cold dissection medium (see section 2.3.1). Using a stereomicroscope, the cerebellum was cut off and the brain hemispheres (Figure 6D) were separated with narrow spatulas. Thalamus (Figure 6D, Th) and basal ganglia were carefully removed before flipping out the “banana shaped” structure that makes up the hippocampus (Figure 6D, HC; Figure 6E) from each cortex cup. Hippocampi were transferred to an extra dish with ice-cold dissection medium for their metabolism to slow down for approximately 30 min. Immediately afterwards, the tissue was dissolved in 0.1 % PBS/trypsin in a 15 ml tube on a horizontal rocker for 20-30 min. To stop trypsinization, the same amount of HBSS (-Mg²⁺/-Ca²⁺, Gibco) supplemented with 10 % FCS was added. Cells were completely dissociated by carefully triturating the solution with fire-polished Pasteur pipettes until no visible cell clumps remained. After centrifugation at 200 *g* for 4 min the cell pellet was resuspended in full Neurobasal A medium (see section 2.3.1) and the appropriate amount of cells was seeded into poly-D-lysine coated culture plates. Cultures were kept *in vitro* at 37 °C and 5 % CO₂ for at least 7 days prior to experiments and 50 % of the cell medium in each well was replaced with fresh medium every 2-3 days.

To evaluate the ratio of glia to neuronal cells in the prepared cultures, a few samples were immunostained with antibodies directed against GFAP (glia marker), β-tubulin, NeuN or MAP2

(neuronal markers). If too many glia cells were present in a single preparation batch, cultures were treated with mitotic inhibitors (e. g. 5 μ M AraC, Calbiochem) to prevent further proliferation and overgrowing of neuronal cells. Immunostaining protocol, see section 3.11.6.

3.5 Preparation and Maintenance of Hippocampal Slice Cultures

Organotypic hippocampal slices were prepared from the same mice at age P3-6 and in the same fashion as described in section 3.4. Maintenance of slices in culture was adapted from the interface technique developed by Stoppini et al. (1991) allowing for optimal supply of oxygen and nutrients through capillary forces. After incubation in dissection buffer for 30 min, hippocampi (Figure 6E) were placed in parallel on the sterilized table of a McIlwain tissue chopper that had been supplied with a sterile razor blade (Figure 6F). After removal of excessive medium, hippocampi were cut into slices of 400 μ m thickness and carefully dissociated with a spatula (Figure 6G). Utilizing a stereomicroscope, only healthy and non-lesioned slices (Figure 6H) were selected and placed on Millipore membrane culture inserts (3-4 slices each, Figure 6I) in six-well-plates filled with 1.2 ml ice-cold pH-adjusted (pH 7.2) culture medium (cf. 2.3.1) per well. Dishes were transferred to a humidified incubator kept at 5 % CO₂ and 37 °C to warm up slowly. Culture medium was changed every 2-3 days and slices were maintained *in vitro* for 5-6 days before experiments commenced. Until then slices had shrunk from 400 μ m thickness to approximately 200 μ m.

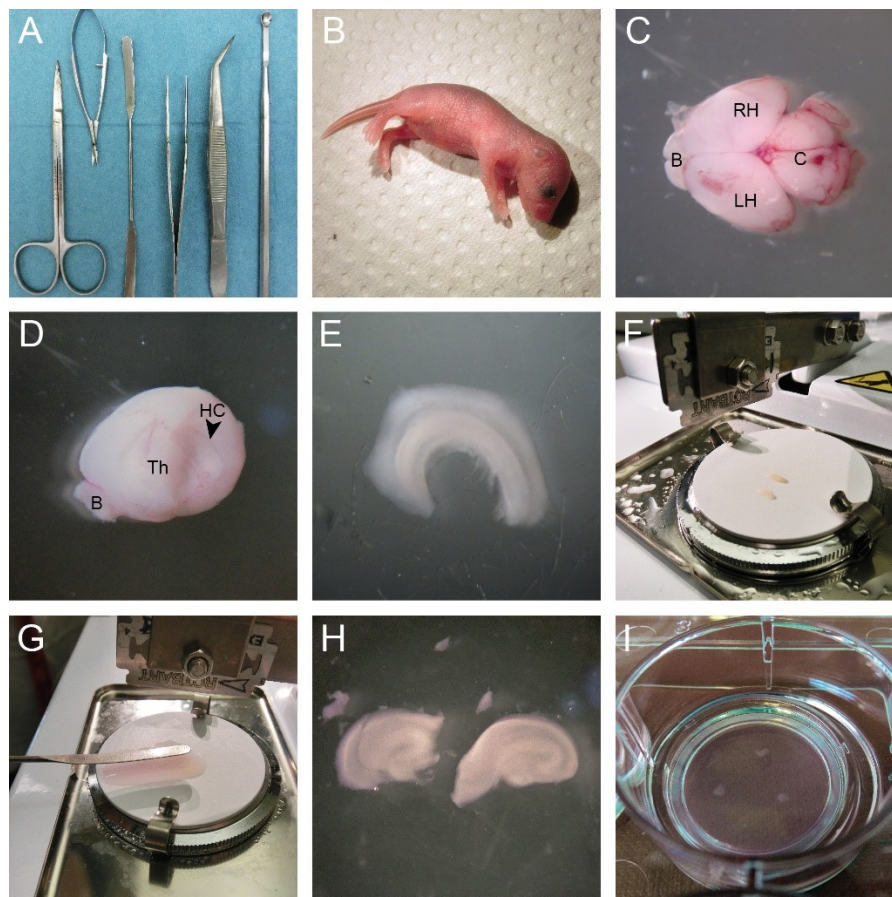


Figure 6. Preparation of hippocampal slices. (A) Suitable instruments, from left to right: pointy scissors, microsurgical scissors with curved blades, round spatula, pointy forceps, blunt/curved forceps, hollow spatula. (B) Mouse pup at age P3. (C) Freshly prepared mouse brain. B – bulbus olfactorius, RH – right hemisphere of the cortex, LH – left hemisphere of the cortex, C – cerebellum. (D) Right hemisphere with hippocampus (HC) and thalamus (Th) laid open. B – bulbus olfactorius. (E) Freshly prepared hippocampus. (F) Two hippocampi placed in parallel on sterilized chopper table. (G) Spatula used for dissociating single hippocampal slices after chopping. (H) Hippocampal slices, left: slice that will be discarded due to extensive lesions, right: slice without lesions suitable for culture. (I) Three hippocampal slices cultured on a Millipore insert (porous membrane).

3.6 Transfection of Plasmids

Transfection is the process of introducing a plasmid of choice into specific target cells. This may be performed by incubating the DNA in a cationic lipid mixture, which leads to the formation of liposomes. In turn, liposomes fuse with the cell membrane and transfer their cargo inside for expression (Behr et al., 1989). Here, transfection of MEF APP-KO and other target cells with APP mutant constructs was performed with FuGENE HD Transfection Reagent (Roche Diagnostics) according to the manufacturer's instructions and verified in a western blot.

To this end, an appropriate number of cells was seeded into 6-well-plates to achieve 60-70 % confluence on the following day. For each well to be transfected a mixture of 3 μ l Fugene transfection reagent (Roche Diagnostics) and 97 μ l serum-free DMEM was blended. After incubation for 5 min at RT, 1 μ g of the cDNA was added and the solution was again incubated at RT for 30 min. Cell culture medium was exchanged into fresh serum-containing medium. Finally, 100 μ l of the Fugene/DNA mixture were added to each well.

Given that the cDNA plasmid contained a fluorophore (such as EGFP-coupled APP constructs) transfection rates were checked under a microscope 24-48 h later. Expression of constructs was also confirmed on a protein level in western blots with cell lysates harvested 48-96 h after transfection. In most cases, transfection was performed transiently, which meant that after >96 h, levels of the desired protein rapidly declined. For this reason, experiments had to be performed in a narrow time window of 48-96 h. However, in a few cases stable transfection was achieved by treatment with the respective antibiotic, such as puromycin, G418 or hygromycin, as most constructs carry a specific resistance (protocol see 3.7).

3.7 Production of Lentiviral Particles

For stable loss-of-function experiments, lentiviral particles were generated in HEK293T cells. In comparison to transient knockdown of proteins, the shRNA will be expressed and the DNA will be integrated into the host genome after infection. The adhesive fibroblast cell line HEK293T is useful

for transformation as well as stable or transient transfection and is capable of replicating a wide variety of viruses (Ivanusic et al., 2014).

Mission® shRNA Plasmid DNA containing the pLKO.1-puro vector was purchased from Sigma-Aldrich (see section 2.4.4). Generation of lentiviral particles was performed following Addgene's pLKO.1 TRC Cloning Vector Protocol (2006) utilizing packaging (psPAX2) and enveloping (pMD2.G) plasmids (Moffat et al., 2006). In brief, 7×10^5 HEK293T cells were seeded into 6 cm tissue culture dishes in medium without antibiotics (pen/strep) to grow overnight. A master mix of 2 µg shRNA plasmid (APP, APLP1 or APLP2), 1.5 µg packaging plasmid and 0.5 µg enveloping plasmid was mixed in 57 µl OPTI-MEM medium (Gibco) in plasticizer-free polypropylene tubes. Afterwards, 6 µl FuGENE transfection reagent were diluted in 30 µl serum-free OPTI-MEM, mixed and incubated for 5 min at RT. This master mix was added to the shRNA solution, carefully blended and incubated for 30 min at RT. The DNA-FuGENE-mixture was then added dropwise to the cells and incubated for 15 h at 37 °C and 5 % CO₂. On the next day, the medium was changed into full medium containing all supplements. Another 24 h later, the supernatant, now containing the viral particles, was collected and fresh medium was added to the cells. This was repeated again after 24 h to pool virus-containing cell media from both days. Virus stocks were filtered through 0.45 µg filter units and stored in polypropylene tubes at -80 °C for long-term storage.

3.8 Generation of Stable Knockdown Cell Lines

Stable APP/APLP1/APLP2 knockdowns were obtained by infecting wt SH-SY5Y cells with lentiviral particles to stably express shRNAs directed against human APP or APLPs. Due to the shRNA's complementary sequence it builds a hair pin structure after transcription, which in turn will be processed by an RNase into siRNA. In combination with the RNA-induced silencing complex (RISC), the siRNA will bind to its specific complementary mRNA, which leads to RNA interference, the degradation of the mRNA and thereby to the silencing of the respective gene (Hamilton and Baulcombe, 1999).

Initially, the optimal antibiotic concentration was determined. As the three APP and APLP constructs carry a puromycin resistance, the best concentration had to be assessed in SH-SY5Y cells for selection of knockdown cells after transduction. To this aim, cells were plated, grown overnight and treated with different concentrations ranging from 1-6 µg/ml puromycin. Cultures were checked microscopically every day and the minimum concentration of puromycin that had resulted in complete cell death after 4-5 days was chosen for future cell selection. In SH-SY5Y cells 1.5 µg/ml puromycin were deemed optimal.

For infection with lentiviral particles, target cells were plated and grown on 6 cm dishes to approximately 70 % confluence. Cultures were changed to fresh medium containing 8 µg/ml

hexadimethrine bromide (polybrene, Sigma-Aldrich) that helps to increase efficiency of viral infection. Multiplicity of infection (MOI) rates refer to the amount of infecting viral particles per cell. The optimal MOI rate for the respective cell line was estimated by evaluating knockdown levels after infection with different virus amounts ranging from 0.1-1.0 ml. Ultimately, 0.8-1 ml of the freshly thawed virus stock was added to each plate and incubated overnight. Medium was changed into puromycin-containing fresh medium on the following day. Protein knockdown could be evaluated by western blot as early as 4 days after infection.

The resulting polyclonal culture of APP/APLP-knockdown cells was further cultured into a monoclonal cell line to achieve a defined, genetically homogenous cell population. After reaching confluence, 200 cells were seeded into 10 cm dishes to select single colonies. Under on-going puromycin selection, single colonies were picked and transferred into smaller dishes using cloning rings. As soon as one clone reached 90 % confluence, they were transferred into bigger dishes. The procedure of single cell cloning was repeated until an estimated 100 % clonal purity was achieved. Again, the protein knockdown was verified by western blot and the clones with best knockdown levels were chosen for experiments and stocked in liquid nitrogen for long-term-storage.

3.9 Cytotoxic Stress Stimuli and Treatments

Different stress stimuli were applied to induce cell death. Trophic factor and nutrient withdrawal as induced by serum and/or glucose deprivation is known to activate a stress response in neuronal and non-neuronal cells which ultimately triggers apoptosis (reviewed in Mielke and Herdegen, 2000). The ubiquitin-proteasome system (UPS) mediates protein degradation and clearance of misfolded, accumulated and otherwise damaged substrates (protein quality control). For this reason, it is thought to play a major role during brain aging and neurodegenerative diseases such as AD (Copanaki et al., 2010; Glickman and Ciechanover, 2002). Inhibition of the proteasome by MG132 (a potent reversible inhibitor of the 26S complex) therefore mimics similar stress conditions as seen during brain aging and AD leading to an accumulation of damaged proteins, which causes activation of stress pathways and cell death (Meng et al., 1999).

For trophic factor deprivation experiments, cells were seeded into appropriate culture dishes and grown overnight at 37 °C. Hippocampal neurons and organotypic hippocampal slices were cultured 5 and 7 days before experiments, respectively. Cultures were pre-treated with either 10-50 nM recombinant yeast-derived sAPP α , E1 domain, GFLD, Δ GFLD or 20 nM human IGF1 (Sigma-Aldrich) for 24 h, as indicated in Results. IGF1 was used as a negative control as it is known to activate cell survival. On the following day, cells/tissues were washed with sterile PBS and changed into media (cf. 2.3.1) lacking serum (FCS or HS) or trophic factors (B27) except for the

control group that was changed into full medium. In some cases, induction of stress-triggered cell death was enhanced by additional withdrawal of glucose. During starvation for 24-48 h, the same substances as administered during pre-treatments were applied. As indicated, the specific ADAM10 (α -secretase) inhibitor GI254023X (5 μ M; Weyer et al., 2011) was used on hippocampal slices to investigate the effect of the absence of endogenous sAPP α . To this end, 5 μ M of the substance or its carrier DMSO (used as negative control) were added to slices 24 h prior to serum/glucose deprivation. Treatment was continued for another day after serum/glucose removal. IGF1 was added every 24 h due to its short half-life. In the experiments using pertussis toxin (PTX, Enzo, Lörrach, Germany), a selective G_{i/o}-protein family inhibitor, 100 ng/ml of the toxin were applied 30 min before sAPP α /E1 was added to the medium. The PI3K inhibitor LY294002 (Enzo, 10 μ M) was used in the same manner.

For experiments using a proteasomal inhibitor as activator of cell death, pre-treatments were administered as described above. After 24 h, 5-10 μ M MG132 were added to fresh medium containing sAPP α /E1. DMSO served as negative control.

3.10 Cell Viability and Cell Death Assays

3.10.1 Caspase Assay

The caspase-dependent form of apoptosis can be measured in a caspase assay, which quantifies mainly the effector caspase-3 that stimulates apoptosis, but also caspases-6 and -7. Aminomethylcoumarin (AMC)-coupled DEVD (N-Acetyl-Asp-Glu-Val-Asp, Enzo) serves as a substrate for these caspases and is proteolytically cleaved upon addition of reaction buffer to caspase-3 containing cell lysates. The released fluorophore AMC may then be measured fluorometrically (ex/em: 360/460 nm) over a time course of 2 h in a plate reader.

Cells were seeded into 24-well-plates and treated as described in 3.9. After the respective treatment time, cells were lysed with CA lysis buffer (cf. 2.2) directly on the plate and plates were frozen at -21 °C overnight. The following steps were performed on ice to avoid enzymatic reactions after lysis. Protein contents were determined with the Bradford-based protein assay Roti-Quant (Carl Roth) according to the product instructions including CA lysis buffer as blank and bovine serum albumin [BSA] for a standard curve. Afterwards, 50 μ l of lysate were transferred to black 96-well-plates and 150 μ l reaction buffer (cf. 2.2) were added. Samples were assayed in triplicate. Plates were measured in a fluorescence plate reader at 37 °C, an extinction wavelength of 360 nm and emission at 460 nm over 2 h recording data every 10 min. Data analysis was performed plotting the absorbance as a function of substrate cleavage against time. Consequently, Caspase-3 activity was expressed as change in arbitrary fluorescence units per μ g protein and hour.

3.10.2 Bioluminescence ATP Assay

Cell viability could also be measured with a commercial kit from Promega (CellTiter-Glo Luminescence Assay) according to the manufacturer's instructions. The assay photometrically quantitates ATP levels, an indicator of metabolically active cells, in multi-well plates. Cell washing, removal of medium or multiple pipetting steps are not required, making it a highly accurate method as claimed by the manufacturer. After adding of a single reagent, a luciferase reaction produces a strong luminescent signal with a half-life of >5 h, which can be quantified in a luminescence plate reader.

Cells were grown in opaque/white 96-well-plates in 100 µl medium and treated as described in section 3.9. Controls without treatment (+FCS and -FCS) were also included on the plate. Before the assay, the plate was equilibrated to RT for ~30 min. Next, 10 ml of CellTiter-Glo Buffer and lyophilized substrate mixture were thawed to RT and mixed gently. To each well, 100 µl of the reagent were added and the plate was mixed on an orbital shaker for 2 min followed by incubation at RT for another 10 min. Luminescence was recorded with an integration time of 1 s. Background values of the respective controls (+FCS or -FCS) were subtracted from sample values.

3.10.3 PI/Hoechst Staining

Another useful method to quantify cell death is the *in vitro* staining with red-fluorescent propidium iodide (PI, Sigma-Aldrich), a DNA-intercalating agent. PI enters cells through lesioned cell membranes only, which is the case in late-apoptotic and necrotic cells. The blue-fluorescent cell stain Hoechst is cell-permeable and also binds to DNA. It is used to stain viable and dead cells alike. Stained cells can be counted manually under a fluorescence microscope or analyzed with a FACS cytometer (section 3.10.4) for quantification of cell death.

Cells were treated as described in chapter 3.9. and stained with 0.8 µg/ml PI in PBS (Sigma-Aldrich) to visualize dead cells which emit red light at 617 nm when excited at 535 nm. At the same time, cells were counter-stained with 1 µg/ml Hoechst solution (ex/em: 355/465 nm, Sigma-Aldrich). Both dyes were directly added to the cell medium and incubated at 37 °C for 10-15 min. PI positive (dead) cells were counted manually under a fluorescence microscope in three random visual fields (> 150 cells). Hoechst stained cells were counted as well to calculate the percentage of dead cells versus the total number of visualized cells.

3.10.4 FACS Analysis

Flow cytometry or fluorescence activated cell sorting (FACS) analysis allows for a highly accurate and high-throughput cell analysis. The cytometer measures single cells in suspension, their fluorescence and characteristic light scattering. Single cells are passing a laser, which is scattered depending on the size (forward scatter) and structure (side scatter) of the cell. If cells are stained

with specific fluorescent antibodies or dyes (e. g. PI, annexin), they can be sorted and quantified according to their different wavelengths. In (early) apoptotic cells, the phospholipid phosphatidylserine (PS) is flipped from the inner cell membrane (cytosolic side) to the outer surface of the cell (Verhoven et al., 1995). Cells may then be stained with the fluorescent dye annexin-V (ex/em: 488/518 nm), which specifically binds PS. As described in chapter 3.10.3, propidium iodide (ex/em: 535/617 nm) will enter late-apoptotic cells through their porous membranes. Therefore, double-stained cells may be differentiated into early-apoptotic (annexin-positive) as well as late-apoptotic and necrotic cells (annexin/PI- and PI-positive).

Cells were seeded into 24-well-plates and treated as described in section 3.9. Next, cultures were harvested by trypsinization and transferred to single-use FACS tubes. After centrifugation at 2000 x g for 4 min, cell pellets were resuspended in 50 µl HEPES buffer (see 2.2) and stained with 0.8 µg/ml PI and 0.8 µl Annexin-V-Fluos (Roche Diagnostics). Samples were incubated for 10-15 min at 37 °C in the dark before being measured in a BD FACS Canto II V96100345 cytometer (BD Biosciences). Prior to use, the cytometer was calibrated with standardized beads according to the manufacturer's instructions. As there is considerable overlap of emission spectra of PI and annexin, spectral compensation was performed and a template with optimized scatter parameters was generated for each specific cell type. For every treatment, four samples with 10000 cells each were measured. Results were analyzed with the corresponding software FACS DIVA (BD Biosciences). Cell death was calculated by subtracting the number of unstained cells from 100 % (all cells).

3.10.5 Live-dead Assay

The live-dead staining kit (PromoKine) provides a useful fluorescence-based assay to assess two recognized parameters of cell viability – intracellular esterase activity and plasma membrane integrity. The provided dyes stain live cells with calcein (green) and dead cells with ethidium-homodimer-3 (red, EthD-III). EthD-III has a higher DNA binding affinity and thus brighter fluorescence than its alternative, EthD-I, as claimed by the manufacturer. The cell-permeant calcein is enzymatically converted to intensely green fluorescent calcein by intracellular esterase activity in live cells (ex/em: 495/515 nm). EthD-III on the other hand, will only enter damaged cell membranes and emits a bright red fluorescence after binding to nucleic acids in dead cells (ex/em: 530/635 nm).

The assay was performed according to the manufacturer's protocol. Briefly, cells were seeded into 24-well-plates and treated as described in section 3.9. Serum-deprived cells were used as negative control (dead cells) and cells grown in full medium were used as positive control (live cells). After treatment, cells were washed with 500 µl PBS. A working solution of calcein/EthD-III was prepared containing 4 µM EthD-III and 2 µM calcein diluted in PBS of which 200 µl were added

to each well. The plate was incubated at RT for 30-45 min before microscopic evaluation with the respective absorbance filters.

3.11 Protein Analysis

3.11.1 Cell Harvest and Protein Concentration

Cells were harvested for protein analysis by sodium dodecyl sulfate polyacrylamide gel electrophoresis (SDS-PAGE). First, cells were washed with ice-cold PBS and lysed with freshly prepared SDS lysis buffer (see section 2.2) or lysis buffer provided in the Akt kinase assay kit supplemented with 1 mM PMSF. To further enhance cell break-up, lysates were sonicated for 7 s at a sonication power of 45 %. Lysates were either used freshly (especially for phospho-antibody probing) or frozen at -80 °C for storage.

As equal loading of samples is essential for the analysis of protein expression changes, protein concentration was quantified using the Pierce BCA Protein Assay Kit (Thermo Fisher) according to the manual. Cell lysates were tested in duplicates by diluting 1 µl lysate in 150 µl 0.9 % NaCl. Lysis buffer was used as blank and BSA was tested at increasing concentrations in a standard curve. After addition of 150 µl bicinchonine acid (BCA) copper ions quantitatively reacted with proteins and the samples changed color within 30-45 min during incubation at 37 °C. Afterwards, their relative absorbance was measured in a fluorescence plate reader at 560 nm and lysate values were compared to the BSA standard curve to calculate their protein content.

3.11.2 Akt Kinase Assay

The Akt activity assay represents a more elaborate way of measuring Akt kinase activity in the cell rather than simply staining for pAkt. Immobilized pAkt antibody is used to immunoprecipitate pAkt from cell extracts followed by an *in vitro* kinase assay using ATP and GSK3 fusion protein as a substrate. Phosphorylation of GSK3 is eventually measured by western blot using pGSK-3α/β (Ser21/9) antibody.

Cells were treated with 10-50 nM yeast-derived sAPPα/E1 or 20 nM human IGF1 under glucose and/or serum starvation for 24-48 h as described in chapter 3.9. Afterwards, lysates were prepared (see section 3.11.1) for the analysis of Akt kinase activity, which was measured *in vitro* with a commercial kit (Akt kinase assay kit, Cell Signaling) according to the manufacturer's instructions.

First, the protein content in cell lysates was determined as described in 3.11.1 and aliquots of 200 µl with equal protein content were prepared. Next, 20 µl of immobilized pAkt (Ser473) antibody bead slurry were added to each 200 µl lysate sample and incubated in an over-head roller overnight at 4 °C to immunoprecipitate endogenous levels of pAkt. After centrifugation at

13000 x g for 1 min at 4 °C, the pellet was washed twice with 500 µl 1x cell lysis buffer (from kit) and again twice with 1x kinase buffer (from kit). Next, the kinase assay was performed by resuspending the pellet in 50 µl 1x kinase buffer supplemented with 10 mM ATP and 1 µl GSK3 fusion protein as a substrate. After incubation of samples for 30 min at 30 °C, the reaction was stopped with 12 µl 5x SDS loading buffer. Samples were centrifuged, heated to 95 °C for 5 min and loaded on SDS-PAGE gels. The *in vitro* inactivation of GSK3 was visualized in a western blot detecting pGSK3 α/β (Ser 21/9, 27 kD) levels.

3.11.3 SDS-PAGE

Sodium dodecyl sulfate polyacrylamide gel electrophoresis (SDS-PAGE) is the gold standard of protein analysis. The method was originally developed by Ulrich Laemmli (Laemmli, 1970) and separates proteins according to their molecular mass in an electrical field in a Tris buffer system. Sodium dodecyl sulfate (SDS), an anionic detergent, linearizes proteins by breaking up their secondary and tertiary structure. Proteins will carry a negative charge that draws them to the anode. The Laemmli-based loading buffer containing β -mercaptoethanol that is added to the protein lysates before loading provokes an additional break-up of disulfide bonds. Two gels are poured and polymerize to form a polyacrylamide separation matrix with varying pore size, which depends on the acrylamide concentration. The upper gel layer (stacking gel) with a lower pH of 6.8 and a wide pore size due to its lower acrylamide concentration (5 %) accumulates stacks of proteins in the order of their mobility. The lower gel (separation gel) with a higher pH of 8.8 has a smaller pore size (10-12 % acrylamide) and separates the proteins. For easy estimation of protein size, a pre-stained protein ladder is loaded as reference.

Protein samples were diluted with ddH₂O and 1x loading buffer to achieve equal protein concentrations and heated at 95 °C for 4 min to enhance denaturation. Gels were prepared with APS and TEMED as a catalyst (see section 2.2) and poured between 1-1.5 mm glass spacers, run in electrophoresis running buffer (see section 2.2) at 90 V constant current for ~30 min followed by 145 V for ~2 h.

3.11.4 Western Blot

Before immunodetection, proteins were immobilized by electrotransferring (blotting) them from gels onto membranes in a semi-dry fashion.

Whatman filter papers, gels and membranes were equilibrated in transfer buffer (see section 2.2) and placed on the blotter. Gel and membrane were positioned between filter papers to face the blotter's anode. Bubbles were removed carefully and the transfer was run at 17 V constant current for 36 min. Afterwards, membranes were rinsed with 0.1 % TBS/Tween-20 and processed for immunodetection (section 3.11.5). To check transfer quality and equal protein loading, gels

were stained with Coomassie-based Imperial Protein Stain (Thermo Scientific) overnight and destained with ddH₂O until bands became visible.

3.11.5 Immunodetection

To enhance the specific binding of primary antibodies to their respective antigens, unspecific background binding was blocked by incubating membranes in 5 % milk powder diluted in 0.1 % TBS/Tween-20 for 1 h at RT on a roller. After three washing steps in 0.1 % TBS/Tween-20 for 5 min each, membranes were incubated in primary antibody solution (antibody + 5 % BSA in TBS/Tween-20) rolling at 4 °C overnight. Antibodies and dilutions are listed in section 2.4.2. After washing, membranes were incubated in the corresponding infrared-labeled or horseradish peroxidase (HRP)-coupled secondary antibodies diluted in 5 % BSA (in 0.1 % TBS/Tween-20) on a roller for 60 min. After repeated washing, detection of infrared-labelled antibodies was performed with the LI-COR Odyssey Infrared Imager. For HRP-coupled antibody detection, blots were incubated in enhanced chemoluminescence (ECL) reagents luminol and hydrogen peroxide (Western Lightning, PerkinElmer, Hamburg, Germany) at equal amounts for 1 min, drained and developed on X-ray film with the Curix 60 film developer (Agfa, Mortsel, Belgium). Films were developed at different exposure times until optimal band intensities were achieved.

3.11.6 Immunostaining/In-cell-western

The in-cell-western is an immunocytochemical alternative to regular western blots, that is performed in multi-well-plates and makes use of target-specific primary and infrared-labeled secondary antibodies. The antibodies detect proteins in fixed cells, and the fluorescent signal from each well is quantified in a fluorescence plate reader or with an infrared imaging scanner. The method provides a very accurate, sensitive and quantifiable analysis of signaling pathways, especially because proteins are detected in their cellular context. It is possible to detect two different targets at 700 and 800 nm, respectively, and increase quantification accuracy if normalizing against pan-protein or housekeeping genes/DNA strains, especially if cell numbers vary from well to well.

The assay was adapted from the recommended protocols by LI-COR Odyssey (Bad Homburg, Germany). First, cells were seeded into 24- or 96-well-plates to grow overnight. The optimal cell density was found to be 50-70 %. Experiments were performed in duplicates and for each treatment, two wells were planned as blanks. After treatments according to section 3.9, cell media were aspirated, and cells were fixed with fixing solution (see section 2.2) for 20 min at RT. For permeabilization, cultures were washed five times with 0.1 % Triton X-100 (in PBS) for 5 min shaking on a rotator. Cells were blocked with LI-COR Odyssey Blocking Buffer or 5 % goat/horse serum in PBS for 1.5 h at RT with moderate shaking. Two primary antibodies, pGSK3 β (Ser 9, rabbit, 1:200) and GSK3 β (mouse, 1:200), were diluted in blocking buffer and added to the cells

to incubate overnight at 4 °C with no shaking. Blanks were treated with blocking buffer only. On the following day, wells were washed five times with 0.1 % Tween-20/PBS for 5 min each with gentle shaking. Fluorescently-labeled secondary antibodies, 680RD anti-rabbit (1:800) and 800CW anti-mouse (1:800), were diluted in blocking buffer and 0.5 % Tween-20. Cells were incubated in the mixture for 60 min with gentle shaking at RT protected from light. After extensive washing, 20 µl PBS were added to each well and the plate was scanned on the Odyssey Imager Scanner. Both red and green infrared channels (700 and 800 nm) were scanned at a focus offset of 3 mm. Infrared signals were measured as arbitrary fluorescence units (pixel count) within a predefined shape and calculated from trim signals. The trimmed signal is the sum of the individual pixel intensity values for a shape minus the product of the average intensity values of the pixels in the background and the total number of pixels enclosed by the shape. Both the highest and lowest 5 % count is excluded from the calculation (see also LI-COR Image Studio Manual, Vers. 2.0.8). Values were normalized to background staining to correct for non-specific binding and pGSK3 β /GSK3 β value ratios were calculated manually.

3.11.7 On-cell-western

The on-cell-western is performed in a very similar fashion to in-cell-westerns described in 3.11.6. However, in contrast to intracellular and/or total protein detection, this assay enables quantitative detection of cell surface protein expression only. It also allows monitoring receptor internalization. As opposed to in-cell-western assays, in on-cell-westerns unpermeabilized cells are stained with antibodies directed against extracellular proteins, thus only cell surface antigens are detected. In this work, on-cell-westerns were performed to evaluate cell surface expression of APP C-terminal domain mutants after transfection relative to wt APP expression levels.

The assay was adapted from similar cell surface assay techniques described in Gonzalez-Gronow et al. (2007) and Delisle et al. (2009). MEF wt and APP-KO cells were grown in 24-well-plates to reach ~70 % confluence. After 24 h MEF APP-KO cells were transfected with the respective APP mutants, Δ PEER and Δ NPTY. Transfection was performed in duplicates. 48 h post transfection, primary antibody directed against the N-terminus of APP (22C11, 1:180) was directly added into the medium of live, unpermeabilized mutant and control cultures for 4 h at 37 °C. For each construct, two background controls were planned that were not treated with primary antibodies. After incubation, wells were washed with PBS three times and incubated in secondary antibody (IRDye goat anti-mouse from LI-COR; 1:1000) diluted in fresh medium for 1 h at 37 °C. Following three more washing steps, plates were dried and scanned using the LI-COR Odyssey Infrared Imager at a focus offset of 3 mm and both 700 and 800 nm channels. Fluorescence signals were quantified using Image Studio 3.1 software (LI-COR Odyssey) as described in 3.11.6. Values were normalized to background staining to correct for non-specific

binding. After fluorescence analysis, cells were lysed and used for conventional western blots to correlate data with total protein levels.

3.12 Purification of sAPP α /E1 from Yeast

Recombinant sAPP α and APP-E1 domain were purified from the yeast *Pichia pastoris*. Yeast stocks and isolation protocols were developed by Frederik Baumkötter, Dep. of Human Biology and Human Genetics, University of Kaiserslautern, Germany (Kins lab). The coding sequences of sAPP α (aa 18-611 of APP695) and E1 (aa 18-189 of APP695) had been cloned in frame as his-tagged fusions in a pBLHIS-SX derived expression vector and expressed in *Pichia pastoris* GS115 cells (Figure 7). The α mating factor signal sequence allows for secretion of the proteins into the culture medium of the stably transformed yeast strain upon addition of methanol. The asparagine residue at position 467 of APP695 (glycosylation site) was replaced with serine by site directed mutagenesis. Therefore, the ectodomains were secreted non-glycosylated into the yeast medium to be able to correlate data with crystallography studies in the Kins lab. As both APP ectodomains were secreted carrying a polyhistidin tag they could be isolated by affinity resins (sepharose beads) containing bound bivalent nickel ions that bind histidine with micromolar affinity. As opposed to other sources such as commercially available sAPP α derived from *Escherichia coli* (*E. coli*), yeast-derived APP ectodomains carry eukaryotic modifications. Furthermore, the purification process yields particularly pure proteins, as confirmed by crystallography experiments in the Kaiserslautern lab. For more detail see paragraph 4.1.

Yeast was cultured in buffered glycerol complex medium (BMGY, cf. 2.3.1) by adding ~ 100 μ l of yeast glycerol stock into 1000 ml medium and incubating at 30 °C for 2 days at 250-300 rpm in sterile baffled flasks in a horizontal shaker. To guarantee ideal oxygen ventilation and sterile atmosphere, porous filter membranes were used to seal the flasks. On the third day, the turbid solution was centrifuged at 1500 x *g* for 5 min, medium was aspirated and replaced with 200 ml buffered methanol complex medium (BMMY, cf. 2.3.1) as methanol induces the protein secretion. Cultures were incubated overnight at 30 °C and 250-300 rpm.

For the purification from 200 ml yeast medium, ~10 ml Ni-sepharose beads were equilibrated in 1x LEW buffer (cf. 2.2) by washing and centrifuging at 1500 rpm three times for 5 min. Yeast culture was centrifuged at 1500 rpm for 10 min at 4 °C, sterile-filtered and distributed to 50 ml falcon tubes. For his-tagged protein binding to nickel, 2-2.5 ml equilibrated Ni-beads were added to each 50 ml falcon and incubated overnight in an over-head roller at 4 °C. On the following day, solutions were pelleted at 1500 rpm for 5 min at 4 °C and pellets were washed with ice-cold 1x LEW buffer three times to remove unspecifically bound proteins.

Elution of sAPP α /E1 was performed with 1x LEW buffer containing 500 nm imidazole (cf. 2.2) for 30 min in an over-head roller at 4 °C. Fresh elution buffer was added to the beads two more times until all three fractions were combined and concentrated by ultracentrifugation. To this aim, 50 ml centricon tubes (Centrifugal Filter Units Amicon Ultra-15, Millipore) were equilibrated with 1x LEW buffer by centrifugation at 3000 rpm. Afterwards, the eluted protein solution was centrifuged at 3000 rpm and 4 °C for ~40 min or until the end volume in each tube was less than 2.5 ml.

To remove imidazole from the protein solution, PD10 desalting columns (GE Healthcare) were equilibrated with PBS or Tris/HCl buffer (cf. 2.2, pH 8.0). Desalting was performed according to the product's manual. The final volume of the protein solution was approximately 3.5 ml. Samples were supplemented with 10 % sterile glycerol, shock-frozen in liquid nitrogen and stored at -80 °C. Protein concentration was determined with a photometer (Nanodrop) by assuming a MW of 110000 Da for sAPP α (with the extinction coefficient $\epsilon = 59735$) and 20000 Da for APP-E1. Protein amount and purity was also assessed in Coomassie gels in comparison to BSA standards.

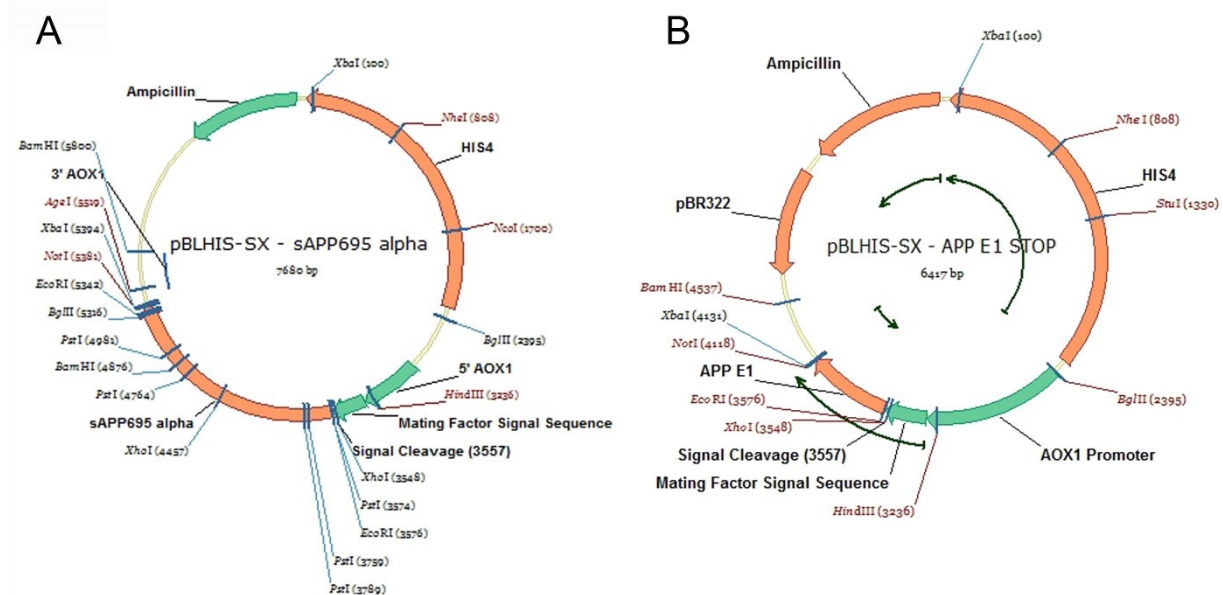


Figure 7. Vector maps of APP ectodomain constructs expressed in *Pichia pastoris*. The coding sequences of sAPP α (A) and E1 (B) were cloned in frame as his-tagged fusions in a pBLHIS-SX derived expression vector and stably transformed in *Pichia pastoris* GS115 cells. Note the α mating factor signal sequence fused to the AOX1 promoter that allows for secretion of the proteins into the yeast medium.

3.13 Plasmid Preparation from *E. coli*

3.13.1 Transformation of *E. coli*

For high-yield plasmid DNA replication, the competent *E. coli* strain DH5 α was utilized. Agar plates were poured with autoclaved LB agar (cf. 2.3.1) and 100 μ g/ml ampicillin into 10 cm dishes and

left to cool down overnight. An aliquot with 90 µl competent DH5α bacteria was quickly thawed on ice. Approximately 8 µl or 5 ng of plasmid DNA were added, mixed and incubated on ice for 30 min. Next, the mixture was heat-shocked at 42 °C for 45-60 s followed by incubation on ice for 2 min. Afterwards, 900 µl of LB medium (cf. 2.3.1) without antibiotics were added and incubated at 37 °C and 225 rpm for 45 min. The solution was centrifuged at 5000 rpm for 2 min and the pellet was resuspended in 50 µl LB medium. The resulting culture was then spread on LB agar plates containing the appropriate antibiotic (100 µg/ml ampicillin) with a sterile spatula. Successfully transformed *E. coli* colonies grew overnight at 37 °C.

3.13.2 Bacterial Culture and Plasmid Preparation

After 16-24 h, a single colony was picked and transferred to 5 ml LB medium containing 100 µg/ml ampicillin. The culture incubated at 37 °C and sufficient oxygen ventilation for 10-12 h at 300 rpm in a horizontal shaker. Depending on the density of bacteria, the culture was transferred to 200-400 ml LB medium containing ampicillin and incubated overnight in baffled flasks at 37 °C and 300 rpm. Cultures were centrifuged at 6000 rpm for 20 min on the following day and isolation of plasmid DNA from the cell pellets was performed with the Endo-free Plasmid Maxi Kit from Qiagen according to the manufacturer's instructions.

3.13.3 Determination of DNA Concentration

The resulting plasmid DNA pellet from section 3.13.2 was resuspended in ~100-150 µl TE buffer and measured in a UV photometer or fluorophotometer (Nanodrop) at 280 nm wavelength to determine DNA content. Purity was considered optimal with an absorbance ratio of 260/280 nm between 1.8 and 2.

3.14 Microscopy

For fluorescence pictures of hippocampal neurons, cells were grown on poly-D-lysine coated glass slips in 24-well-plates, fixed and stained as described in chapter 3.11.6. Neuronal markers β-3-tubulin, NeuN or MAP2, the glia marker GFAP and Hoechst were used to dye cells (see also 2.4.2). After incubation with the respective Cy2- (green) or Cy3- (red) coupled secondary antibody, glass slips were washed with 0.1 % Tween-20/PBS and mounted on objectives with mounting medium (Permafluor, Immunotech, Krefeld, Germany), sealed with transparent nail polish and examined microscopically. For manual PI counting experiments, samples were prepared as described in section 3.10.3 and analyzed in triplicate by counting >150 cells in three random visual fields.

Fluorescence microscopy was performed with the Nikon Eclipse TE2000-S with Plan Fluor x4, x10 or x20 dry objectives, a 100 W mercury lamp and FITC (green, ex: 465-495 nm, dichroic mirror: 505 nm, em: 515-555 nm) or Texas Red (red, ex: 540-580 nm, dichroic mirror: 595 nm,

em: 600-660 nm) excitation filters. Images were acquired with a DS-5Mc cooled color digital camera (Nikon, Düsseldorf, Germany) and NIS Elements AR (version 3.22) software from Nikon. Image adjustments such as changes of contrast and brightness were applied equally across the entire image.

3.15 Data Analysis

Unless stated otherwise, results are expressed as mean \pm standard error of the mean (SEM) and normalized to control treatments where depicted. All experiments were repeated at least twice yielding similar results. Statistical analyses were performed using SPSS (IBM, Armonk, NY, USA) with one-way ANOVA followed by Tukey HSD post hoc comparisons. P-values < 0.05 were considered as statistically significant. Western blot quantifications were performed with LI-COR Odyssey Image Studio 3.1 software to guarantee analysis of fluorescence signals in a linear range. Values were normalized to serum/glucose treated controls (dashed line in figures). Band intensities in blots with whole cell lysates were normalized to their corresponding loading control (GAPDH) and plotted as pGSK3 β /GAPDH ratios. All graphs show means of $n = 3$ blot quantifications \pm SEM.

4 Results

4.1 Yeast-derived sAPP α and E1 Have Neuroprotective Properties

As outlined before, several studies showed that sAPP α has neuroprotective and neurotrophic properties under various stress conditions (Kögel et al., 2012b). Previous data from the Kögel lab demonstrating this neuroprotective action were gained with secreted APP from different sources (Copanaki et al., 2010; Eckert et al., 2011). Purified COS7 cell-derived recombinant sAPP α as well as secreted sAPP α from conditioned supernatants obtained from HEK cells overexpressing wt APP were applied to reproduce these results. In initial experiments, sAPP α from both sources was confirmed to possess neuroprotective properties in different cell death and viability assays (data not shown). However, these sources of sAPP α , especially commercially available products derived from *E. coli* exhibited unfavorable limitations such as inefficient production yield, inadequate purity or even inconsistent reproducibility. In consequence, a newly designed technique was established for this work to produce recombinant yeast-derived sAPP α and APP-E1 with reliable performance. The yeast *Pichia pastoris* as an expression system allows for the production of high yields of recombinant and highly purified APP cleavage products. Furthermore, as opposed to some other sources like *E. coli*-derived sAPP α mentioned above, yeast-derived APP ectodomains carry eukaryotic modifications (Cereghino and Cregg, 2000) and the purification process yields particularly pure proteins as confirmed by crystallography experiments (Stefan Kins lab, Kaiserslautern). However, as mentioned in Methods the asparagine residue at position 467 of APP695 (glycosylation site) was replaced with serine by site directed mutagenesis. In consequence, the APP ectodomains were secreted non-glycosylated into the yeast medium. This was done to be able to correlate data with structural results from crystallographic approaches performed in the Kins lab (Kaiserslautern), because especially N-glycosylation hampers crystal formation (Davis and Crispin, 2011). While N-linked glycosylation of sAPP α should be completely abolished by the introduced mutation, there is a possibility that the secreted protein was O-glycosylated by *Pichia*, which differs from higher eukaryotes.

As seen in Figure 8, sAPP α was usually detected as a double band at an apparent molecular weight of ~75 and 110 kD on Coomassie stained gels and western blots (not shown). It is to assume that these bands correspond to the mature, O-glycosylated form (~110 kD) and the immature non-glycosylated form (~75 kD), respectively. A similar observation was made by members of the Kins lab in Kaiserslautern (unpublished data) and Eggert and colleagues (2004). Alternatively, other bands on the gel and seemingly unspecific bindings of anti-N-terminal APP Ab 22C11 could also correspond to APP fragments of different sizes that were cleaved by (still unknown) secretases present in yeast. In this context, several reports show APP cleavage by the

metalloprotease meprin, which releases APP fragments of various sizes (Bien et al., 2012). *Pichia* itself does not secrete any proteins into its medium (Cereghino and Cregg, 2000), which rules out other protein fragments. In contrast to sAPP α , the purified APP-E1 domain does not exhibit any glycosylation sites, which is in line with the finding that no additional bands appear on Coomassie gels (Figure 8, right). Purity and concentration of each protein batch were always confirmed spectrometrically, on Coomassie gels (Figure 8) and in crystallography experiments (Kins lab, Kaiserslautern) before experiments.

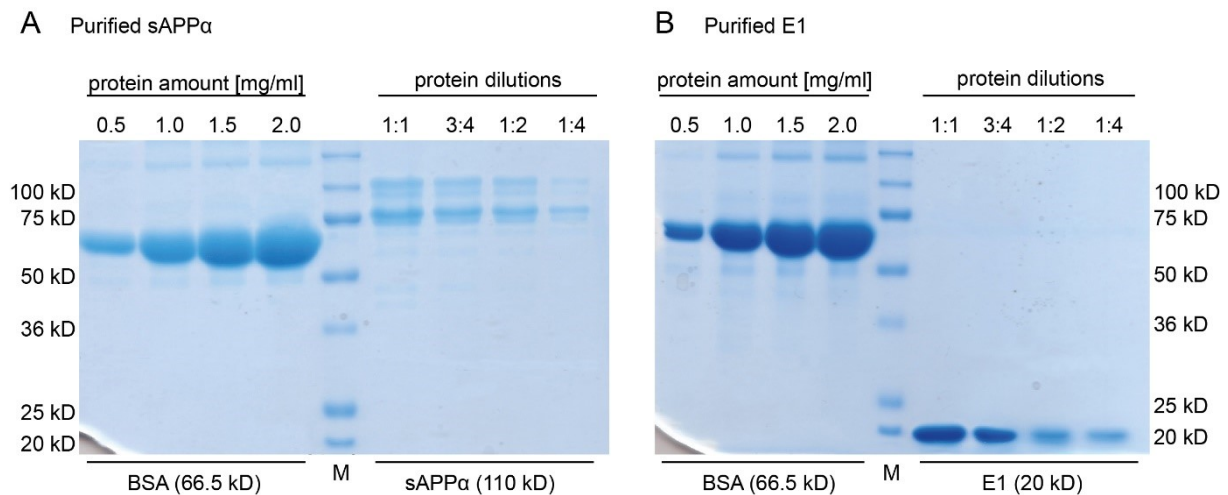


Figure 8. Purified APP cleavage products from *Pichia pastoris*. Recombinant sAPP α or APP-E1 domain were purified from yeast supernatants and tested on Coomassie gels at different dilutions to evaluate purity and concentration. Bovine serum albumin (BSA, 66.5 kD) was loaded at concentrations ranging from 0.5-2 mg/ml to compare band intensities to the loaded APP domains. Recombinant sAPP α (**A**) usually appeared as a double band around 110 kD and 75 kD, which may be due to differences in glycosylation status or processing by APP secretases. Purified E1 (**B**) appeared highly pure and ran as a single band at ~20 kD. M = pre-stained protein marker, kD = kilo daltons.

Ultimately, *Pichia*-derived sAPP α showed the same biological and neuroprotective activity as (fully glycosylated) sAPP α purified from mammalian COS7 cells (Copanaki et al., 2010). Moreover, non-glycosylated E1 was also able to induce neuroprotection rendering any yeast-mediated glycosylation irrelevant for this effect. Single yeast purification batches were tested for their biological and neuroprotective activity in several control experiments with different cell lines subjected to proteasomal stress or serum deprivation. Additionally, possible protective activities caused by components of the yeast medium still present in purified APP fragments were ruled out by testing heat-inactivated fractions (see also Figure 18).

Protection by sAPP α obtained from conditioned supernatants from APP overexpressing HEK cells was already established in PC12 cells subjected to proteasomal stress in the Kögel lab (Copanaki et al., 2010; Eckert et al., 2011). Figure 9 confirms these findings depicting caspase activity assays performed with human SH-SY5Y cells subjected to proteasomal stress (1 μ m

MG132, 24 h) and simultaneous treatment with sAPP α /E1. Both recombinant peptides significantly antagonize apoptotic cell death (as measured by effector caspase activity) induced by proteasome inhibition.

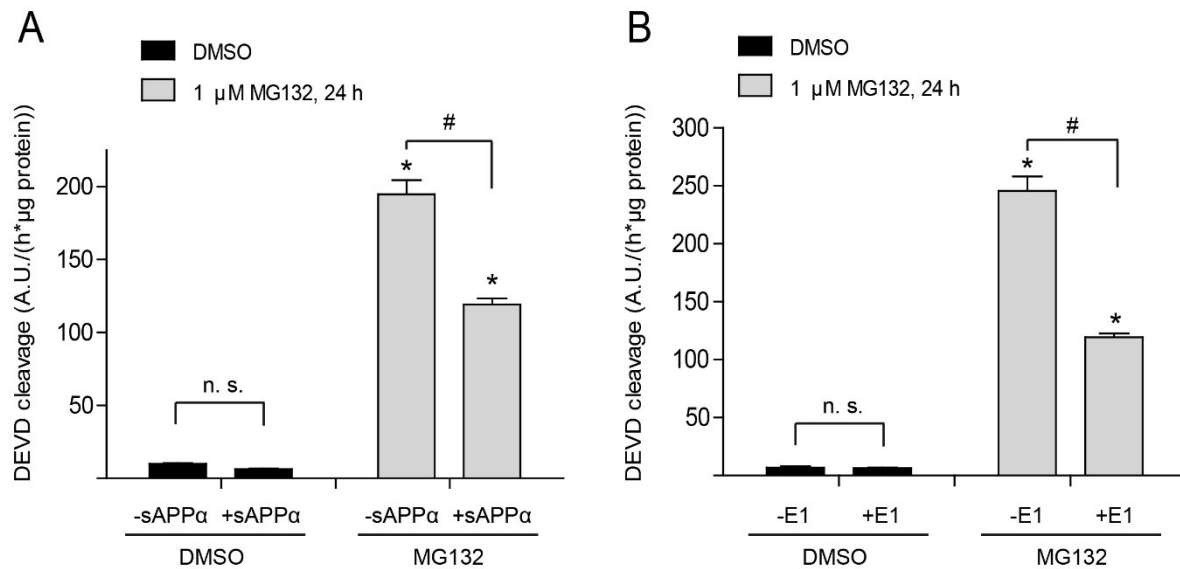


Figure 9. Yeast-derived sAPP α and APP-E1 antagonize stress-triggered cell death. SH-SY5Y cells were pre-treated with 25 nM recombinant yeast-purified sAPP α (A) or E1 domain (B) for 24 h before treatment with 1 μM MG132 or volume-equivalent DMSO as negative control for 24 h to induce proteasomal stress. Both APP cleavage products reduced caspase activity significantly as measured by DEVD cleavage. Data are means from four independent cultures \pm SEM. Statistical significance: *, p < 0.05 compared to controls (DMSO); #, p < 0.05 compared to MG132 treated cultures in the absence of sAPP α /E1; n. s. = not significant.

4.2 Recombinant sAPP α and E1 Promote Cell Survival Only in the Presence of Holo-APP

It is established that APP and APLPs are integral transmembrane proteins that can form homo- and heterodimers and may function as membrane-bound signaling receptors and/or adhesion molecules (Baumkotter et al., 2012; Soba et al., 2005). In this context, it was suggested that sAPP α may act as a competitive inhibitor disrupting membrane-bound APP homodimers, thereby inducing cell survival (Gralle et al., 2009). Yet, the cellular receptor linking sAPP α to downstream survival signaling remains unidentified.

To investigate the potential contribution of endogenous APP for sAPP α -induced neuroprotection, a stable lentiviral knockdown of APP was performed in human SH-SY5Y cells (cf. 3.8). For experiments, both polyclonal APP-KD cultures and isolated single clones were used. Different batches of polyclonal cultures were screened for the most apparent APP knockdown efficiencies in western blots. Additionally, single cell clones were isolated from polyclonal cultures

utilizing cloning rings (cf. 3.8) and the resulting single clone cell line was again subjected to western blots to confirm depletion of APP (Figure 10).

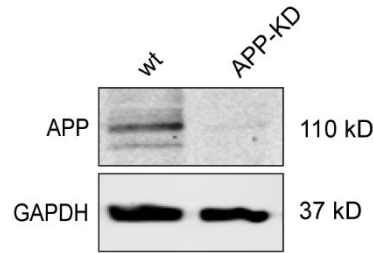


Figure 10. Knockdown of APP in SH-SY5Y cells. Stable knockdown of APP was obtained by infecting wt human neuroblastoma SH-SY5Y cells with lentiviral particles to express shRNAs directed against human APP. The blot shows a representative single cell clone with efficient suppression of APP expression utilized in this work.

Again, cell death was induced by proteasomal stress (10 μ M MG132, 24 h) as described in chapter 3.9 and was analyzed by FACS analysis of PI/Annexin-V stained cells. As depicted in Figure 11, increasing amounts of recombinant yeast-derived sAPP α antagonized cytotoxic stress significantly, but only in holo-APP expressing SH-SY5Y cells and not in APP-KD cells.

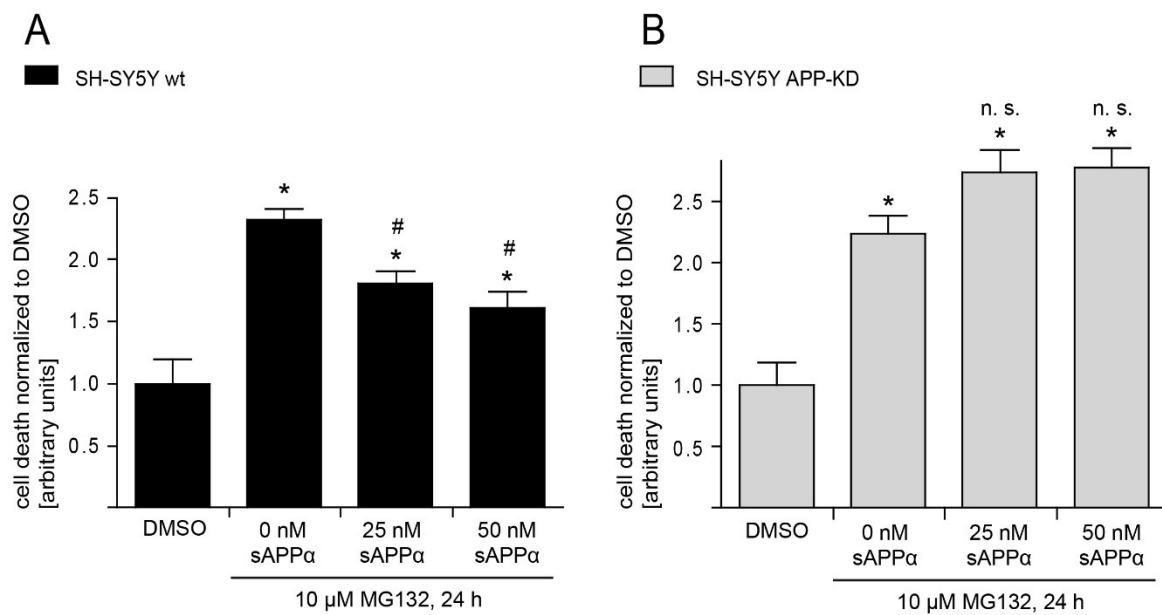


Figure 11. Recombinant sAPP α antagonizes cell death induced by proteasomal stress only in the presence of endogenous APP. Human wt (A) or APP-KD (B) SH-SY5Y cells were pre-treated with increasing doses of yeast-derived sAPP α for 24 h followed by treatment with 10 μ M MG132 or volume-equivalent DMSO as negative control for 24 h to induce proteasomal stress. PI/annexin positive cells were measured in a FACS cytometer and normalized to DMSO-treated controls. Data are means from four independent cultures \pm S.E.M. Statistical significance: *, $p < 0.05$ compared to controls (DMSO); #, $p < 0.05$ compared to MG132 treated cultures in the absence of sAPP α ; n. s. = not significant.

It is now widely acknowledged that loss of trophic factors and a diminished glucose metabolism may contribute to brain aging and the pathogenesis of AD (Furst et al., 2012; Hyman and Yuan, 2012; Pluta et al., 2013). Therefore, also trophic factor withdrawal as induced by serum (-FCS/-HS) and/or glucose deprivation (-FCS/-HS/-Gluc) was used to induce cell death in the utilized cell and tissue cultures.

Cell viability/death was analyzed in various assays, e. g. by quantification of ATP levels (Figure 12A+B) and microscopical evaluation of propidium iodide (PI) uptake (Figure 12C+D). Human IGF1 served as a positive control for activation of cell survival. As already seen in experiments with proteasomal stress, recombinant sAPP α and even its subdomain APP-E1 alone exerted protective effects in wt human SH-SY5Y subjected to trophic factor withdrawal (Figure 12A+C; A was performed by Master student Gaye Tanriöver). Again, both sAPP α and E1 failed to antagonize stress-triggered cell death in cells lacking endogenous APP, suggesting that the expression of holo-APP is necessary for the neuroprotective functions of exogenously applied APP ectodomains (Figure 12B+D).

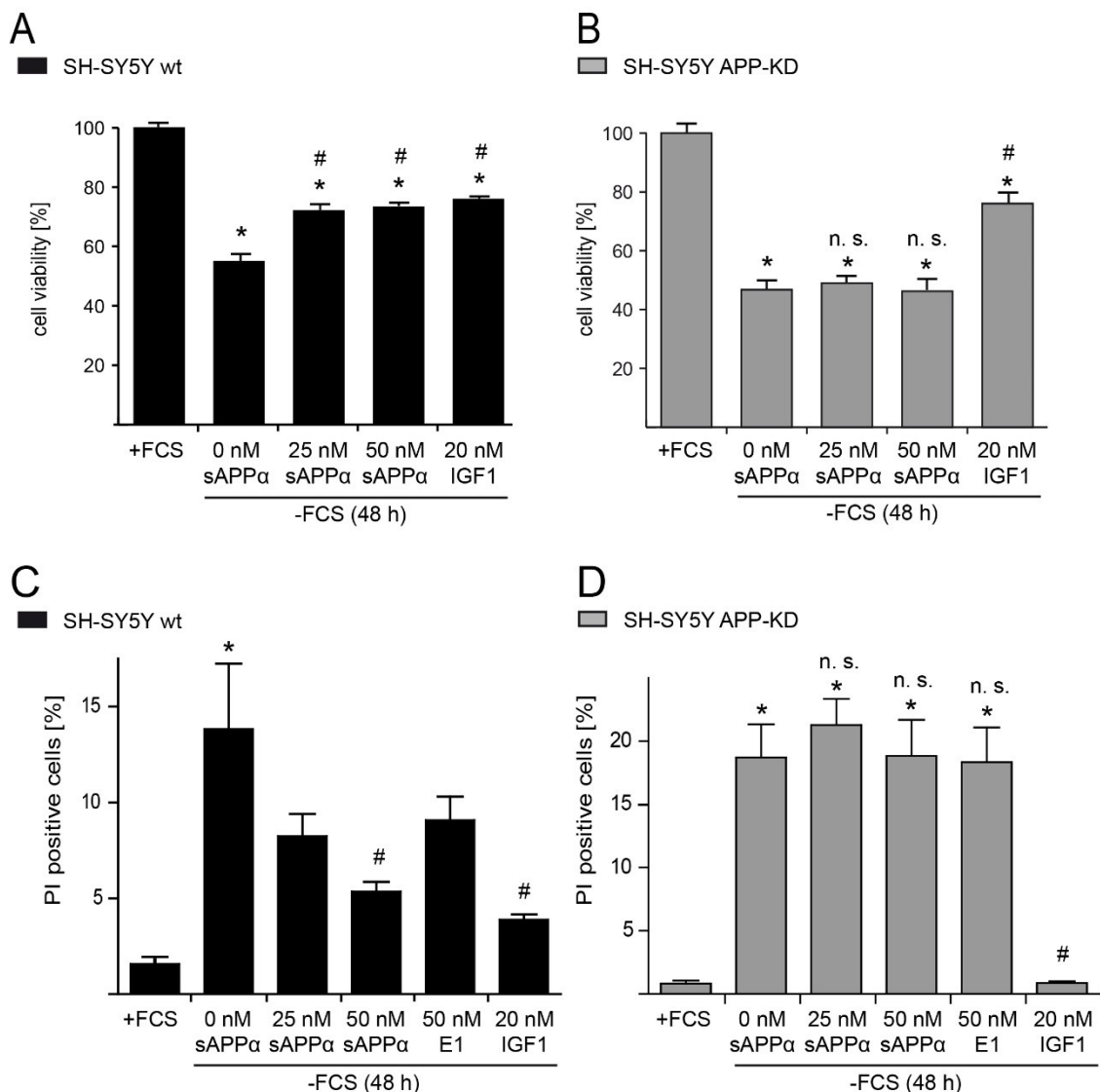


Figure 12. Cell survival promoted by recombinant sAPP α /E1 depends on the presence of endogenous holo-APP. Human wt or APP-KD SH-SY5Y neuroblastoma cells were cultured in full medium (+FCS) or in medium lacking trophic factors (-FCS) for 48 h to induce cell death (**A and B**). In parallel, cells were treated with increasing doses of sAPP α purified from yeast or IGF1 as positive control activating cell survival. Cell viability was measured photometrically in a bioluminescence assay by quantifying ATP levels. (A) was performed by Gaye Tanriöver. Serum-deprived SH-SY5Y wt (**C**) or APP-KD (**D**) cells were treated with increasing doses of sAPP α or recombinant E1. Cell death was assessed microscopically by counting PI stained (dead) cells in 3 random visual fields (> 150 cells) and calculated as a percentage of the total number of visualized cells (Hoechst staining). Data are means from 4-10 cultures \pm SEM. Statistical significance: *, $p < 0.05$ compared to controls (+FCS); #, $p < 0.05$ compared to serum withdrawal in the absence of sAPP α /E1/IGF1; n. s. = not significant.

The requirement of endogenous APP for the protective effects of sAPP α was also confirmed in a non-neuronal cell model - mouse embryonic fibroblasts (MEFs) derived from APP-KO mice. MEFs were subjected to trophic factor/glucose withdrawal employing a calcein/ethidium homodimer-3-based assay (Figure 13A) and FACS analysis of PI uptake (Figure 13B). Green calcein dye is only incorporated by viable cells whereas red ethidium homodimer-3 stains dead cells only.

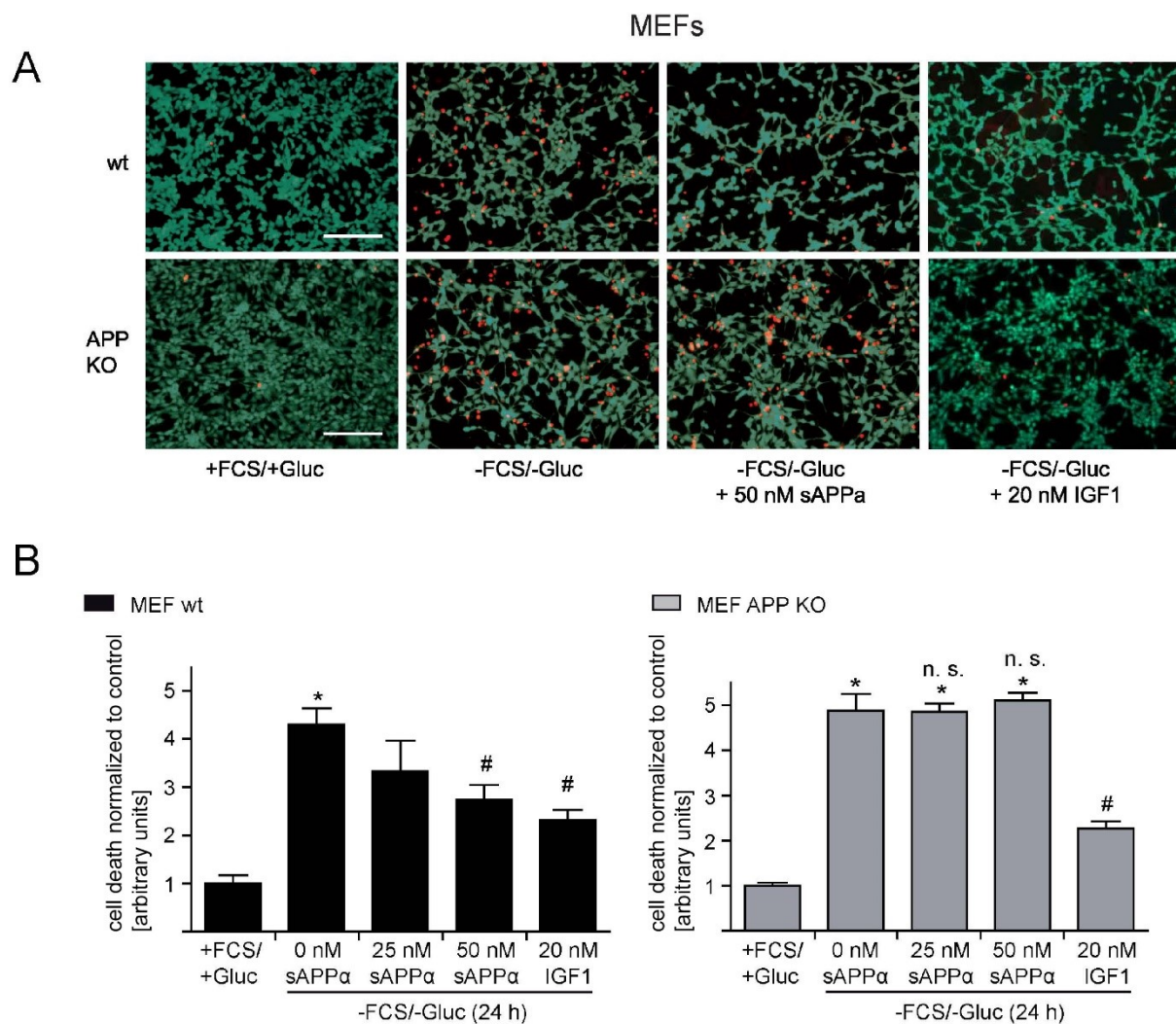


Figure 13. sAPP α -mediated suppression of cell death depends on the presence of holo-APP. (A) MEFs prepared from wt or APP-KO mice were cultured in glucose- and serum-free medium for 24 h to induce cell

death. In parallel, cells were treated with yeast-derived sAPP α or IGF1 as a positive control. Cells were stained with green-fluorescent calcein to indicate intracellular esterase activity. This dye exclusively stains live cells (green). Cultures were simultaneously stained with red-fluorescent ethidium homodimer-3 to visualize loss of plasma membrane integrity (red, dead cells). Scale bar: 500 μ m. **(B)** MEFs obtained from wt (left panel) or APP-KO mice (right panel) were cultured in glucose- and serum-free medium for 24 h and treated with the indicated amounts of sAPP α or IGF. PI-stained cells were analyzed with a FACS cytometer and the extent of cell death was normalized to control cells (+FCS/+Gluc). Data are means from four cultures \pm SEM. Statistical significance: *, $p < 0.05$ compared to controls (+FCS/+Gluc); #, $p < 0.05$ compared to serum/glucose withdrawal in the absence of sAPP α /IGF1; n. s. = not significant.

The neuroprotective function of sAPP α was further substantiated in tissue models when analyzing organotypic hippocampal slice cultures prepared from wt or APP-KO mice (Figure 14). As outlined in the introduction the hippocampus is one of the most sensitive brain regions that is affected earlier than most other regions in neurological disorders such as (global) ischemia or AD (Fjell et al., 2014). There was a pronounced increase of PI positive cells in serum/glucose-deprived hippocampal slice cultures which was significantly reduced in the presence of recombinant sAPP α . Importantly, this effect was only visible in wt slices (Figure 14, upper panel) and not in slices from APP-KO animals (Figure 14, lower panel). Quantification of PI stained slices by manual counting confirmed these results (Figure 16).

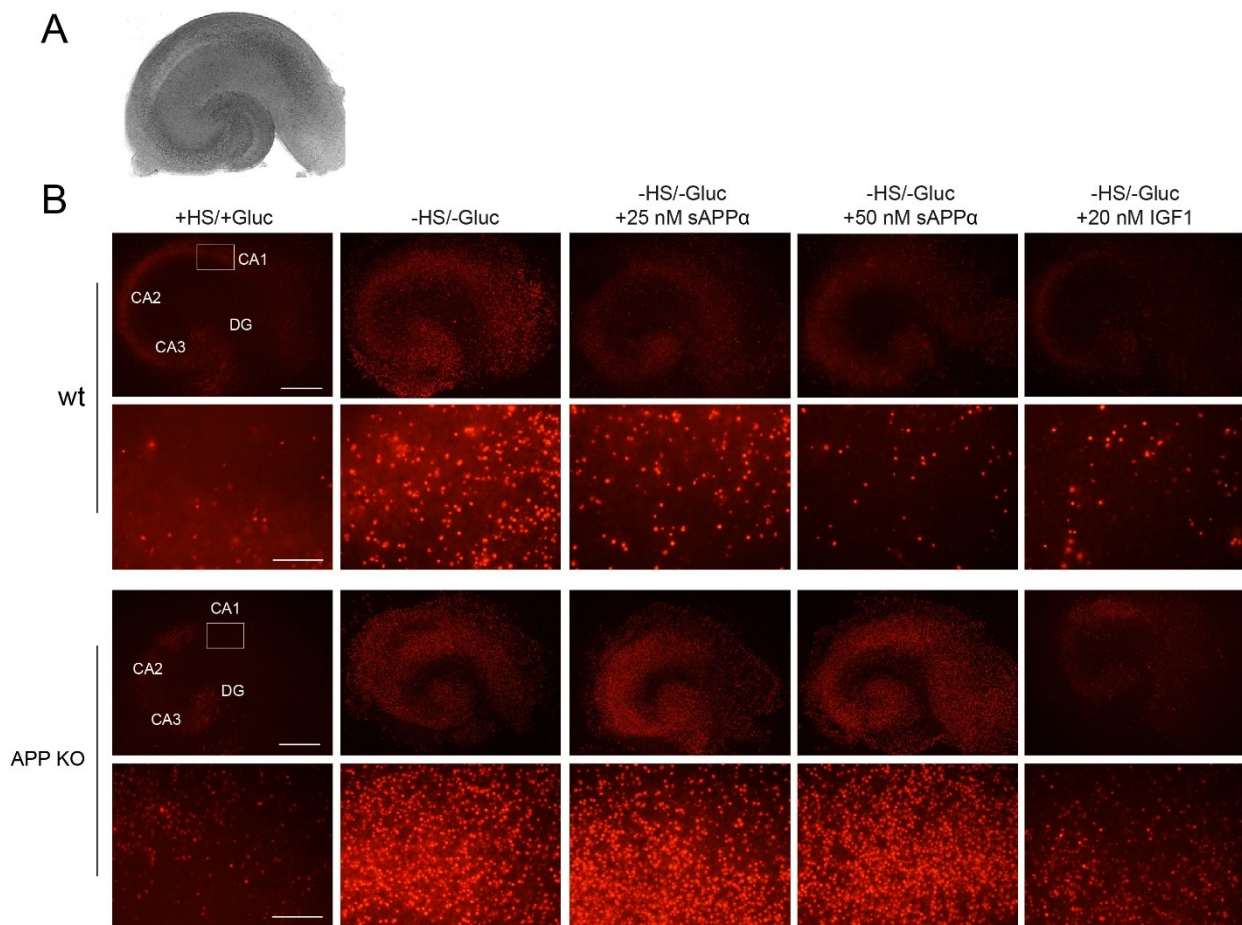


Figure 14. sAPP α induces neuroprotection in organotypic hippocampal slices from wt mice but not from APP deficient mice. (A) Representative light microscopic image of a hippocampal slice culture. **(B)**

Organotypic hippocampal slices dissected from wt or APP-deficient (APP-KO) mice were cultured on permeable membrane inserts in full medium containing 5 % (v/v) horse serum and glucose. After 5 days *in vitro* (DIV), slices were transferred into serum- and glucose-free neurobasal A medium with 25/50 nM sAPP α or 20 nM IGF1 for 24 h. Cell death was visualized microscopically by PI staining. Major hippocampal areas cornu ammonis 1-3 (CA1-3) and dentate gyrus (DG) are designated. Whole slices are shown in the upper panel of each genotype; magnification: $\times 4$, scale bar: 400 μm . A representative area in the CA1 region of the hippocampus (as depicted in the white square) is shown in the lower panel of each genotype; magnification: $\times 20$, scale bar: 100 μm .

When applying the specific ADAM10 (α -secretase) inhibitor GI254023X (5 μM) to serum/glucose-deprived slices, PI counts were significantly increased in comparison to DMSO (carrier)-treated controls (Figure 15+16C). This observation suggests that the absence of endogenous sAPP α exacerbates cell death under these conditions. This cell death-enhancing effect of GI254023X could be completely rescued by applying exogenous sAPP α , thereby supporting the notion that recombinant sAPP α can substitute endogenous sAPP α function (Figure 15, far right).

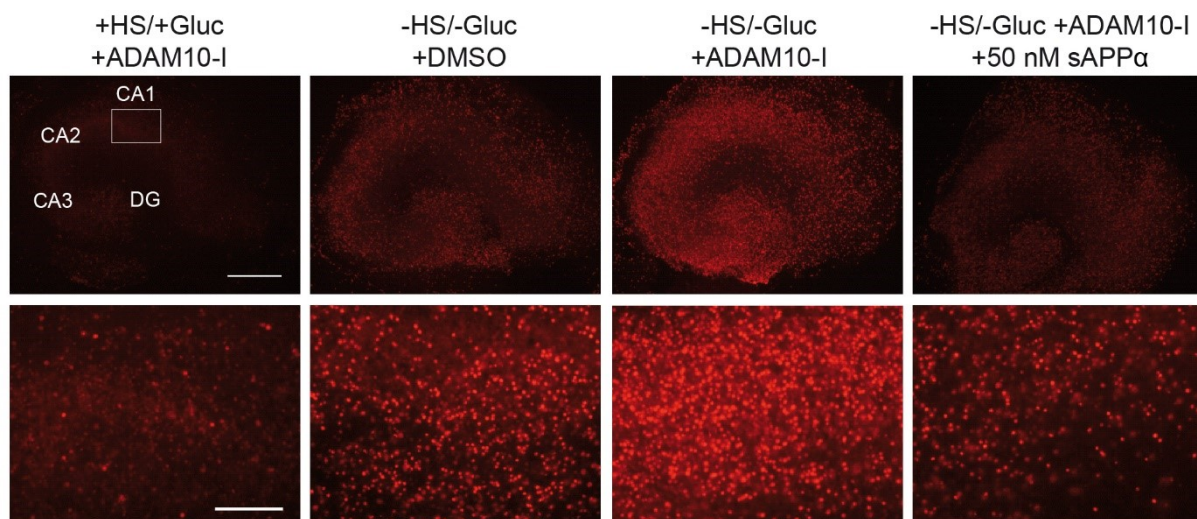


Figure 15. The absence of endogenous sAPP α exacerbates cell death in hippocampal slices under nutrient deprivation, which is rescued by exogenously applied recombinant sAPP α . Organotypic hippocampal slices from wt mice subjected to serum/glucose deprivation in the presence of the ADAM10 (α -secretase) inhibitor GI254023X show increased PI staining in comparison to serum/glucose-deprived controls. This effect is reversed by recombinant sAPP α (50 nM, far right). Whole slices are shown in the upper panel; magnification: $\times 4$; scale bar: 400 μm . A representative area in the CA1 region of the hippocampus (as depicted in the white square) is shown in the lower panel; magnification: $\times 20$; scale bar: 100 μm .

The major histologically distinct subregions of the hippocampus include the cornu ammonis regions 1-4 (CA1-4), of which CA1 and CA3 are connected by pyramidal neurons of the Shaffer collaterals. Axons of the CA1 region project into the subiculum and the entorhinal cortex (EC). Furthermore, the CA1 region has been a major area of focus investigating the molecular dynamics

of synaptic plasticity underlying learning and memory (long-term-potential) due to its simple neural network anatomy (Bliss and Collingridge, 1993). As it was shown to be one of the most vulnerable brain regions following traumatic brain injury, ischemia and epilepsy, it is also the preferred area for cell death studies (Hatch et al., 2014; Lee et al., 2014).

To quantify cell death induced by serum/glucose deprivation in hippocampal slices, PI stained cells were analyzed microscopically in a pre-defined area in the CA1 region of the hippocampus as depicted in Figure 14+15 (white squares and lower panels). Numbers were normalized to cells counted in serum/glucose-treated controls and confirmed sAPP α -dependent neuroprotection in wt versus APP-KO cultures (Figure 16A+B) as well as significantly increased cell death in ADAM10 inhibitor (GI254023X) treated slices that was compensated by application of recombinant sAPP α (Figure 16C).

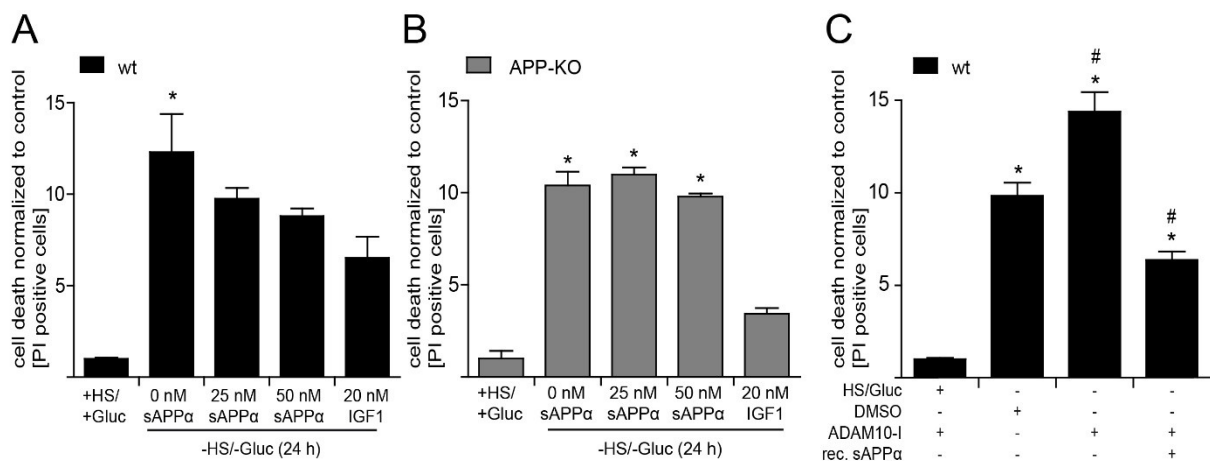
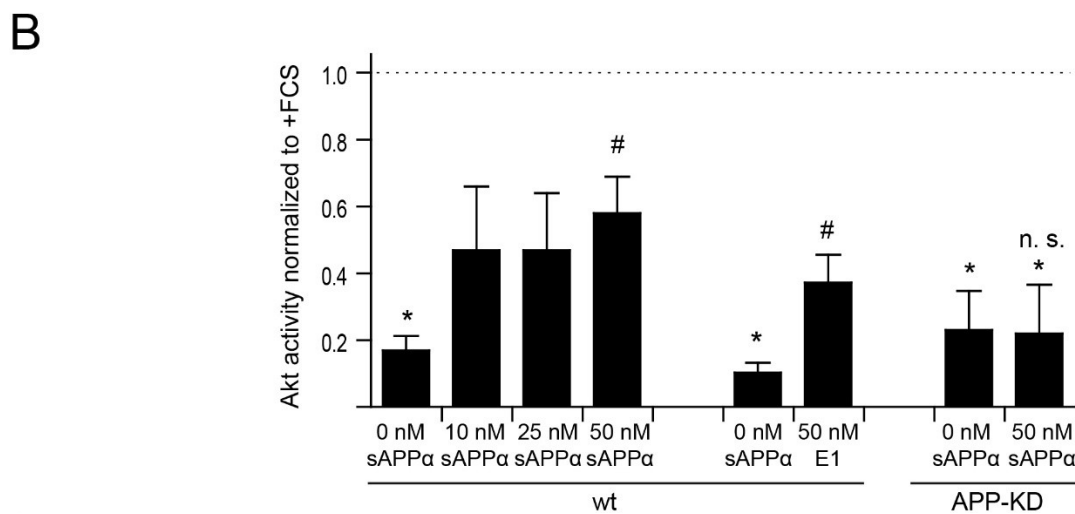
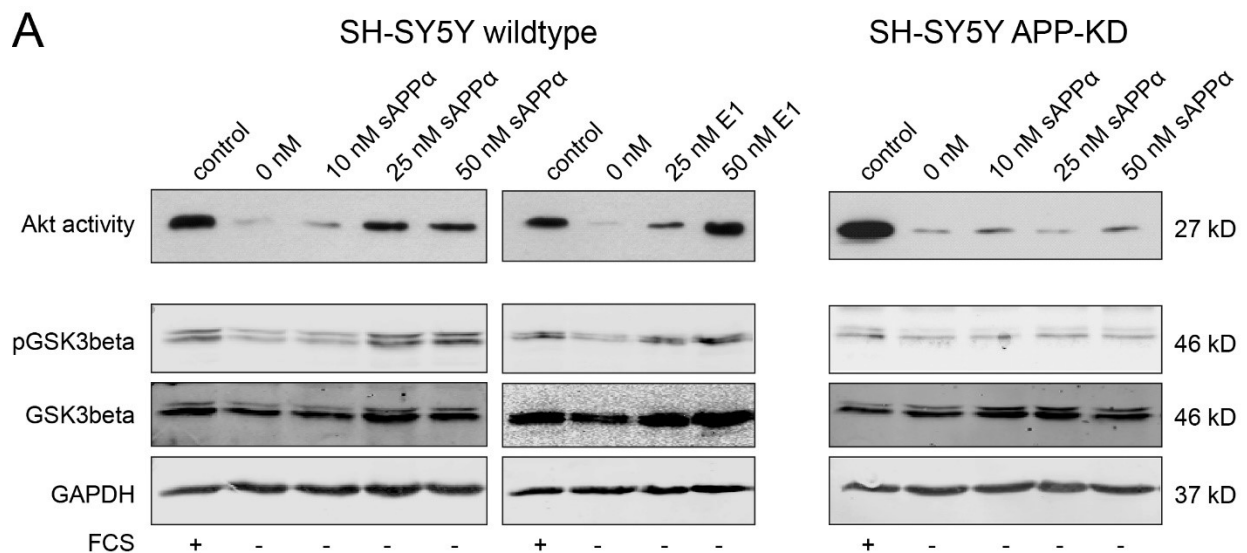


Figure 16. sAPP α reduces neuronal death in the CA1 region of the hippocampus from wt mice but not in an APP-deficient background, while ADAM10 inhibitor treatment further exacerbates cell death. Extent of cell death in wt (A) versus APP-KO (B) slices and slices treated with ADAM10 inhibitor (C) was calculated by counting PI-stained (dead) cells in a specified area in the CA1 region and subsequent normalization to serum-/glucose-treated controls. Data are means from four to six cultures \pm SEM. Statistical significance: *, $p < 0.05$ compared to controls (+HS/+Gluc); #, $p < 0.05$ compared to serum/glucose withdrawal + DMSO or ADAM10 inhibitor in the absence of sAPP α .

4.3 Recombinant sAPP α and APP-E1 Domain Activate the PI3K/Akt Survival Pathway, which Requires the Expression of Holo-APP

As outlined in the introduction, earlier studies (Copanaki et al., 2010; Eckert et al., 2011; Jimenez et al., 2011) suggested that the PI3K/Akt survival signaling pathway is involved in mediating the protective function of sAPP α , i. a. by making use of synthetic inhibitors. However, the putatively involved cellular receptors and the exact molecular mechanisms underlying sAPP α -dependent neuroprotective signaling have remained elusive.

To further analyze the activation of neuroprotective PI3K/Akt signaling by sAPP α *in vitro* Akt kinase assays were performed with serum-deprived SH-SY5Y neuroblastoma cells. As seen in Figure 17, trophic factor withdrawal led to a pronounced decrease of Akt activity and levels of Ser 9 phosphorylated GSK3 β , which was prevented by increasing doses of yeast-derived sAPP α and the APP-E1 domain alone. Again, this was only observed in APP-expressing wt cells (Figure 17A, left panel) while SH-SY5Y APP-KD cells did not show any sAPP α -mediated Akt activation (Figure 17A, right panel). Quantification of blots (n = 3) verified significant induction of Akt activity (Figure 17B) and enhanced pGSK3 β (Ser 9) levels (Figure 17C) for sAPP α and recombinant E1 in wt cells. In APP-KD cells, only treatment with IGF1 induced phosphorylation of GSK3 β to a significant degree. These results were also confirmed quantitatively in an in-cell-western approach (data not shown).



C

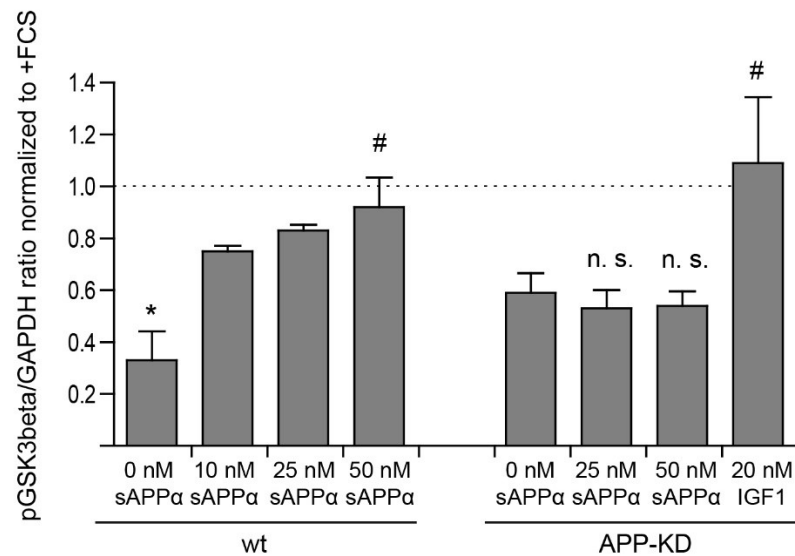


Figure 17. Recombinant sAPPα/E1 activate the PI3K/Akt survival pathway which requires the expression of holo-APP. SH-SY5Y wt or APP-KD cells **(A)** were stressed by serum deprivation (-FCS) for 48 h with concomitant treatment with sAPPα or APP-E1 domain. Akt kinase activity was measured *in vitro* as outlined in section 3.11.2. Note that treatment of cells with increasing amounts of either sAPPα or APP-E1 increased kinase activity in a dose dependent manner. Akt kinase activation was associated with inactivation of GSK3 as measured by western blot with antibodies specific for phosphorylated pGSK3α/β (Ser 21/9, 27 kD). Additionally, whole cell lysates were tested with anti-pGSK3β and anti-GSK3β. GAPDH was used as a loading control. Quantification of Akt kinase activity **(B)** and pGSK3β/GAPDH ratios in whole-cell lysates **(C)**. Data are means ± SEM from three blots. Values were normalized to serum-treated controls (dashed line). Conventional blots were normalized to their corresponding loading control (GAPDH) and plotted as pGSK3β/GAPDH ratios. Statistical significance: *, $p < 0.05$ compared to controls (+FCS); #, $p < 0.05$ compared to serum withdrawal in the absence of sAPPα/E1/IGF1; n. s. = not significant.

Possible protective activities caused by components of the yeast medium still present in purified APP fragments were ruled out by testing heat-inactivated fractions, which did not show any rescuing effects (Figure 18). Heat-inactivation at 95 °C and above is a convenient method to denature proteins and thereby inactivate enzymatic reactions. However, heat-induced protein inactivation may be decreased by known protein stabilizers such as glycerol, which was also added to sAPPα/E1 working solutions (Pinto et al., 1991). This may explain the slight but nonsignificant activation of Akt activity still visible in Figure 18.

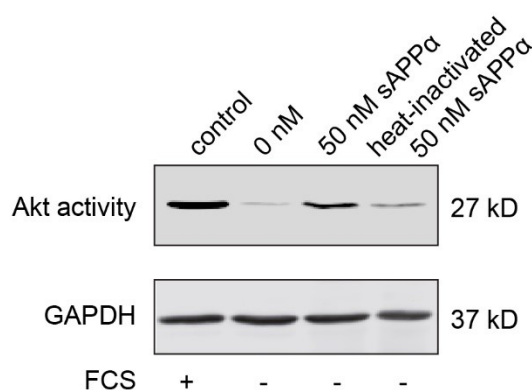
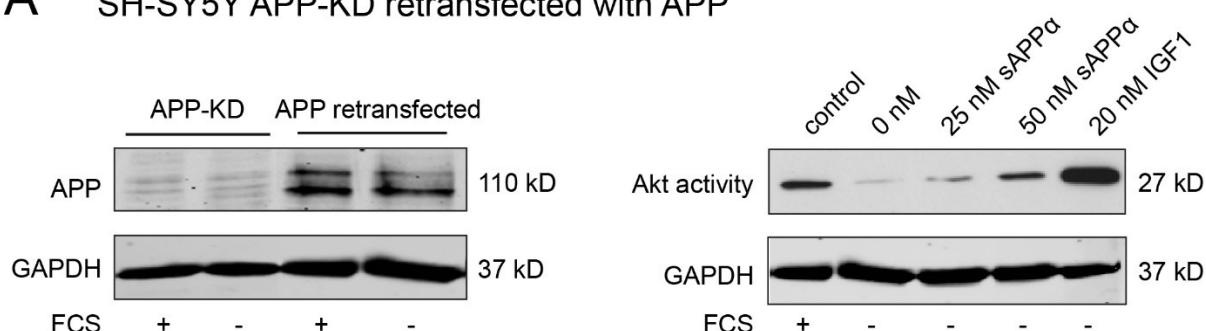


Figure 18. Heat-inactivated recombinant yeast-derived sAPPα does not activate the PI3K/Akt survival pathway. Increased Akt kinase activity in serum-deprived SH-SY5Y wt cells treated with 50 nM sAPPα. The heat-inactivated protein did not show activation of PI3K/Akt signaling. In parallel to Akt immunoprecipitation, the same whole cell lysates were tested with anti-GAPDH as a loading control.

As APP was shown to be indispensable for the protective effect of sAPPα, a rescue experiment with a holo-APP construct was performed to verify this observation. In contrast to APP-KD, that did not show increased Akt activity induced by sAPPα/E1, retransfection of APP-KD cells with a holo-APP construct restored the sAPPα-dependent Akt activation (Figure 19A). To further substantiate these findings hippocampal neurons derived from wt and APP-KO mice were also used. As seen in APP-depleted neuroblastoma cells before, APP-KO neurons failed to show sAPPα-dependent Akt activation, that could, however, be readily detected in wt neurons (Figure 19B). Again, these observations could be verified by quantification of western blot data both for Akt activity from immunoprecipitation and pGSK3β levels in the corresponding whole cell lysates (Figure 19C). Similar results were also acquired in hippocampal neurons obtained from rats (data not shown).

A SH-SY5Y APP-KD retransfected with APP



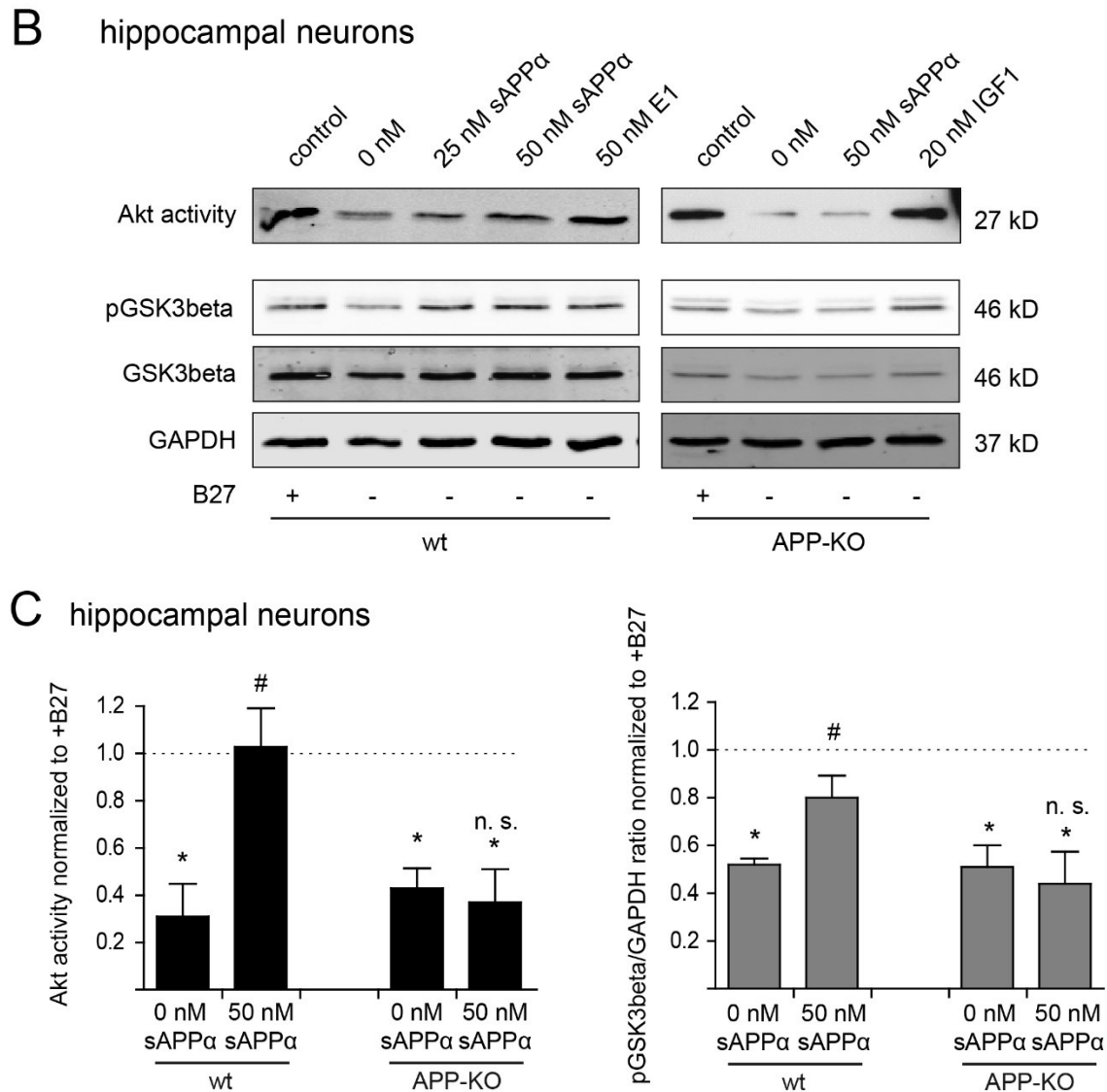


Figure 19. sAPPα/E1-mediated PI3K/Akt signaling is restored in APP-retransfected APP-KD cells and can be detected in hippocampal neurons from wt mice. SH-SY5Y APP-KD cells (**A, left**) were retransfected with a holo-APP construct. (**A, right**) Cells were stressed by serum deprivation (-FCS) for 48 h and treated with sAPPα or IGF1 as positive control for Akt activity. PI3K/Akt signaling was restored by sAPPα treatment in cells retransfected with holo-APP in contrast to APP-KD cells. (**B**) sAPPα-induced Akt activity and pGSK3β levels in serum-deprived hippocampal neurons obtained from wt or APP-KO mice. GAPDH was used as a loading control. (**C**) Quantification of Akt kinase activity (left panel) and pGSK3β/GAPDH ratios in whole-cell lysates (right panel). Data are means ± SEM from three blots. Statistical significance: *, $p < 0.05$ compared to controls (+B27); #, $p < 0.05$ compared to serum withdrawal in the absence of sAPPα/E1/IGF1; n. s. = not significant.

4.4 PI3K/Akt Survival Signaling Mediated by sAPPα and APP-E1 Domain Does Not Depend on the Expression of APLP1 or APLP2

The APP family members and mammalian paralogues APLP1 and APLP2 share most of their sequence and are cleaved in a fashion very similar to APP (Endres and Fahrenholz, 2012; Hög et al., 2011). It is therefore expected that they also share physiological functions.

To test the possible redundancy of endogenous APP with APLP1 and APLP2 in regulating neuroprotection, stable knockdowns of APLP1 and APLP2 were established in SH-SY5Y cells (Figure 20).

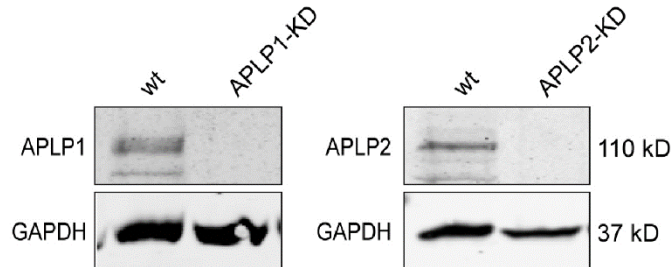
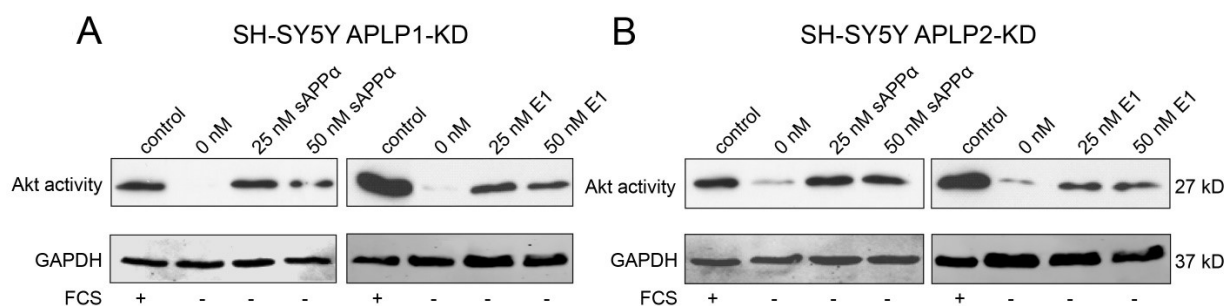


Figure 20. Knockdown of APP family members APLP1 and APLP2. Stable knockdown of APLP1 and APLP2 was obtained by infecting wt human neuroblastoma SH-SY5Y cells with lentiviral particles to stably express shRNAs directed against the respective APP family member. The blots show a representative knockdown level that was achieved in single cell clones isolated from polyclonal cultures. Cell lines were established by Andreas Zymny (Zymny, 2010).

The role of both APLPs in sAPP α -mediated neuroprotection and PI3K/Akt survival signaling was analyzed in an *in vitro* Akt kinase assay as described in chapter 3.11.2. Interestingly, both Akt pathway activity (Figure 21A+B) and cell survival as measured by PI staining (Figure 21C+D; performed by Master student Gaye Tanriöver) were mediated by sAPP α and the E1 domain independent of APLP1 or APLP2 expression. Therefore, none of the two APP homologues seem to share the specific physiological function of APP in this context, even though it is established that APP and APLPs can form homo- and heterodimers (Baumkotter et al., 2012; Soba et al., 2005).



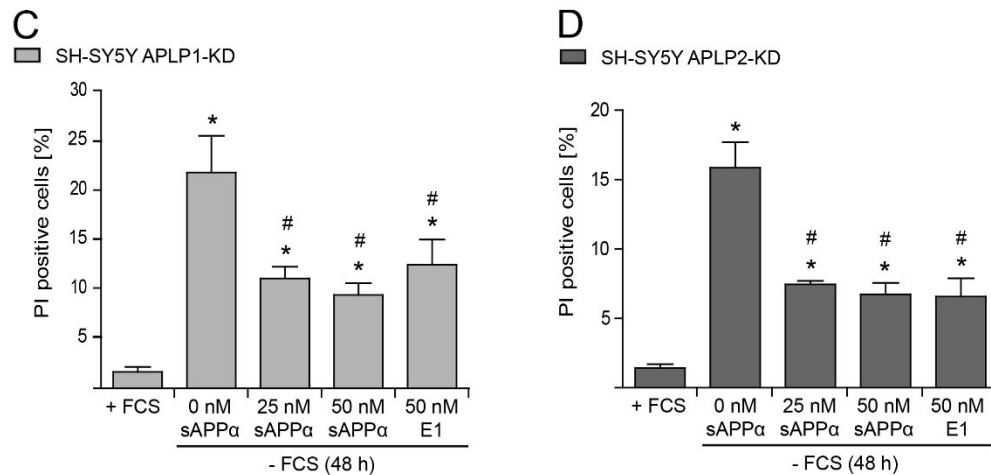


Figure 21. Akt pathway activation and neuroprotection by sAPPα/E1 does not require APLP1 or APLP2. Akt pathway activation by sAPPα and APP-E1 domain in APLP1 (A) and APLP2 KD (B) cells under serum deprivation. (C+D) Cell death was assessed microscopically by counting PI stained (dead) cells in 3 random visual fields (> 150 cells) and calculated as a percentage of the total number of visualized cells (Hoechst staining). Counting performed by Master student Gaye Tanriöver. Data are means from 4 cultures ± SEM. Statistical significance: *, $p < 0.05$ compared to controls (+FCS); #, $p < 0.05$ compared to serum withdrawal in the absence of sAPPα/E1.

4.5 The AICD but Not the YENPTY Motif Is Required for sAPPα-mediated Akt Signaling

The APP intracellular domain (AICD) links APP to diverse intracellular signaling pathways. Given the finding that APP expression is essential for the neuroprotective function of sAPPα, the possible role of the AICD in sAPPα-mediated survival signaling was scrutinized in subsequent experiments. In particular the YENPTY motif in its C-terminal tail is known to be the binding site for the majority of AICD interaction partners (Aydin et al., 2012; Merdes et al., 2004).

To investigate the contribution of the AICD and possibly pinpoint the exact motif responsible for sAPPα-dependent survival signaling, several AICD deletion constructs were utilized and expressed in an APP-KO background. Figure 22 shows a schematic illustration of the APP constructs that were used in this work.

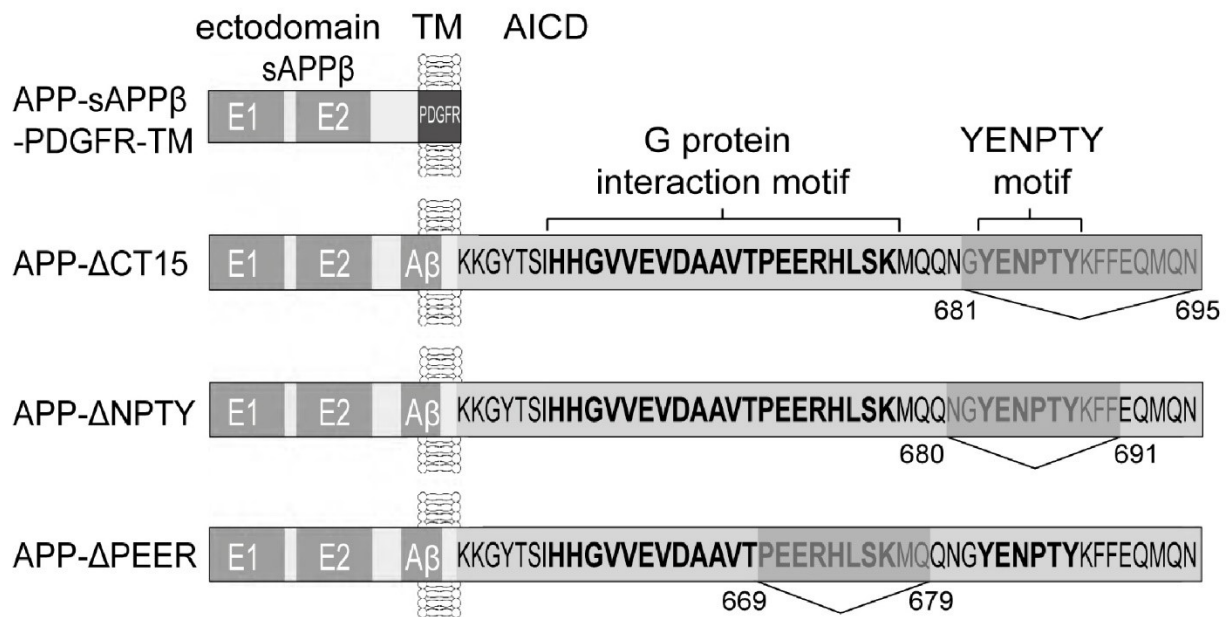


Figure 22. Mutant APP constructs utilized in this work. The upper lentiviral construct (APP-sAPPβ-PDGFR-TM) encodes for the extracellular part of APP including E1 and E2 domains, but lacks the AICD and the transmembrane domain (TM) of APP, which is replaced by the TM of the platelet-derived growth factor receptor (PDGFR). The APP-ΔCT15 mutant (available as ΔCT15 mice only) contains the complete ectodomain of APP, but lacks the last 15 C-terminal amino acids including the YENPTY motif. APP-ΔNPTY was available as cDNA ready for transient transfection and also lacked the YENPTY motif of the AICD. APP-ΔPEER constructs were available for transfection as well and contained a mutated G-protein interaction motif incapable of binding G-proteins.

To determine whether the AICD was required for sAPPα-induced Akt activation, a lentiviral construct encoding the extracellular part from the amino-terminus to the β-secretase cleavage site of APP (\triangleq sAPPβ) coupled to the transmembrane domain of the platelet-derived growth factor receptor (PDGFR) was transfected into MEF APP-KO cells. The resulting cell line expressed membrane-anchored APP lacking the AICD with its transmembrane domain; sufficient expression was confirmed in a western blot (Figure 23A).

Interestingly, as shown in Figure 23B, sAPPα and APP-E1 were not able to activate the Akt pathway in the absence of the APP C-terminal domain as determined by conventional western blots or *in vitro* kinase assays. Quantification of protein levels confirmed the lack of Akt activity induction that could only be stimulated by IGF1 treatment (Figure 23C). This suggests a crucial role of the intracellular domain of APP for sAPPα-mediated PI3K/Akt survival signaling.

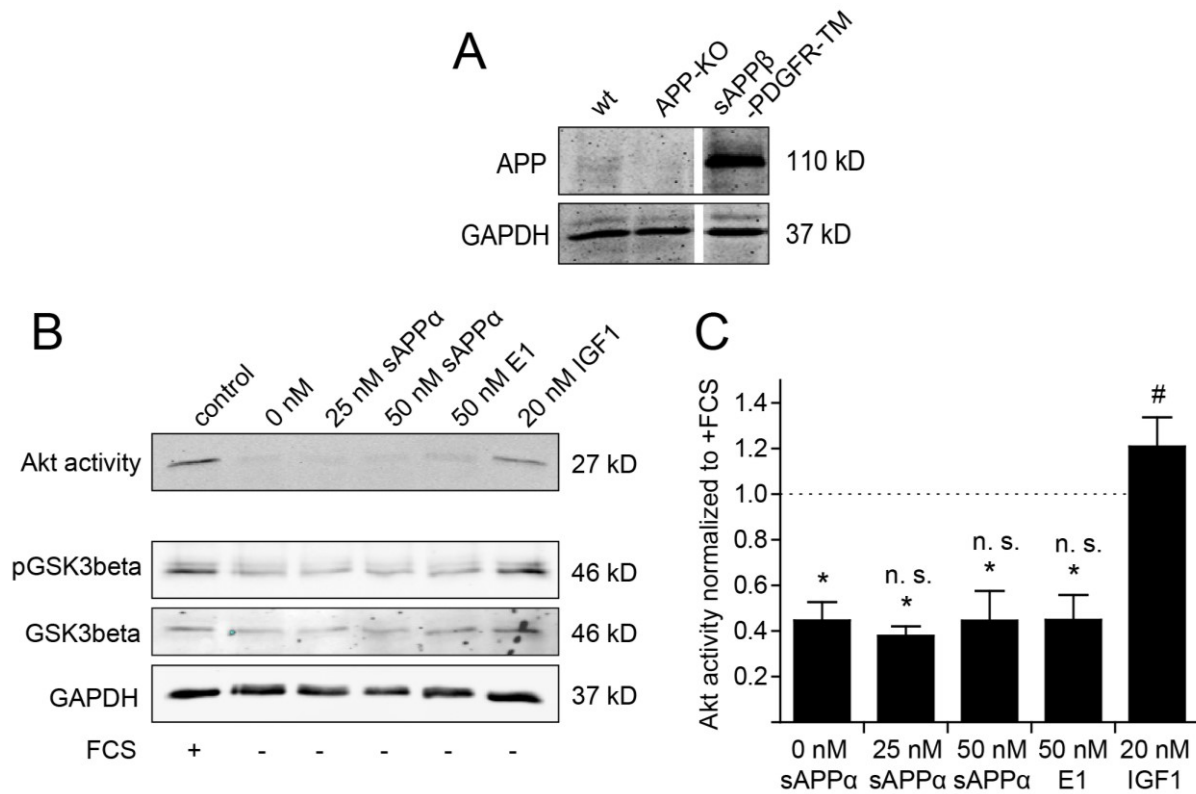


Figure 23. Akt survival signaling requires the APP intracellular C-terminal domain (AICD). (A) MEF APP-KO cells were transduced with a lentiviral construct encoding sAPPβ fused to the PDGFR TM (sAPPβ-PDGFR-TM). Expression of this APP construct lacking the AICD was confirmed in a western blot. (B) No sAPPα-induced Akt activity was observed in the generated cell line suggesting that the AICD is necessary for this effect. Human IGF1 served as positive control. In parallel to Akt activity detection, whole cell lysates were tested with anti-pGSK3β, anti-GSK3β and anti-GAPDH (loading control) antibodies. (C) Akt activity was quantified by normalizing values to serum-treated controls (dashed line). Data are means ± SEM from three blots. Statistical significance: *, $p < 0.05$ compared to controls (+FCS); #, $p < 0.05$ compared to serum withdrawal in the absence of sAPPα/E1/IGF1; n. s. = not significant.

As the AICD was found to be essential for Akt signaling, the specific domain responsible for this effect was localized by testing different AICD mutants. First, primary hippocampal neurons from APP-ΔCT15 mice were tested. These lack the last 15 C-terminal aa of APP, including the YENPTY motif that interacts with several adaptor proteins including Fe65 and is crucial for transcriptional activation by the (released) AICD as described earlier (Müller et al., 2008; Ring et al., 2007).

Akt signaling was potently activated in these cells, despite the absence of the YENPTY motif (Figure 24A) excluding AICD-mediated effects on transcription as the underlying cause of sAPPα-dependent Akt signaling. Quantification of protein levels confirmed significant Akt activity induction in APP-ΔCT15 mice (Figure 24B).

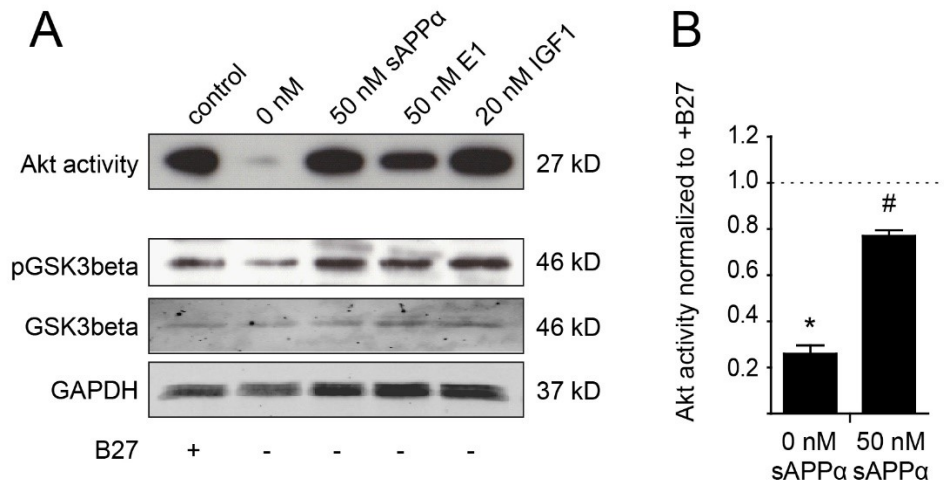


Figure 24. AICD-dependent PI3K/Akt signaling does not require the YENPTY motif of APP. (A) Potently activated Akt signaling by sAPP α and the E1 domain in hippocampal neurons from mice lacking the 15 C-terminal aa of APP (Δ CT15) including the YENPTY motif. In parallel to Akt activity detection, whole cell lysates were tested with anti-pGSK3 β , anti-GSK3 β and anti-GAPDH (loading control) antibodies. **(B)** Akt activity was quantified by normalizing values to serum-treated controls (dashed line). Data are means \pm SEM from three blots. Statistical significance: *, $p < 0.05$ compared to controls (+B27); #, $p < 0.05$ compared to serum withdrawal in the absence of sAPP α ; n. s. = not significant.

4.6 Activation of the PI3K/Akt Pathway by sAPP α /E1 Is Mediated by G-protein-dependent Signaling

To further map the regions of the AICD required for sAPP α -induced Akt activation, two APP deletion mutants (illustrated in Figure 22) lacking the YENPTY motif (Δ NPTY) or a central sequence motif (Δ PEER) of the AICD (Back et al. 2007, Merdes et al. 2004) were transfected into an APP-deficient background. The Δ PEER mutant lacks the membrane-proximal G-protein binding site (Deyts et al., 2012a).

Again, transfection efficiency and overall expression of the APP constructs was verified by western blot (Figure 25A). Additionally, an on-cell-western approach was applied to quantify their cell surface expression after transfection in comparison to wt control cells. As shown in Figure 25B, cell surface expression levels of both constructs were comparable with those detected in wt cells.

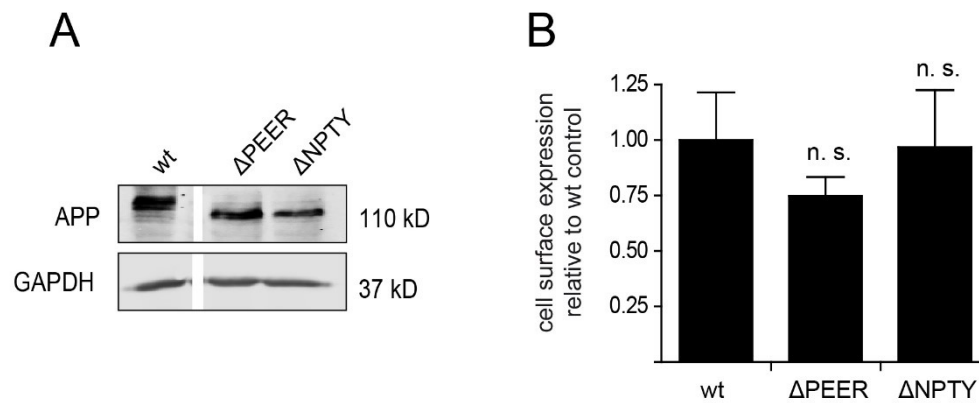


Figure 25. Transfection efficiency and cell surface expression of AICD mutant constructs in comparison to wt control cells. (A) The two AICD mutants, APP-ΔPEER and APP-ΔNPTY, were described in Merdes et al. (2004). Both constructs were transfected into MEF APP-KO cells; expression was confirmed in a western blot. **(B)** Cell surface expression of the two APP C-terminal domain mutants after transfection relative to wt APP expression levels. Fluorescence signals measured in an on-cell-western with unpermeabilized cells were normalized to background staining. Data are means \pm SEM from three experiments. Statistical significance: n. s. = not significant compared to wt control.

Similar to SH-SY5Y cells and neurons, significant sAPP α -dependent induction of Akt activity under serum deprivation was also observed in MEF wt cells, which was readily confirmed by blot quantification (Figure 26A+B). This indicates that MEF cells represent a suitable non-neuronal model to study the modification of signaling pathways by APP ectodomains after induction of cell stress.

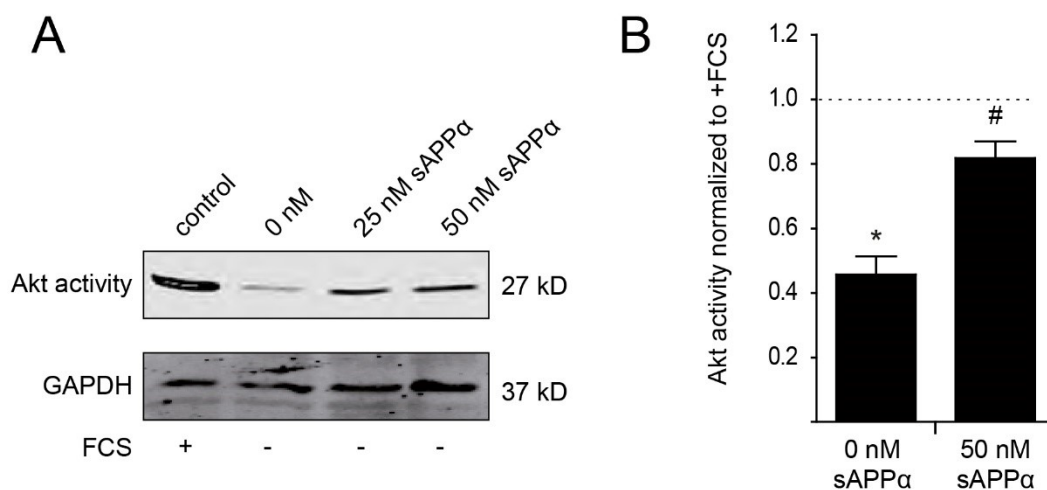


Figure 26. Significant sAPP α -dependent induction of Akt activity in MEF cells. (A) Akt activity in MEF wt cells treated with sAPP α and its corresponding blot quantification **(B)**. Data are means \pm SEM from three blots. Values were normalized to serum treated controls (dashed line). Statistical significance: *, $p < 0.05$ compared to control (+FCS); #, $p < 0.05$ compared to serum withdrawal in the absence of sAPP α .

In line with result obtained in Δ CT15 neurons, Akt signaling was strongly activated in Δ NPTY-transfected MEF cells (Figure 27A, right). However, the Δ PEER mutant, despite being expressed at similar levels as APP Δ NPTY, did not rescue activation of the Akt pathway (Figure 27A, middle). Although not reaching significance, the trend of Akt activation in Δ NPTY mutants as opposed to Δ PEER transfected cells is well visible in quantified western blot results (Figure 27B). This suggests that Akt pathway activation by sAPP α requires G-protein-mediated signaling.

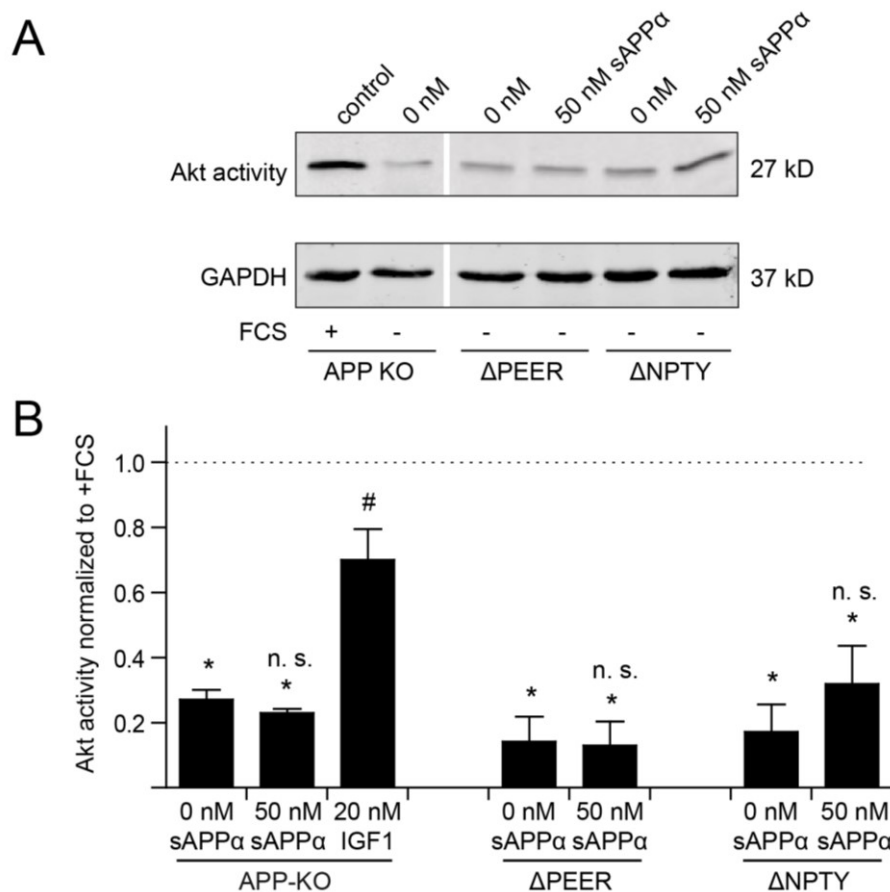


Figure 27. Akt pathway activation depends on the expression of the G-protein interaction motif. (A) Recombinant sAPP α activated Akt in serum-deprived wt and Δ NPTY cells (right), but not in APP-KO (left) and Δ PEER cells (middle) lacking an interaction motif for G-proteins. **(B)** Blot quantification values were normalized to serum-treated controls (dashed line). Data are means \pm SEM from three blots. Statistical significance: *, $p < 0.05$ compared to controls (+FCS); #, $p < 0.05$ compared to serum withdrawal in the absence of sAPP α ; n. s. = not significant.

Indeed, applying pertussis toxin (PTX), a selective $G_{i/o}$ inhibitor (Ayoub et al., 2009; Horgan et al., 1995), efficiently blocked sAPP α -mediated Akt signaling in wt MEFs (Figure 28A), which was readily confirmed in blot quantifications (Figure 28B). Even though the G-protein subunit $G_{s\alpha}$ was recently shown to be involved in APP-induced modulation of GSK3 β (Deyts et al., 2012a) the abolished Akt signaling after PTX treatment seen here argues for G_o -dependent signal

transduction. This is also in line with findings by Nishimoto and Shaked who showed that APP interacts with G_o (Nishimoto et al., 1993; Shaked et al., 2009).

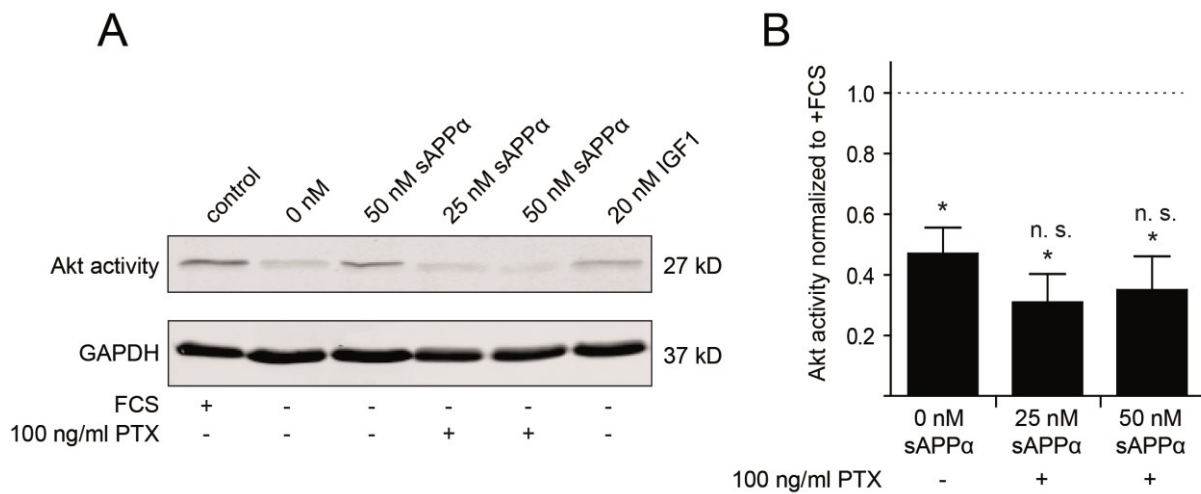


Figure 28. sAPP α -dependent activation of the PI3K/Akt is mediated by G-protein signaling. (A) MEF wt cells preincubated with 100 ng/ml PTX, a specific $G_{i/o}$ inhibitor, showed no induction of Akt activity by sAPP α . **(B)** Blot quantifications ($n = 3$ blots \pm SEM) confirmed these results (right). Values were normalized to serum-treated controls (dashed line). Statistical significance: *, $p < 0.05$ compared to control (+FCS); n. s. = not significant.

Additionally, FACS analysis was performed with MEF wt cells simultaneously treated with sAPP α and the $G_{i/o}$ inhibitor PTX or the PI3K inhibitor LY294002 to quantify cell death of cultures under serum/glucose deprivation. As depicted in Figure 29, treatment with PTX and the PI3K inhibitor completely abolished sAPP α -mediated cell survival. This observation further substantiates the findings with APP deletion constructs that sAPP α initiates cell survival via G_o -mediated activation of the PI3K/Akt pathway.

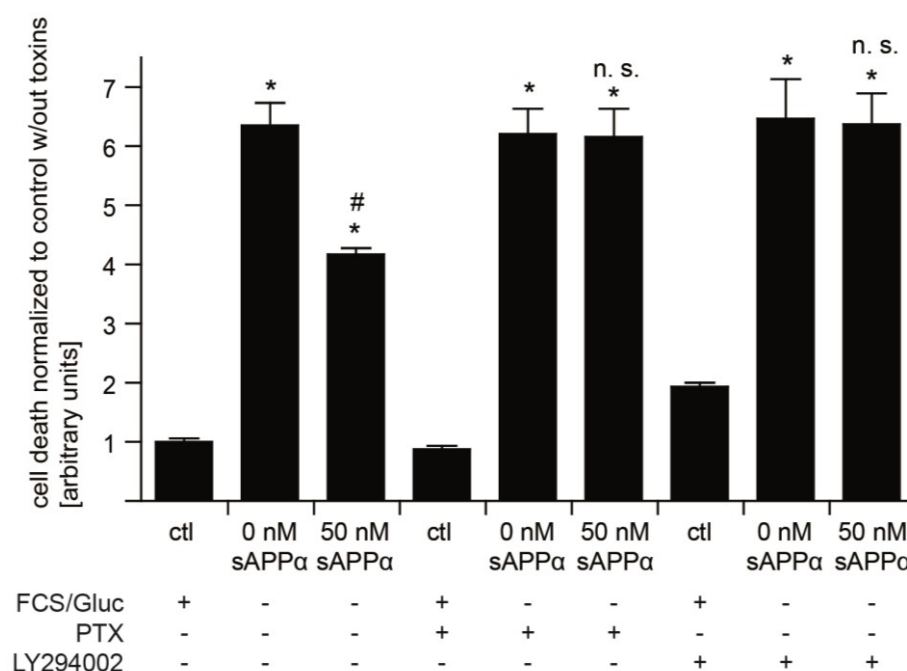


Figure 29. sAPPα-mediated cell survival is induced by G_o-dependent activation of the PI3K/Akt pathway. FACS analysis with MEF wt cells treated with G_o-selective PTX (100 ng/ml, 24 h) or PI3K inhibitor LY294002 (10 μM, 24 h) abolished sAPPα-mediated cell survival under serum/glucose deprivation. Values are normalized to serum/glucose-treated control without inhibitors. Data are means from four cultures ± SEM. Statistical significance: *, $p < 0.05$ compared to controls (+FCS/+Gluc); #, $p < 0.05$ compared to serum/glucose withdrawal in the absence of sAPPα; n. s. = not significant.

4.7 IGF1-R Expression Is Not Required for sAPPα-dependent Survival Signaling

Recently, Jimenez et al. (2011) suggested that sAPPα-dependent neuroprotection may require the expression of IGF1 receptor (IGF1-R) and insulin receptor (IR) as both receptors have been shown to play a major role in the development/onset of neurodegenerative diseases and AD (see also Carro and Torres-Aleman, 2004). The authors proposed a model in which sAPPα acts through IGF1 and/or insulin receptors to activate the PI3K/Akt pathway and to phosphorylate and inhibit the activity of GSK3β. However, their experimental data was exclusively obtained using pharmacological inhibitors of the two receptors, which has several limitations such as target specificity and efficacy.

Therefore, in this work complete IGF1-R-KO MEFs prepared from homozygous IGF1-R-KO (IGF1-R^{-/-}) late gestation embryos were utilized to investigate the effect of sAPPα on cells lacking the receptor. Figure 30 shows an Akt activity assay performed with IGF1-R-deficient MEF cells, which argues against a contribution of IGF1-R in sAPPα-mediated neuroprotection. Despite the proposed involvement of IGF1-R as a co-receptor, sAPPα and APP-E1 treatment clearly activated

Akt activity in serum-deprived IGF1-R-KO cells while the application of IGF1 (served as negative control in this case) did not (Figure 30).

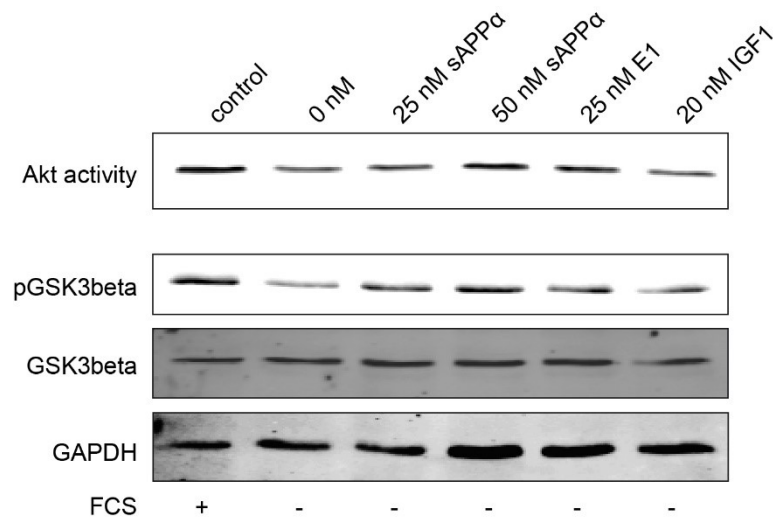


Figure 30. IGF1 receptor expression is not required for sAPPα-mediated PI3K/Akt pathway activation. Akt kinase activity assay with MEFs from IGF1-R-KO mice. Despite the lack of IGF1-R the Akt pathway was activated with increasing doses of sAPPα or recombinant E1 domain. Similarly, pGSK3β levels increased in full lysates, while GSK3β levels did not change. Here, IGF1 served as a negative control. GAPDH was used as a loading control.

4.8 The Growth Factor-like Domain (GFLD) of APP Is Protective, but Not the Mutated Copper Binding Domain

Results in this work demonstrate that besides sAPPα, the recombinant APP-E1 domain alone induces neuroprotection and activates the PI3K/Akt survival pathway. E1, however, is further subdivided into the cysteine-rich growth factor-like domain (GFLD) and the copper binding domain (CuBD) and was identified as the major interaction interface for APP dimerization (Baumkötter et al., 2012+2014; Gralle and Ferreira, 2007; Reinhard et al., 2005). It was shown that copper binding to the GFLD enhances APP dimerization (Noda et al., 2013) and that ablating copper binding in the E1 domain of APP diminished its cytoprotective abilities (Gough et al., 2014).

We therefore tested the recombinant GFLD and mutant GFLD (H108/110A) incapable of binding copper purified from yeast (friendly gift from Baumkötter/Kins, University of Kaiserslautern). In agreement with the authors cited earlier, Figure 31 confirms that the GFLD's ability to bind copper and to form dimers may indeed be required for cytoprotection via PI3K/Akt signaling. This further indicates that direct interaction of sAPP and APP might be involved (see also Discussion). The treatment with recombinant GFLD readily induced Akt activation in serum-

deprived MEF wt cells, whereas the mutant GFLD (Δ GFLD) that cannot bind copper did not show any induction. Yet, further research has to confirm these findings.

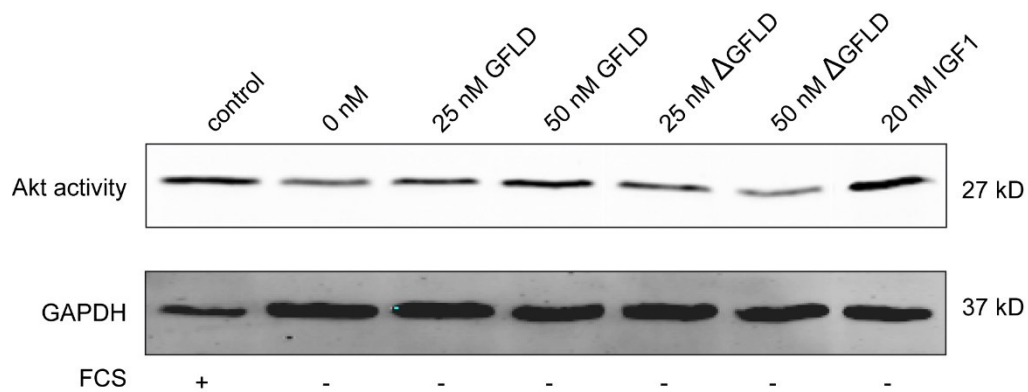


Figure 31. The GFLD of APP activated Akt signaling, but not the mutant GFLD incapable of binding copper. MEF wt cells were deprived of serum and treated with increasing doses of recombinant GFLD or mutant GFLD (Δ GFLD) purified from yeast. The Akt survival pathway was readily activated by GFLD, but not by the mutant form that cannot bind copper. GAPDH was used as a loading control in the corresponding whole cell lysates.

5 Discussion

The Amyloid Precursor Protein (APP) and its mammalian paralogues APP-like proteins 1 and 2 (APLP1 and APLP2) share most of their sequence motifs except the A β region that is unique to APP. Generation of the toxic peptide A β is prevented by α -secretase cleavage within the A β region. This liberates the neuroprotective soluble ectodomain sAPP α under physiological conditions along the non-amyloidogenic pathway (Endres and Fahrenholz, 2012). A β is produced by β - and γ -cleavage in the amyloidogenic pathway of APP processing and is seen as the major (toxic) component of senile plaques in the brains of patients suffering from AD. The two downstream amyloidogenic processing fragments A β and AICD have largely been linked to neurodegeneration and apoptosis (Kögel et al., 2012b). In contrast, previous studies from this and other labs suggested that sAPP α exerts potent neurotrophic and neuroprotective effects (Kögel et al. 2012b, Kögel et al. 2012a). APP and sAPP α were also shown to play a crucial role in neuronal plasticity, axonal growth and synaptogenesis (Zheng and Koo, 2011). Therefore, loss of these functions may render neurons more susceptible to cellular stress. Several studies revealed diminished APP processing during aging causing less secretion of sAPP α (Kern et al., 2006). Yet, most of the existing experimental work has been devoted to decipher the pathophysiological, neurotoxic roles of APP and the exact mechanisms of sAPP α /APP-mediated neuroprotection are not established so far (Kögel et al., 2012b). They most likely involve a complex interplay between survival/stress pathways and interaction with surface receptors and other targets (Table 12).

Early observations of sAPP α protecting significantly against excitotoxic stress were solely detectable after incubation with sAPP α over several hours. This suggests that a persistent activation of cell survival signaling pathways such as PI3K/Akt, ERK and NF- κ B may be necessary (Kögel et al., 2012b, Table 12). Accordingly, previous studies from this lab reported that the JNK/c-Jun stress pathway, which has a decisive function in brain aging and neurodegeneration, is antagonized by APP overexpression and sAPP α treatment (Kögel et al., 2005). More importantly, also the PI3K/Akt survival signaling pathway was found to be involved in mediating the protective function of sAPP α (Copanaki et al., 2010; Eckert et al., 2011). The PI3K/Akt pathway is a central survival pathway that can be activated by several neurotrophic cytokines such as IGF1 and plays a critical role in various neurodegenerative diseases. Downstream phosphorylation of Akt eventually activates pro-survival proteins like Bcl-xL or Bcl2, inhibits caspases and stimulates cell growth, whereas stress-triggered proteins (e. g. GSK3 β) are inhibited (Chong et al., 2012; Manning and Cantley, 2007). This may include the activation of pro-survival genes with simultaneous suppression of pro-apoptotic genes (e. g. c-Jun) most likely involved in stress responses and neuronal survival such as manganese superoxide dismutase (MnSOD), peroxiredoxins, catalase,

insulin-like growth factor 2 (IGF2) (Kögel et al., 2005; Stein et al., 2004, Table 12). Additionally, certain crosstalk between stress and survival pathways was also proposed with activation of the PI3K/Akt survival pathway that may consequently inhibit the JNK stress pathway (Barthwal et al., 2003; Kögel et al., 2012b). Table 12 lists possible mechanisms of APP/sAPP α -mediated neuroprotection by interaction with putative, yet unidentified, co-factors and/or consecutive activation of survival/stress signaling pathways or by inducing the expression of downstream genes. For more details, see also 1.3.3 and 1.5 of the introduction or refer to the review by Kögel et al. (2012b).

Table 12. Mechanisms of APP/sAPP α -mediated neuroprotection.

APP/fragment	Co-factor	Mechanism	Reference
sAPP α	IGF1-R? I-R?	↑PI3K/Akt pathway	Eckert et al., 2011; Jimenez et al., 2011; Cheng et al., 2002 Venezia et al., 2006
sAPP α	?	↑NF- κ B pathway	Guo et al., 1998; Cheng et al., 2002
sAPP α	GRB2 ShcA	↑ERK pathway	Cheng et al., 2002; Greenberg et al., 1995; Nizzari et al., 2007; Venezia et al., 2006
sAPP α , APP	?	↓c-Jun transcription, ↓JNK/c-Jun pathway	Kögel et al. 2005; Copanaki et al. 2010; Eckert et al., 2011
APP	?	↑p38 MAPK/MEF2 pathway	Burton et al., 2002
sAPP α , APP, APLP1	?	↓cdk5 pathway	Han et al., 2005 Hartl et al., 2013
sAPP α	APP	↑survival signaling	Gralle et al., 2009
APP/sAPP α	?	↑neuroprotective target genes: MnSOD, peroxiredoxin-2, catalase, transthyretin, IGF2 and insulin-like growth factor-binding protein 2 (IGF-BP2) etc.	Stein et al., 2004; Kögel et al., 2005

5.1 Yeast-derived sAPP α and E1 Have Neuroprotective Properties

As outlined above, several studies revealed neuroprotective properties of APP and its subdomain sAPP α (Mattson et al., 1993; Müller et al., 2012). APP overexpressing cells were reported to be protected against genotoxic and ER stress (Kögel et al., 2003, 2005). Besides its function as a neurotrophic growth factor stimulating cell proliferation and synaptogenesis (Chasseigneaux and Allinquant, 2012), sAPP α was suggested to act as a neuroprotective agent after brain injury (Corrigan et al., 2011; Thornton et al., 2006). Similar to the observations in this work, it was also

shown to rescue neurons from cell death induced by hypoglycemia (Mattson et al., 1993) and trophic factor deprivation (Cheng et al., 2002). Suggested mechanisms for this effect are the modulation of ion homeostasis through rapid effects on ion channel function (LaFerla, 2002; Mattson et al., 1997) and delayed activation of protective signaling pathways (Kögel et al., 2012b).

In this work, previous data from the Kögel lab demonstrating neuroprotective action by sAPP α from different sources were confirmed and reproduced with recombinant sAPP α and APP-E1 domain purified from *Pichia pastoris*. The APP ectodomains were applied to various cell models under proteasomal stress or trophic factor deprivation and metabolic stress. In agreement with the mentioned reports, the present results unequivocally demonstrate that recombinant sAPP α and even its subdomain E1 alone, which has not been shown before, are capable of providing a robust neuroprotection in an array of viability and cell death assays in a dose-dependent manner. As described in 4.1, *Pichia*-derived APP subdomains showed clear biological and neuroprotective activity as compared to sAPP α from other sources.

5.2 Recombinant sAPP α and E1 Antagonize Stress Induced by Trophic Factor Deprivation and Proteasomal Inhibition

In the course of this study, different stress stimuli were applied to cell and tissue models to induce cell death and investigate the protective abilities of APP fragments.

Brain aging and AD are characterized by various stress mechanisms leading to a progressive loss of neurons (Goedert and Spillantini, 2006). Some hallmarks suggest an important role of apoptosis, but also non-apoptotic, inflammatory and necrotic features are controversially discussed. Especially since apoptosis is considered a relatively rapid process leading to cell deterioration within hours rather than decades as is the case in (sporadic) AD (Hyman and Yuan, 2012) and changes in synaptic plasticity and neural circuits appear much earlier than neuronal death (de Calignon et al., 2010; D'Amelio et al., 2012), non-apoptotic stress pathways may be involved. Accordingly, D'Amelio et al. (2011) describe a non-apoptotic baseline caspase-3 activity that induces synaptic loss and contributes to cognitive dysfunction in an AD model. On the other hand, Hyman and Yuan propose that a lack of trophic factors may induce an active, caspase-independent mechanism of cell death such as necroptosis (Hyman and Yuan, 2012; Vandenabeele et al., 2010). As described in 1.4.4, TUNEL-positive neurons and upregulated initiating and executioner caspases detected in the aging brain and AD patients support apoptosis as an important mediator (reviewed in Hyman and Yuan, 2012). Thus it was suggested that neurons may tolerate a certain level of caspase activity without undergoing immediate cell death, but caspase activation and caspase-dependent protein cleavage might promote an apoptotic program. Still, the numerous stress signaling pathways that are activated during brain aging and altered by

APP/sAPP α may also trigger caspase-independent non-apoptotic cell death mechanisms, neuroinflammation or even induction of tau hyperphosphorylation with toxic abilities.

In consequence to the reports discussed above, the analysis of sAPP α -mediated protection in response to neuronal stress also contributes important information about possible mechanistic features during brain aging. For this reason, sAPP α was applied to various cell models treated with different stimuli to trigger neuronal death. The results give an impression of the consequences of the aging-associated loss of sAPP α and its neuroprotective function.

It was established in this lab before that sAPP α is able to protect PC12 cells and neurons from apoptosis induced by epoxomicin, an irreversible inhibitor of the 20S proteasome (Copanaki et al., 2010). In agreement, sAPP α and even its subdomain APP-E1 alone were able to antagonize cell stress triggered by proteasome inhibition with MG132 in this study. As discussed in 1.4.4, inhibition of the proteasome mimics similar stress conditions as seen during brain aging and AD leading to an accumulation of damaged proteins, which causes cell death and activation of stress pathways. Cell stress as induced by serum and/or glucose deprivation represents another convenient model of investigating APP ectodomain-mediated protective mechanisms. Removal of glucose and trophic factors leads to metabolic stress impairing cell growth and survival in a very stringent way (Mielke and Herdegen, 2000; Yuan and Yankner, 2000). Furthermore, it is now widely acknowledged that loss of trophic factors and a diminished glucose metabolism may contribute to brain aging and the pathogenesis of AD (Furst et al., 2012; Hyman and Yuan, 2012; Pluta et al., 2013).

Initial experiments with time-dependent single (serum) and double (serum/glucose) deprivation revealed a potent reduction of cell survival as measured by metabolic cell activity (intracellular ATP levels in bioluminescence assays and esterase activity with calcein staining) and PI or ethidium homodimer-3 staining of stressed cells (lightmicroscopical evaluation and FACS analysis). Concomitant treatment with purified recombinant sAPP α and APP-E1 potentially antagonized stress-triggered cell death in a dose- and time-dependent manner in an array of different cell and tissue models. IGF1, a neurotrophic factor activating cell survival, was used as a positive control. Neuroprotection mediated by sAPP α and E1 was evident in mouse fibroblasts (MEFs), human neuroblastoma cells (SH-SY5Y) as well as primary (hippocampal) neurons and organotypic slices. The latter offer an authentic and complex CNS environment maintaining functional synaptic networks and the original cell architecture in an *ex vivo* model. Neuronal cells continue to differentiate. At the same time, the system combines accessibility and easy maintenance of *in vitro* cultures. Results gained from this far more elaborate approach therefore offer a more comprehensive understanding of the physiological conditions.

In summary, sAPP α and E1 promoted a robust neuroprotection after stress stimuli in different cell and tissue models. Pharmacological intervention to enhance the secretion of sAPP α or modulate APP processing in favor of sAPP α cleavage may indeed represent a useful therapy option for AD or neurodegeneration triggered by ischemic events. However, most clinical trials with seemingly promising compounds targeting these mechanisms were discontinued early as they failed to show cognitive improvements in these patients (Schneider et al., 2014).

5.3 APP Fragments Promote Cell Survival Only in the Presence of Holo-APP

Several studies propose that APP acts as a (membrane-bound) cell surface receptor or adhesion molecule for various interaction partners (Haass et al., 2012). Co-receptors and molecules interacting with APP that were described before include LINGO-1 (Bai et al., 2008), DISC1 (Young-Pearse et al., 2010), Fe65, Tip60, CP2 (Müller et al., 2008), DR6 (Nikolaev et al. 2009), p75 (Yaar et al., 1997), Netrin-1 (Lourenço et al., 2009), sorLA (Andersen et al., 2006), integrin- β 1 (Young-Pearse et al., 2008), I-R, IGF1-R (Jimenez et al., 2011) and several others (see also Table 12). These candidates may facilitate APP's neuroprotective abilities and form a protein network under physiological conditions. In this context, sorLA receptors were shown to decrease APP processing and internalization (Fjorback et al., 2012). In a similar fashion, APP was found to compete with sAPP α in the binding to integrin- β 1, which regulates apoptotic signaling mechanisms by protecting cells from cytotoxic stimuli (Grossmann, 2002; Young-Pearse et al., 2008). Furthermore, integrins, acting as mechanoreceptors, were shown to regulate cell viability via the PI3K/Akt pathway (Tian et al., 2002). It is also clearly established that holo-APP can form homo- and heterodimers with APLPs (Baumkotter et al., 2012; Soba et al., 2005). Nevertheless, the cellular receptor linking sAPP α to downstream survival signaling remains unidentified. Rohn et al. (2000) proposed that APP antibody 22C11 binding to APP activates caspases and neuronal death possibly by facilitating its dimerization. Based on this assumption, another study suggested that enforced APP homodimerization induces cell death unless disrupted by sAPP α as a competitive inhibitor rendering holo-APP expression necessary for sAPP α -mediated neuroprotection (Gralle et al., 2009). The same authors also argue that due to structural equality of sAPP α and the APP extracellular domain sAPP α most likely directly interacts with APP to exert its neuroprotective function (Gralle et al., 2009). Moreover, sAPP α and E1 were shown to dimerize in solution (Gralle et al., 2006; Kaden et al., 2012), which further supports the hypothesis of self-interaction in the APP protein family (Kaden et al., 2012).

To investigate the potential contribution of endogenous APP for sAPP α -induced neuroprotection, experiments were performed with stable lentiviral APP-KD human SH-SY5Y neuroblastoma cells, APP-KO MEFs and hippocampal neurons/slices obtained from APP-KO mice. Despite the somewhat different conclusions drawn by Gralle et al. (2009) their major finding, i. e.

that APP is required for the protective effect of sAPP α , is consistent with the above presented observations. Neuroprotection mediated by sAPP α /E1 as measured in viability and cell death assays depended on the expression of holo-APP in the present study. In addition, here, the activation of survival signaling pathway PI3K/Akt by sAPP α /E1 was also exclusively seen in APP expressing cells and tissues. This is in line with another report suggesting that the *Drosophila* orthologue of sAPP α , sAPPL, only exhibited protective abilities in the presence of membrane-bound APPL (Wentzell et al., 2012). Yet, other groups also presented contradictory results, e. g. by proposing that exogenous sAPP α was sufficient to (at least partly) restore functional outcome that had been lost due to APP deficiency in APP $^{-/-}$ mice (Ring et al., 2007). Similar effects on function and histological changes were shown by another group testing wt mice vs. APP-KO animals after traumatic brain injury (Corrigan et al., 2012). However, the latter acknowledge that sAPP α may act via alternative mechanisms *in vivo* compared to those described *in vitro* to account for the controversial findings (Corrigan et al., 2012). Furthermore, the present study solely focused on APP-dependent neuroprotection mediated by sAPP α and did not investigate its dependence on APP in histological or behavioral analyses, e. g. by examining its effect on synapto- and neurogenesis.

The specific ADAM10 (α -secretase) inhibitor GI254023X (Weyer et al., 2011) utilized in this work significantly increased PI counts in serum/glucose-deprived hippocampal slices in comparison to DMSO (carrier)-treated controls. This observation suggests that the absence of endogenous sAPP α exacerbates cell death under stress conditions. In turn, the effect could be completely rescued by applying exogenous sAPP α ; thereby supporting the notion that recombinant sAPP α can substitute endogenous sAPP α function. Furthermore, the present study revealed differences in basal cell death levels (e. g. PI counts in SH-SY5Y cells, Figure 12) between wt and APP-deficient cells. This is in agreement with numerous studies that provide evidence for an enhanced susceptibility of neurons to cellular stress in an APP-KO background in which neither holo-APP nor sAPP α is expressed (reviewed in Kögel et al. 2012).

5.4 APP-dependent Cell Survival Involves Activation of the PI3K/Akt Pathway

Synthetic inhibitors of the PI3K/Akt pathway were observed to abrogate sAPP α -dependent neuroprotection (Cheng et al., 2002; Copanaki et al., 2010; Eckert et al., 2011). In agreement with these findings, data from this thesis provide first direct evidence that sAPP α indeed represents a key activator of the PI3K/Akt signaling pathway. As presented in Results, sAPP α and APP-E1 potently stimulated the Akt survival pathway under stress conditions and - in line with data from viability/cell death assays - this activation is dependent on the expression of endogenous APP.

Moreover, FACS analysis with the PI3K inhibitor LY294002 (Vlahos et al., 1994) could abolish sAPP α -mediated neuroprotection in cells under metabolic stress and neurotrophic factor deprivation further supporting the notion that protection is in fact induced via the PI3K/Akt pathway.

Recently, Jimenez et al. also demonstrated that sAPP α can activate the PI3K/Akt pathway, which may require the expression of IGF1-R and I-R (Jimenez et al., 2011). Both receptors were shown to play a major role in physiological survival signaling. Likewise, IGF1 signaling was shown to trigger anti-amyloidogenic cleavage of APP and ectodomain shedding of APLP1 and APLP2 (Adlerz et al., 2007). Alterations in these receptors may induce the development/onset of neurodegenerative diseases and AD (Carro and Torres-Aleman, 2004; Schulte-Herbrüggen et al., 2008). Jimenez and colleagues further suggested that sAPP α acts through IGF1 and/or insulin receptors to activate the PI3K/Akt survival pathway by phosphorylating and inhibiting the activity of GSK3 β (Jimenez et al., 2011). However, their experimental data were exclusively obtained using pharmacological inhibitors of the two receptors, which has several limitations such as target specificity and efficacy and therefore makes interpretation of the results difficult. Despite the proposed contribution of these co-receptors experiments with IGF1-R-deficient cells in this work did not confirm a role of IGF1-R in sAPP α -mediated neuroprotection. Interestingly though, Stein and colleagues could show that high levels of sAPP α increase the expression of IGF2 in mice, which they suggested might bind to IGF1-R in a comparable manner than IGF1. This, in turn, would stimulate the PI3K/Akt survival pathway (Stein et al., 2004). Consistently, altered insulin signaling, IGF1 resistance and/or deficiency were shown during brain aging and AD suggesting that neurodegeneration is a result of impaired IGF1 input (Talbot et al., 2012). This notion of “brain-type diabetes” is contradicted by other authors claiming that reduced insulin signaling delays aging and that long-term IGF1 signaling might rather be harmful (reviewed in Freude et al., 2009). Certainly, I-R/IGF1-R signaling plays an important role in APP processing, A β clearance and cognitive performance (Bassil et al., 2014).

Data obtained in this study clearly demonstrate that in the absence of endogenous holo-APP, Akt activation by sAPP α is completely abolished. Present results also suggest that the E1 domain alone can substitute for sAPP α in rescuing the activity of the Akt pathway under stress conditions. Again, this could not be observed in APP-depleted cells, emphasizing that the E1 domain, containing the growth factor like domain, encompasses the neuroprotective active part of sAPP α . Surprisingly, observations from this and other labs have previously demonstrated that sAPP β , which is generated via β -secretase cleavage of APP, lacks the neuroprotective properties of sAPP α (Copanaki et al., 2010; Furukawa et al., 1996). Although actively regulating gene expression, sAPP β failed to rescue perinatal lethality and synapse defects of APP- and APLP2-KO animals (Li et al., 2010). Given the fact that sAPP β also carries the E1 domain, this lack of neuroprotective

properties of sAPP β vs. sAPP α is currently difficult to explain, but may involve conformational differences between these two molecules. Future studies will have to address this important topic of APP biology in more detail.

In light of the high structural similarity between APP and APLPs (Aydin et al., 2012) we hypothesized that APLP1 and APLP2 may possess similar or overlapping physiological functions as APP in neuroprotection. Furthermore, it is well established that APP and APLPs can form homo- and heterodimers, arguing for a functional connection between these molecules (Soba et al., 2005). APLP1 and APLP2 do not contain an A β -domain, but their ectodomains are shed in an ADAM10-dependent manner similar to APP (Endres and Fahrenholz, 2012; Höggl et al., 2011). To analyze the potential role of APLP1 and APLP2 in sAPP α -mediated neuroprotection, a former member of the Kögel lab, diploma student Andreas Zymny, established stable lentiviral knockdowns in SH-SY5Y cells. Data from his preliminary works ("Untersuchungen zur Rolle von APP und APLPs bei der Zellalterung", Andreas Zymny, 2010) and findings from the present study clearly demonstrate that APP, but not APLP1 and APLP2 specifically functions as a surface receptor for sAPP α -mediated neuroprotection. Both APP family members certainly seem to have a vital physiological role (Korte et al., 2012), which may be concealed by functional compensation of the other paralogues (Ring et al., 2007). Although not many data exist on APLP1/2-dependent neuroprotection, Midthune and colleagues found that APLP2 expression was dispensable for the maintenance of dendritic structures, spine density or synaptic function (Midthune et al., 2012). Also, CA1 neurons from APLP1-KO and APLP2-KO mice exhibited normal neuronal architecture and spine density, whereas APP-KO mice revealed a highly reduced spine density and dendritic complexity. This was only partly restored in sAPP α -knockin (KI) mice lacking transmembrane holo-APP (Weyer et al., 2014).

Consistent with the above findings on the GSK3 β -regulating function of sAPP α , GSK3 β activity has been found to be upregulated in the aging brain, promoting tau hyperphosphorylation, tangle formation and diminished synaptic plasticity (Bradley et al., 2012; Hernandez et al., 2013; Jimenez et al., 2011). Moreover, A β was observed to activate caspase-3 cleavage, which in turn cleaved Akt and activated GSK3 β (Cavallucci et al., 2012). These investigations support the hypothesis that the aging-associated decline of sAPP α and its neuroprotective function (Endres and Fahrenholz, 2012; Fahrenholz, 2007; Kögel et al., 2012b) may contribute to this upregulation of GSK3 β , thereby sensitizing neurons to cellular stress stimuli. Based on this notion, one could hypothesize that the shift towards amyloidogenic APP processing and therefore promoting the enhanced generation of A β with concomitant loss of the sAPP α -dependent function in neuroprotection may synergize in rendering neurons more prone to neurodegeneration in the aging brain.

Collectively, the present data demonstrate a key role of sAPP α and E1 in neuronal survival by activating neuroprotective signaling through activation of Akt and consecutive inhibition of the

GSK3 β stress pathway in the presence of holo-APP. This suggests that other targets may have a function in this mechanism, too.

5.5 Cytoprotection Depends on the AICD and G-Protein Signaling

The observation that endogenous APP was required for sAPP α -mediated neuroprotection suggested a signaling role of the APP C-terminal domain and its interactors in this context. As outlined in Aydin et al. the APP C-terminal domain couples APP to diverse intracellular signaling pathways (Aydin et al., 2012). For example, it was proposed that the Src homology 2 (SH2) domain of Abl or the phosphotyrosine-binding domain (PTBD) of Shc may interact with the YENPTY motif of APP. This would suggest a role for APP in tyrosine kinase-mediated signal transduction (Venezia et al., 2006). Additional putative interactors binding to the APP intracellular domain at the YENPTY, PEER and YTSI motifs are displayed in Figure 32 and discussed in further detail in Aydin et al. (2012).

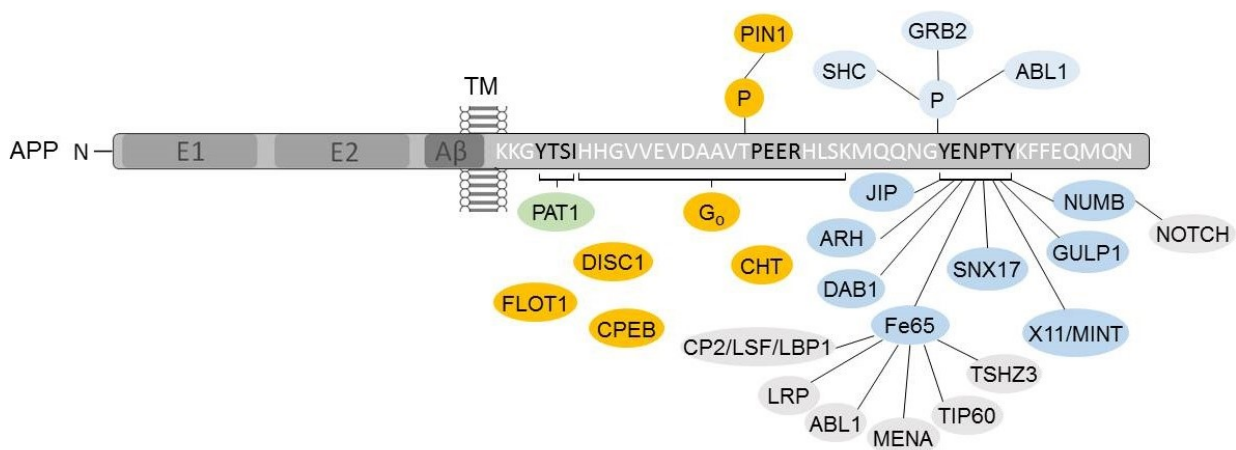


Figure 32. Interaction partners of APP at the AICD. APP was shown to interact with various proteins at its intracellular domain. Confirmed binding is indicated with a line. Green color corresponds to interaction partners of the YTSI motif, orange corresponds to PEER domain binding molecules and blue corresponds to YENPTY motif interactors. Figure adapted from Aydin et al. (2012), refer to the same review for protein function, abbreviations and references. TM – transmembrane domain.

In an alternative scenario to intracellular signaling involved in the neuroprotective function of APP, we hypothesized that membrane-tethering of APP alone may suffice for sAPP α -mediated activation of the Akt pathway. To characterize the functional domains of holo-APP required for sAPP α -induced signaling, a construct composed of the E1 and E2 domains of APP fused to the heterologous PDGFR transmembrane domain was overexpressed in an APP-KO background (see Figure 22). This construct lacked the complete C-terminal domain of APP. However, it was not able to restore sAPP α -mediated Akt activation under serum deprivation, indicating that the APP C-terminal domain is indeed required for neuroprotection. To further investigate the putative

function of PTBD-interactors, primary neuron cultures of APP Δ CT mice (lacking the 15 C-terminal aa of APP) were utilized to investigate the possible contribution of PTBD-containing interactors to sAPP α -stimulated Akt signaling. Intriguingly, the resulting data revealed that the last C-terminal 15 amino acids of the APP C-terminal domain are dispensable for mediating the neuroprotective effect of sAPP α . This domain comprises the YENPTY motif (Ring et al., 2007) to which the vast majority of the APP C-terminal domain interactors bind (Figure 32), including Fe65 (Aydin et al., 2012; Müller et al., 2008). Furthermore, the YENPTY is crucial for transcriptional activation by the (released) APP intracellular domain (AICD). The finding that it is nonessential for survival rules out AICD-mediated effects on transcription as the underlying cause of sAPP α -dependent Akt signaling. In compliance with the result from this work, APP-KI animals lacking the YENPTY motif have been shown to protect against several different deficits seen in APP-KO mice. Likewise, YENPTY-deficient APP, APLP1 and APLP2 single KO mice showed only mild phenotypes (Guo et al., 2012; Ring et al., 2007).

The outlined observation that the APP C-terminal domain, but not the YENPTY motif is essential for mediating sAPP α /APP-induced neuroprotection suggested that YENPTY-independent interactors are required for sAPP α action. Indeed, Nishimoto and colleagues could show that APP forms a complex with the heterotrimeric G-protein G_o , which binds in a YENPTY motif-independent manner to the APP C-terminal domain (Nishimoto et al., 1993). Similarly, the G-protein subunit $G_{s\alpha}$ was recently shown to be involved in APP-induced modulation of GSK3 β and neurite outgrowth (Deyts et al., 2012a). Furthermore, A β -induced cell death was shown to be dependent on APP and G-protein activation suggesting a direct interaction of APP and G_o in humans (Shaked et al., 2009). Therefore, to further map the APP C-terminal domain region mediating sAPP α -dependent neuroprotection in the present study, APP-KO cells were reconfigured with a deletion mutant (Δ PEER) lacking the G-protein interaction motif (Figure 32). In contrast to the Δ NPTY mutant, expression of the Δ PEER mutant (described in Back et al., 2007; Merdes et al., 2004) did not rescue sAPP α -induced Akt activation after serum starvation, indicating that G-protein-mediated signaling is causally involved. Consistently, the G-protein inhibitor PTX that selectively inhibits the heterotrimeric $G_{i/o}$ protein family (Ayoub et al., 2009; Horgan et al., 1995) completely abolished sAPP α -induced Akt activation and cell survival. This is in line with the findings by Nishimoto and Shaked mentioned above, who showed that APP interacts with G_o (Nishimoto et al., 1993; Shaked et al., 2009). Since G_o and $G_{s\alpha}$ were the only G-protein subunits described to interact with APP, this argues for G_o -specific signal transduction induced by sAPP α /APP action as seen here. PI3Ks are activated via different mechanisms. Growth factors, neurotransmitters, several hormones and other stimuli can activate receptor tyrosine kinases (RTKs), integrins, cytokine receptors or B-cell antigen receptors (BCRs), thereby leading to autophosphorylation. In turn, the p85 subunit of PI3K may bind the respective RTK directly or

via an adaptor protein such as IRS in the case of insulin receptor activation or focal adhesion kinase (FAK) after integrin stimulation (Assinder et al., 2009; Sussman et al., 2011). Consequently, PI3K catalyzes PIP2 to PIP3, which activates Akt and downstream proteins. Alternatively, the PI3K/Akt pathway was also found to be stimulated by G-protein-coupled receptors in different cell models (Murga et al., 1998, 2000). The present thesis now confirms this observation by showing that sAPP α -induced PI3K/Akt activation is indeed mediated by G-protein signaling (most likely by G_o) as opposed to stimulation via RTKs.

Numerous groups established that interaction of various bindings partners, e. g. DISC1, with the C-terminus of APP and the YENPTY motif in specific regulates APP trafficking, internalization and therefore also APP processing and overall APP levels (Koo and Squazzo, 1994; Shahani et al., 2014). Also, it was shown that caspase cleavage of APP results in loss of the YENPTY motif and therefore its endocytosis signal. In turn, one would expect reduced APP internalization and therefore less secreted sAPP α and A β . However, Soriano et al. showed that caspase activation by serum withdrawal did not affect A β levels (Soriano et al., 2001). Still, to exclude the possibility of reduced surface levels of the APP C-terminal deletion mutants utilized in this work, their cell surface expression levels were examined. Their internalization would prevent any putative direct or indirect interaction with sAPP α . As outlined in Results, no differences between wt, Δ PEER (G-protein-binding motif) and Δ NPTY were observed. This further strengthens the hypothesis, that sAPP α presumably interacts with cell surface APP, either directly or indirectly, to exert its neuroprotective effect.

Taken together, the presented data provide a detailed understanding of the key signaling components of sAPP α -mediated neuroprotection. They suggest that sAPP α and E1 act through membrane-bound APP activating an intracellular survival cascade via G_o-protein-mediated signaling.

5.6 Copper Binding Abilities of the Growth Factor-like Domain of APP Are Required for Activation of Survival Signaling

As discussed before, it will be interesting to investigate whether sAPP β , which lacks only 17 amino acids in comparison to sAPP α , exhibits similar neuroprotective abilities. However, earlier data from this and other labs suggest that sAPP α is up to 100 times more potent in mediating cytoprotection (Furukawa et al., 1996). This observation is currently difficult to explain as sAPP β also contains the E1 domain, which is shown here to potently induce neuroprotection. Conformational differences between sAPP α and sAPP β could be one explanation for this effect.

E1 is subdivided into the growth factor-like domain (GFLD) and the copper binding domain (CuBD, cf. Figure 2) and was identified as the major interaction interface for APP dimerization

(Baumkotter et al., 2012 and 2014; Gralle and Ferreira, 2007; Reinhard et al., 2005). In this work, experiments performed with recombinant GFLD propose that it is able to induce survival signaling similar to sAPP α and E1 by activating the PI3K/Akt pathway under stress conditions. In agreement, Corrigan and colleagues could show that the neuroprotective function of sAPP α may be mediated by the GFLD and the E2 domain of APP, which are both part of sAPP α (Corrigan et al., 2011). As outlined in Results, further analysis with a mutated GFLD (H108/110A) incapable of binding copper revealed no apparent induction of PI3K/Akt survival signaling. Again, also this finding is in line with earlier studies suggesting that copper binding to the GFLD enhances APP dimerization (Baumkötter et al., 2014; Noda et al., 2013) and that ablating copper binding in the GFLD or the CuBD diminished APP's cytoprotective abilities, synaptogenic function and APP interaction (Baumkötter et al., 2014; Fogel et al., 2014; Gough et al., 2014). In addition, Corrigan and colleagues recently defined the heparin binding site in APP96-110, which corresponds to the GFLD, as the responsible part of sAPP α to induce neuroprotection following traumatic brain injury (Corrigan et al., 2014). Along with other authors, they suggest that the neuroprotective properties relate to sAPP α 's ability to bind heparin sulphate proteoglycans (Corrigan et al., 2011; Small et al., 1994) as experiments with heparinase abolished the protective effects of sAPP α (Furukawa et al., 1996). This also indicates that soluble APP is capable of efficiently binding to cell membranes in a receptor-independent manner (Reinhard et al., 2013). In line with this notion, heparin binding was found to facilitate APP homodimerization and heterodimerization with other APP family members (Gralle et al., 2006; Soba et al., 2005), even though APLP1 was shown to lack a heparin binding site in the GFLD (Anliker and Müller, 2006).

In summary, the data obtained for this work suggest that the ability to bind copper by the GFLD of APP may indeed be required for cytoprotection via PI3K/Akt signaling. Given the findings by Baumkotter et al. (2014) that copper promotes APP trans-dimerization with its copper-binding E1 domain, this would also argue for direct interaction of holo-APP and sAPP α in mediating neuroprotection.

5.7 Conclusion and Outlook

In conclusion, this study identifies key signaling components and mechanisms involved in sAPP α -mediated neuroprotection: the data indicate that sAPP α signals either by direct binding or via an indirect mechanism through membrane-tethered APP. As APP harbors a G-protein interaction domain and sAPP α -mediated neuroprotection is lost upon deletion of this motif, this strongly suggests that APP serves as a receptor to trigger G-protein-dependent activation (most likely via G_o) of PI3K. This activation leads to the recruitment and downstream activation of the pro-survival kinase Akt and subsequent inhibition of its target GSK3 β (Figure 33). These findings support the hypothesis that sAPP α and holo-APP share equal relevance in mediating the neuroprotective

function of APP. They also provide novel mechanistic insights into the physiological function of APP in limiting neuron damage and death in response to neurotoxic stress conditions, as well as the loss of this function during brain aging.

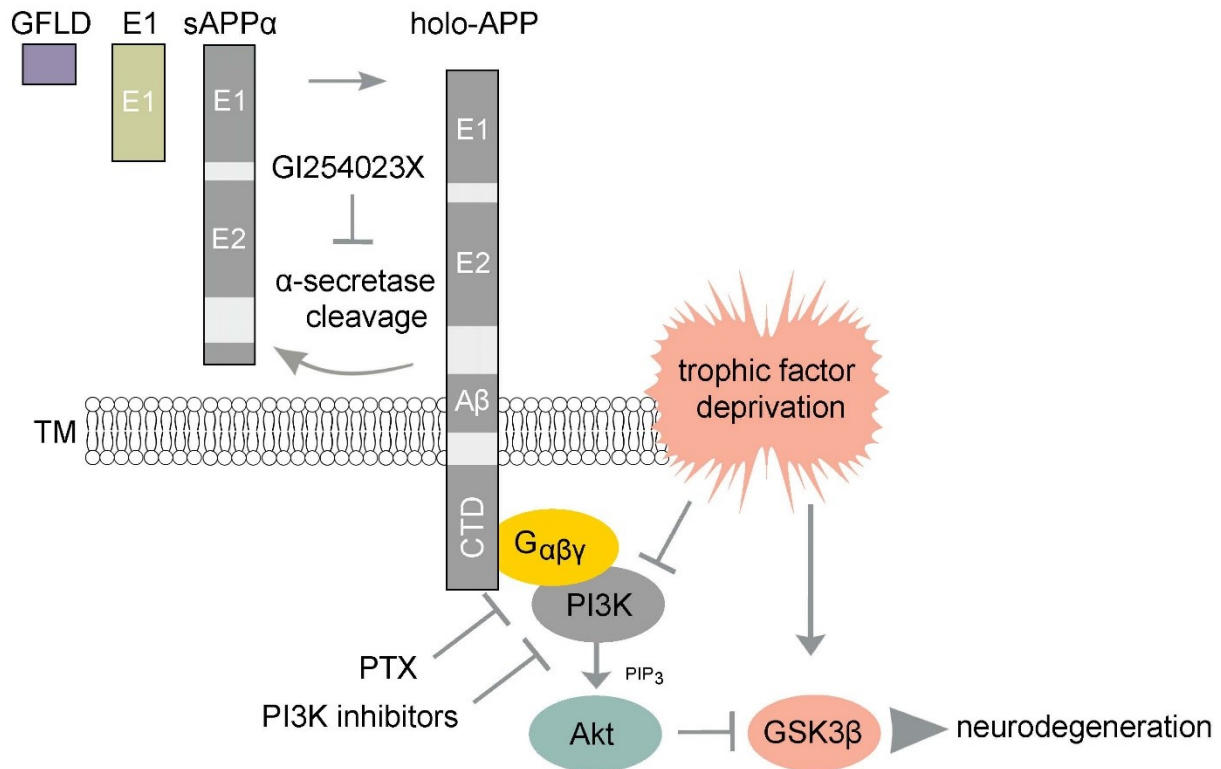


Figure 33. Hypothetical model of sAPP α -mediated Akt activation and survival signaling. In the anti-amyloidogenic processing pathway, APP is cleaved by α -secretase generating sAPP α that can activate induction of the PI3K/Akt survival pathway. Its subdomain E1 and the GFLD alone are shown here to mediate the same effects. This activation depends on the presence of holo-APP and its intracellular G-protein interaction motif, coupling sAPP α to G-protein-dependent induction of PI3K/Akt and downstream suppression of GSK3 β , thereby preventing neurodegeneration and cell death. CTD: APP C-terminal domain, TM: transmembrane domain, PI3K: PI3 kinase, PTX: pertussis toxin.

Direct interaction of sAPP α and APP remains to be insufficiently substantiated and therefore needs further experimental proof. However, as discussed earlier, interaction of the E1 domain and holo-APP was proven before (Baumkötter et al., 2014; Gough et al., 2014; Noda et al., 2013). Consequently, the specific functional (extracellular) domain of holo-APP required for neuroprotective signaling should be investigated. This may be done by employing APP mutant constructs. A lentiviral construct solely composed of the E2 domain coupled to the APP transmembrane domain and C-terminus that is lacking all three secretase sites is already available for testing in the Kögel lab. Additional research with lentiviral/transient KO models, synthetic inhibitors or neutralizing antibodies could also help defining other putative APP co-receptors and (membrane-bound) interaction partners as listed in 5.3. These candidates may facilitate its

neuroprotective abilities and form a protein network under physiological conditions. To this day, most APP interactors have been identified via yeast-two-hybrid screenings, but using a global proteomic approach such as mass spectrometry in combination with pulldown/co-IP and fluorescence resonance energy transfer (FRET) experiments may also expose (indirect) complex building (Kohli et al., 2012), global protein expression and phosphorylation changes (e. g. tau) induced by sAPP α .

To further elucidate the exact survival mechanisms triggered by sAPP α key downstream signaling targets of the PI3K/Akt survival pathway could be investigated. These may include central pro- and anti-apoptotic signaling components such as Bim, PUMA, Bax, Bak, Bcl-2, Bcl-xL, TRIB3, mTOR, FOXO, Jun etc.

Additional experiments with other APP fragments, such as E2 and sAPP β , could contribute to determine the protective domain(s) of APP and under which conditions they exhibit their distinctive functions. As discussed in 5.4, studies with the APP ectodomain sAPP β will be of particular interest, as sAPP β also carries the E1 domain but lacks the neuroprotective properties.

Another interesting issue could be to analyze the effect of sAPP α -mediated GSK3 β inhibition on tau phosphorylation. As discussed earlier, GSK3 β activity was found to promote tau hyperphosphorylation (Bradley et al., 2012; Hernandez et al., 2013). Therefore, findings on changes in tau phosphorylation by sAPP α treatment in wt vs. APP-KO models might expose the missing link between the tau hypothesis and the loss-of-function-theory of APP in the development of neurodegeneration and AD.

Finally, in light of the controversial findings by Corrigan et al. (2014) it will be important to further analyze the *in vivo* relevance of APP/sAPP α (inter-)action in an organotypic brain environment. These experiments could be conducted under conditions of hypoxia/glucose deprivation (transient global forebrain ischemia) since numerous reports claim that cerebral ischemia may contribute to the pathogenesis of AD (Pluta et al, 2013) and since sAPP α was shown to have protective effects after cerebral ischemia due to traumatic brain injury (Corrigan et al., 2011, 2012, 2014; Smith-Swintosky et al., 1994; Thornton et al., 2006). Furthermore, hyperphosphorylated tau (Geddes et al., 1994; Wen et al., 2004) and altered PI3K/Akt signaling (Endo et al., 2006) were observed in models of focal cerebral ischemia. In this context, analyzing sAPP α -mediated neuroprotection, changes in stress signaling and tau phosphorylation after acute ischemia/trauma to investigate the impact on neuronal loss would be highly interesting. In a similar manner, the response to sAPP α treatment after ischemic events in an AD mouse model vs. control animals could be assessed.

Taken together, the generated data from this thesis add significant details to the understanding of APP's physiological function. Further research as described above will shed light on the

pathophysiological consequences of APP loss during brain aging, since aging is still the most reliable risk factor for the development of AD. Ultimately, these insights may expose therapeutic concepts for the treatment of AD targeting A β /tau aggregation by enhancing clearance or neuroprotective pathways via activation of α -secretase or inhibition of hyperactive stress signaling (Crews and Masliah, 2010).

6 References

- Adlerz, L., Holback, S., Multhaup, G., and Iverfeldt, K. (2007). IGF-1-induced processing of the amyloid precursor protein family is mediated by different signaling pathways. *J. Biol. Chem.* *282*, 10203–10209.
- Ahmed, Z., Cooper, J., Murray, T.K., Garn, K., McNaughton, E., Clarke, H., Parhizkar, S., Ward, M.A., Cavallini, A., Jackson, S., et al. (2014). A novel in vivo model of tau propagation with rapid and progressive neurofibrillary tangle pathology: the pattern of spread is determined by connectivity, not proximity. *Acta Neuropathol* *127*, 667–683.
- Akers, J.C., Gonda, D., Kim, R., Carter, B.S., and Chen, C.C. (2013). Biogenesis of extracellular vesicles (EV): exosomes, microvesicles, retrovirus-like vesicles, and apoptotic bodies. *J. Neurooncol.* *113*, 1–11.
- Allsop, D. (2000). Introduction to Alzheimer's disease. *Methods Mol. Med.* *32*, 1–21.
- De Almagro, M.C., and Vucic, D. (2012). The inhibitor of apoptosis (IAP) proteins are critical regulators of signaling pathways and targets for anti-cancer therapy. *Exp. Oncol.* *34*, 200–211.
- Andersen, O.M., Schmidt, V., Spoelgen, R., Gliemann, J., Behlke, J., Galatis, D., McKinstry, W.J., Parker, M.W., Masters, C.L., Hyman, B.T., et al. (2006). Molecular dissection of the interaction between amyloid precursor protein and its neuronal trafficking receptor SorLA/LR11. *Biochemistry* *45*, 2618–2628.
- Ankarcrona, M., Dypbukt, J.M., Bonfoco, E., Zhivotovsky, B., Orrenius, S., Lipton, S.A., and Nicotera, P. (1995). Glutamate-induced neuronal death: a succession of necrosis or apoptosis depending on mitochondrial function. *Neuron* *15*, 961–973.
- Anliker, B., and Müller, U. (2006). The functions of mammalian amyloid precursor protein and related amyloid precursor-like proteins. *Neurodegener Dis* *3*, 239–246.
- Arendt, T. (2009). Synaptic degeneration in Alzheimer's disease. *Acta Neuropathol.* *118*, 167–179.
- Areosa Sastre, A., McShane, R., and Sherriff, F. (2004). Memantine for dementia. *Cochrane Database Syst Rev* CD003154.
- Assinder, S.J., Dong, Q., Kovacevic, Z., and Richardson, D.R. (2009). The TGF-beta, PI3K/Akt and PTEN pathways: established and proposed biochemical integration in prostate cancer. *Biochem. J.* *417*, 411–421.
- Aydin, D., Weyer, S.W., and Müller, U.C. (2012). Functions of the APP gene family in the nervous system: insights from mouse models. *Exp Brain Res* *217*, 423–434.
- Ayoub, M.A., Damian, M., Gespach, C., Ferrandis, E., Lavergne, O., De Wever, O., Banères, J.-L., Pin, J.-P., and Prévost, G.P. (2009). Inhibition of heterotrimeric G protein signaling by a small molecule acting on Galpha subunit. *J. Biol. Chem.* *284*, 29136–29145.
- Back, S., Haas, P., Tschäpe, J.-A., Gruebl, T., Kirsch, J., Müller, U., Beyreuther, K., and Kins, S. (2007). beta-amyloid precursor protein can be transported independent of any sorting signal to the axonal and dendritic compartment. *J. Neurosci. Res.* *85*, 2580–2590.

- Bai, Y., Markham, K., Chen, F., Weerasekera, R., Watts, J., Horne, P., Wakutani, Y., Bagshaw, R., Mathews, P.M., Fraser, P.E., et al. (2008). The in vivo brain interactome of the amyloid precursor protein. *Mol. Cell Proteomics* 7, 15–34.
- Bao, Q., and Shi, Y. (2007). Apoptosome: a platform for the activation of initiator caspases. *Cell Death Differ.* 14, 56–65.
- Barthwal, M.K., Sathyanarayana, P., Kundu, C.N., Rana, B., Pradeep, A., Sharma, C., Woodgett, J.R., and Rana, A. (2003). Negative regulation of mixed lineage kinase 3 by protein kinase B/AKT leads to cell survival. *J. Biol. Chem.* 278, 3897–3902.
- Bassil, F., Fernagut, P.-O., Bezard, E., and Meissner, W.G. (2014). Insulin, IGF-1 and GLP-1 signaling in neurodegenerative disorders: targets for disease modification? *Prog. Neurobiol.* 118, 1–18.
- Baumkotter, F., Wagner, K., Eggert, S., Wild, K., and Kins, S. (2012). Structural aspects and physiological consequences of APP/APLP trans-dimerization. *Exp Brain Res* 217, 389–395.
- Baumkötter, F., Schmidt, N., Vargas, C., Schilling, S., Weber, R., Wagner, K., Fiedler, S., Klug, W., Radzimanowski, J., Nickolaus, S., et al. (2014). Amyloid precursor protein dimerization and synaptogenic function depend on copper binding to the growth factor-like domain. *J. Neurosci.* 34, 11159–11172.
- Behl, C. (2000). Apoptosis and Alzheimer's disease. *J Neural Transm* 107, 1325–1344.
- Behr, J.P., Demeneix, B., Loeffler, J.P., and Perez-Mutul, J. (1989). Efficient gene transfer into mammalian primary endocrine cells with lipopolyamine-coated DNA. *Proc. Natl. Acad. Sci. U.S.A.* 86, 6982–6986.
- Berger, Z., Ravikumar, B., Menzies, F.M., Oroz, L.G., Underwood, B.R., Pangalos, M.N., Schmitt, I., Wullner, U., Evert, B.O., O'Kane, C.J., et al. (2006). Rapamycin alleviates toxicity of different aggregate-prone proteins. *Hum. Mol. Genet.* 15, 433–442.
- Bien, J., Jefferson, T., Causević, M., Jumpertz, T., Munter, L., Multhaup, G., Weggen, S., Becker-Pauly, C., and Pietrzik, C.U. (2012). The metalloprotease meprin β generates amino terminal-truncated amyloid β peptide species. *J. Biol. Chem.* 287, 33304–33313.
- Birks, J., and Harvey, R.J. (2006). Donepezil for dementia due to Alzheimer's disease. *Cochrane Database Syst Rev* CD001190.
- Blennow, K., Hardy, J., and Zetterberg, H. (2012). The neuropathology and neurobiology of traumatic brain injury. *Neuron* 76, 886–899.
- Bliss, T.V., and Collingridge, G.L. (1993). A synaptic model of memory: long-term potentiation in the hippocampus. *Nature* 361, 31–39.
- Braak, H., and Braak, E. (1991). Demonstration of amyloid deposits and neurofibrillary changes in whole brain sections. *Brain Pathol.* 1, 213–216.
- Bradley, C.A., Peineau, S., Taghibiglou, C., Nicolas, C.S., Whitcomb, D.J., Bortolotto, Z.A., Kaang, B.-K., Cho, K., Wang, Y.T., and Collingridge, G.L. (2012). A pivotal role of GSK-3 in synaptic plasticity. *Front Mol Neurosci* 5, 13.
- Brookmeyer, R., Johnson, E., Ziegler-Graham, K., and Arrighi, H.M. (2007). Forecasting the global burden of Alzheimer's disease. *Alzheimers Dement* 3, 186–191.

- Burton, T.R., Dibrov, A., Kashour, T., and Amara, F.M. (2002). Anti-apoptotic wild-type Alzheimer amyloid precursor protein signaling involves the p38 mitogen-activated protein kinase/MEF2 pathway. *Brain Res. Mol. Brain Res.* 108, 102–120.
- Busciglio, J., Lorenzo, A., Yeh, J., and Yankner, B.A. (1995). beta-amyloid fibrils induce tau phosphorylation and loss of microtubule binding. *Neuron* 14, 879–888.
- De Calignon, A., Fox, L.M., Pitstick, R., Carlson, G.A., Bacskai, B.J., Spires-Jones, T.L., and Hyman, B.T. (2010). Caspase activation precedes and leads to tangles. *Nature* 464, 1201–1204.
- Camandola, S., and Mattson, M.P. (2011). Aberrant subcellular neuronal calcium regulation in aging and Alzheimer's disease. *Biochim. Biophys. Acta* 1813, 965–973.
- Carro, E., and Torres-Aleman, I. (2004). The role of insulin and insulin-like growth factor I in the molecular and cellular mechanisms underlying the pathology of Alzheimer's disease. *Eur. J. Pharmacol.* 490, 127–133.
- Cavallucci, V., D'Amelio, M., and Cecconi, F. (2012). A β toxicity in Alzheimer's disease. *Mol. Neurobiol.* 45, 366–378.
- Cereghino, J.L., and Cregg, J.M. (2000). Heterologous protein expression in the methylotrophic yeast *Pichia pastoris*. *FEMS Microbiol. Rev.* 24, 45–66.
- Chasseigneaux, S., and Allinquant, B. (2012). Functions of A β , sAPP α and sAPP β : similarities and differences. *J. Neurochem.* 120 Suppl 1, 99–108.
- Chen, X., and Yan, S.D. (2006). Mitochondrial Abeta: a potential cause of metabolic dysfunction in Alzheimer's disease. *IUBMB Life* 58, 686–694.
- Cheng, G., Yu, Z., Zhou, D., and Mattson, M.P. (2002). Phosphatidylinositol-3-kinase-Akt kinase and p42/p44 mitogen-activated protein kinases mediate neurotrophic and excitoprotective actions of a secreted form of amyloid precursor protein. *Exp. Neurol.* 175, 407–414.
- Chesser, A.S., Pritchard, S.M., and Johnson, G.V.W. (2013). Tau Clearance Mechanisms and Their Possible Role in the Pathogenesis of Alzheimer Disease. *Front Neurol* 4, 122.
- Chiba, K., Araseki, M., Nozawa, K., Furukori, K., Araki, Y., Matsushima, T., Nakaya, T., Hata, S., Saito, Y., Uchida, S., et al. (2014). Quantitative analysis of APP axonal transport in neurons- Role of JIP1 in enhanced APP anterograde transport. *Mol. Biol. Cell.*
- Chong, Z.Z., Shang, Y.C., Wang, S., and Maiese, K. (2012). A Critical Kinase Cascade in Neurological Disorders: PI 3-K, Akt, and mTOR. *Future Neurol* 7, 733–748.
- Congdon, E.E., Wu, J.W., Myeku, N., Figueroa, Y.H., Herman, M., Marinec, P.S., Gestwicki, J.E., Dickey, C.A., Yu, W.H., and Duff, K.E. (2012). Methylthioninium chloride (methylene blue) induces autophagy and attenuates tauopathy in vitro and in vivo. *Autophagy* 8, 609–622.
- Copanaki, E., Chang, S., Vlachos, A., Tschäpe, J.-A., Müller, U.C., Kögel, D., and Deller, T. (2010). sAPP α antagonizes dendritic degeneration and neuron death triggered by proteasomal stress. *Mol. Cell. Neurosci.* 44, 386–393.
- Corbett, A., Pickett, J., Burns, A., Corcoran, J., Dunnett, S.B., Edison, P., Hagan, J.J., Holmes, C., Jones, E., Katona, C., et al. (2012). Drug repositioning for Alzheimer's disease. *Nat Rev Drug Discov* 11, 833–846.

- Corrigan, F., Pham, C.L.L., Vink, R., Blumbergs, P.C., Masters, C.L., van den Heuvel, C., and Cappai, R. (2011). The neuroprotective domains of the amyloid precursor protein, in traumatic brain injury, are located in the two growth factor domains. *Brain Res.* 1378, 137–143.
- Corrigan, F., Vink, R., Blumbergs, P.C., Masters, C.L., Cappai, R., and van den Heuvel, C. (2012). sAPP α rescues deficits in amyloid precursor protein knockout mice following focal traumatic brain injury. *J. Neurochem.* 122, 208–220.
- Corrigan, F., Thornton, E., Roisman, L.C., Leonard, A.V., Vink, R., Blumbergs, P.C., van den Heuvel, C., and Cappai, R. (2014). The neuroprotective activity of the amyloid precursor protein against traumatic brain injury is mediated via the heparin binding site in residues 96–110. *J. Neurochem.* 128, 196–204.
- Coulson, E.J., Paliga, K., Beyreuther, K., and Masters, C.L. (2000). What the evolution of the amyloid protein precursor supergene family tells us about its function. *Neurochem. Int.* 36, 175–184.
- Crews, L., and Masliah, E. (2010). Molecular mechanisms of neurodegeneration in Alzheimer's disease. *Hum. Mol. Genet.* 19, R12–R20.
- Cribbs, D.H., Berchtold, N.C., Perreau, V., Coleman, P.D., Rogers, J., Tenner, A.J., and Cotman, C.W. (2012). Extensive innate immune gene activation accompanies brain aging, increasing vulnerability to cognitive decline and neurodegeneration: a microarray study. *J. Neuroinflammation* 9, 179.
- Cuervo, A.M., Bergamini, E., Brunk, U.T., Dröge, W., Ffrench, M., and Terman, A. (2005). Autophagy and Aging: The Importance of Maintaining “Clean” Cells. *Autophagy* 1, 131–140.
- D'Amelio, M., Cavallucci, V., Middei, S., Marchetti, C., Pacioni, S., Ferri, A., Diamantini, A., De Zio, D., Carrara, P., Battistini, L., et al. (2011). Caspase-3 triggers early synaptic dysfunction in a mouse model of Alzheimer's disease. *Nat. Neurosci.* 14, 69–76.
- D'Amelio, M., Sheng, M., and Cecconi, F. (2012). Caspase-3 in the central nervous system: beyond apoptosis. *Trends Neurosci.* 35, 700–709.
- Davis, S.J., and Crispin, M. (2011). Solutions to the Glycosylation Problem for Low- and High-Throughput Structural Glycoproteomics. In *Functional and Structural Proteomics of Glycoproteins*, R. Owens, and J. Nettleship, eds. (Springer Netherlands), pp. 127–158.
- Dawkins, E., and Small, D.H. (2014). Insights into the physiological function of the β -amyloid precursor protein: beyond Alzheimer's disease. *J. Neurochem.* 129, 756–769.
- Delisle, B.P., Underkofler, H.A.S., Moungey, B.M., Slind, J.K., Kilby, J.A., Best, J.M., Foell, J.D., Balijepalli, R.C., Kamp, T.J., and January, C.T. (2009). Small GTPase Determinants for the Golgi Processing and Plasmalemmal Expression of Human Ether-a-go-go Related (hERG) K⁺ Channels. *J. Biol. Chem.* 284, 2844–2853.
- Deng, Y., Qu, Z., and Naqvi, N.I. (2012). Role of Macroautophagy in Nutrient Homeostasis During Fungal Development and Pathogenesis. *Cells* 1, 449–463.
- Desikan, R.S., Cabral, H.J., Hess, C.P., Dillon, W.P., Glastonbury, C.M., Weiner, M.W., Schmansky, N.J., Greve, D.N., Salat, D.H., Buckner, R.L., et al. (2009). Automated MRI measures identify individuals with mild cognitive impairment and Alzheimer's disease. *Brain* 132, 2048–2057.

- Dewji, N.N., and Do, C. (1996). Heat shock factor-1 mediates the transcriptional activation of Alzheimer's beta-amyloid precursor protein gene in response to stress. *Brain Res. Mol. Brain Res.* 35, 325–328.
- Deyts, C., Vetrivel, K.S., Das, S., Shepherd, Y.M., Dupré, D.J., Thinakaran, G., and Parent, A.T. (2012b). Novel GαS-protein signaling associated with membrane-tethered amyloid precursor protein intracellular domain. *J. Neurosci.* 32, 1714–1729.
- Dunai, Z., Bauer, P.I., and Mihalik, R. (2011). Necroptosis: biochemical, physiological and pathological aspects. *Pathol. Oncol. Res.* 17, 791–800.
- Eckert, G.P., Chang, S., Eckmann, J., Copanaki, E., Hagl, S., Hener, U., Müller, W.E., and Kögel, D. (2011). Liposome-incorporated DHA increases neuronal survival by enhancing non-amyloidogenic APP processing. *Biochim. Biophys. Acta* 1808, 236–243.
- Eggert, S., Paliga, K., Soba, P., Evin, G., Masters, C.L., Weidemann, A., and Beyreuther, K. (2004). The proteolytic processing of the amyloid precursor protein gene family members APLP-1 and APLP-2 involves alpha-, beta-, gamma-, and epsilon-like cleavages: modulation of APLP-1 processing by n-glycosylation. *J. Biol. Chem.* 279, 18146–18156.
- Endo, H., Nito, C., Kamada, H., Nishi, T., and Chan, P.H. (2006). Activation of the Akt/GSK3beta signaling pathway mediates survival of vulnerable hippocampal neurons after transient global cerebral ischemia in rats. *J. Cereb. Blood Flow Metab.* 26, 1479–1489.
- Endres, K., and Fahrenholz, F. (2012). The Role of the anti-amyloidogenic secretase ADAM10 in shedding the APP-like proteins. *Curr Alzheimer Res* 9, 157–164.
- Fahrenholz, F. (2007). Alpha-secretase as a therapeutic target. *Curr Alzheimer Res* 4, 412–417.
- Fjell, A.M., McEvoy, L., Holland, D., Dale, A.M., and Walhovd, K.B. (2014). What is normal in normal aging? Effects of aging, amyloid and Alzheimer's disease on the cerebral cortex and the hippocampus. *Progress in Neurobiology* 117, 20–40.
- Fjorback, A.W., Seaman, M., Gustafsen, C., Mehmedbasic, A., Gokool, S., Wu, C., Militz, D., Schmidt, V., Madsen, P., Nyengaard, J.R., et al. (2012). Retromer binds the FANSHY sorting motif in SorLA to regulate amyloid precursor protein sorting and processing. *J. Neurosci.* 32, 1467–1480.
- Fogel, H., Frere, S., Segev, O., Bharill, S., Shapira, I., Gazit, N., O'Malley, T., Slomowitz, E., Berdichevsky, Y., Walsh, D.M., et al. (2014). APP homodimers transduce an amyloid-β-mediated increase in release probability at excitatory synapses. *Cell Rep* 7, 1560–1576.
- Förstl, H., and Kurz, A. (1999). Clinical features of Alzheimer's disease. *Eur Arch Psychiatry Clin Neurosci* 249, 288–290.
- Franceschi, C., Capri, M., Monti, D., Giunta, S., Olivieri, F., Sevini, F., Panourgia, M.P., Invidia, L., Celani, L., Scurti, M., et al. (2007). Inflammaging and anti-inflammaging: a systemic perspective on aging and longevity emerged from studies in humans. *Mech. Ageing Dev.* 128, 92–105.
- Freude, S., Schilbach, K., and Schubert, M. (2009). The role of IGF-1 receptor and insulin receptor signaling for the pathogenesis of Alzheimer's disease: from model organisms to human disease. *Curr Alzheimer Res* 6, 213–223.
- Fuchs, Y., and Steller, H. (2011). Programmed cell death in animal development and disease. *Cell* 147, 742–758.

- Furst, A.J., Rabinovici, G.D., Rostomian, A.H., Steed, T., Alkalay, A., Racine, C., Miller, B.L., and Jagust, W.J. (2012). Cognition, glucose metabolism and amyloid burden in Alzheimer's disease. *Neurobiol. Aging* 33, 215–225.
- Furukawa, K., and Mattson, M.P. (1998). Secreted amyloid precursor protein alpha selectively suppresses N-methyl-D-aspartate currents in hippocampal neurons: involvement of cyclic GMP. *Neuroscience* 83, 429–438.
- Furukawa, K., Sopher, B.L., Rydel, R.E., Begley, J.G., Pham, D.G., Martin, G.M., Fox, M., and Mattson, M.P. (1996). Increased activity-regulating and neuroprotective efficacy of alpha-secretase-derived secreted amyloid precursor protein conferred by a C-terminal heparin-binding domain. *J. Neurochem.* 67, 1882–1896.
- Galluzzi, L., Maiuri, M.C., Vitale, I., Zischka, H., Castedo, M., Zitvogel, L., and Kroemer, G. (2007). Cell death modalities: classification and pathophysiological implications. *Cell Death Differ.* 14, 1237–1243.
- Galluzzi, L., Vitale, I., Abrams, J.M., Alnemri, E.S., Baehrecke, E.H., Blagosklonny, M.V., Dawson, T.M., Dawson, V.L., El-Deiry, W.S., Fulda, S., et al. (2012). Molecular definitions of cell death subroutines: recommendations of the Nomenclature Committee on Cell Death 2012. *Cell Death Differ.* 19, 107–120.
- Garcia, M.L., and Cleveland, D.W. (2001). Going new places using an old MAP: tau, microtubules and human neurodegenerative disease. *Curr. Opin. Cell Biol.* 13, 41–48.
- Geddes, J.W., Schwab, C., Craddock, S., Wilson, J.L., and Pettigrew, L.C. (1994). Alterations in tau immunostaining in the rat hippocampus following transient cerebral ischemia. *J. Cereb. Blood Flow Metab.* 14, 554–564.
- Ghavami, S., Shojaei, S., Yeganeh, B., Ande, S.R., Jangamreddy, J.R., Mehrpour, M., Christoffersson, J., Chaabane, W., Moghadam, A.R., Kashani, H.H., et al. (2014). Autophagy and apoptosis dysfunction in neurodegenerative disorders. *Prog. Neurobiol.* 112, 24–49.
- Glenner, G.G., and Wong, C.W. (2012). Alzheimer's disease: initial report of the purification and characterization of a novel cerebrovascular amyloid protein. 1984. *Biochem. Biophys. Res. Commun.* 425, 534–539.
- Glickman, M.H., and Ciechanover, A. (2002). The ubiquitin-proteasome proteolytic pathway: destruction for the sake of construction. *Physiol. Rev.* 82, 373–428.
- Goate, A. (2006). Segregation of a missense mutation in the amyloid beta-protein precursor gene with familial Alzheimer's disease. *J. Alzheimers Dis.* 9, 341–347.
- Goedert, M., and Spillantini, M.G. (2006). A century of Alzheimer's disease. *Science* 314, 777–781.
- Gonzalez-Gronow, M., Kaczowka, S.J., Payne, S., Wang, F., Gawdi, G., and Pizzo, S.V. (2007). Plasminogen Structural Domains Exhibit Different Functions When Associated with Cell Surface GRP78 or the Voltage-dependent Anion Channel. *J. Biol. Chem.* 282, 32811–32820.
- Gottfried, Y., Rotem, A., Lotan, R., Steller, H., and Larisch, S. (2004). The mitochondrial ARTS protein promotes apoptosis through targeting XIAP. *EMBO J.* 23, 1627–1635.
- Gough, M., Blanthorn-Hazell, S., Delury, C., and Parkin, E. (2014). The E1 copper binding domain of full-length amyloid precursor protein mitigates copper-induced growth inhibition in brain metastatic prostate cancer DU145 cells. *Biochem. Biophys. Res. Commun.*

- Gralle, M., and Ferreira, S.T. (2007). Structure and functions of the human amyloid precursor protein: the whole is more than the sum of its parts. *Prog. Neurobiol.* 82, 11–32.
- Gralle, M., Oliveira, C.L.P., Guerreiro, L.H., McKinstry, W.J., Galatis, D., Masters, C.L., Cappai, R., Parker, M.W., Ramos, C.H.I., Torriani, I., et al. (2006). Solution conformation and heparin-induced dimerization of the full-length extracellular domain of the human amyloid precursor protein. *J. Mol. Biol.* 357, 493–508.
- Gralle, M., Botelho, M.G., and Wouters, F.S. (2009). Neuroprotective secreted amyloid precursor protein acts by disrupting amyloid precursor protein dimers. *J. Biol. Chem.* 284, 15016–15025.
- Gray, E.G., Paula-Barbosa, M., and Roher, A. (1987). Alzheimer's disease: paired helical filaments and cytomembranes. *Neuropathol. Appl. Neurobiol.* 13, 91–110.
- Greenberg, S.M., Qiu, W.Q., Selkoe, D.J., Ben-Itzhak, A., and Kosik, K.S. (1995). Amino-terminal region of the beta-amyloid precursor protein activates mitogen-activated protein kinase. *Neurosci. Lett.* 198, 52–56.
- Grossmann, J. (2002). Molecular mechanisms of “detachment-induced apoptosis--Anoikis.” *Apoptosis* 7, 247–260.
- Guo, Q., Furukawa, K., Sopher, B.L., Pham, D.G., Xie, J., Robinson, N., Martin, G.M., and Mattson, M.P. (1996). Alzheimer's PS-1 mutation perturbs calcium homeostasis and sensitizes PC12 cells to death induced by amyloid beta-peptide. *Neuroreport* 8, 379–383.
- Guo, Q., Wang, Z., Li, H., Wiese, M., and Zheng, H. (2012). APP physiological and pathophysiological functions: insights from animal models. *Cell Res.* 22, 78–89.
- Gupta, S. (2001). Molecular steps of tumor necrosis factor receptor-mediated apoptosis. *Curr. Mol. Med.* 1, 317–324.
- Haass, C., and De Strooper, B. (1999). The presenilins in Alzheimer's disease--proteolysis holds the key. *Science* 286, 916–919.
- Haass, C., Kaether, C., Thinakaran, G., and Sisodia, S. (2012). Trafficking and Proteolytic Processing of APP. *Cold Spring Harb Perspect Med* 2.
- Hampel, H., Bürger, K., Teipel, S.J., Bokde, A.L.W., Zetterberg, H., and Blennow, K. (2008). Core candidate neurochemical and imaging biomarkers of Alzheimer's disease. *Alzheimers Dement* 4, 38–48.
- Han, P., Dou, F., Li, F., Zhang, X., Zhang, Y.-W., Zheng, H., Lipton, S.A., Xu, H., and Liao, F.-F. (2005). Suppression of cyclin-dependent kinase 5 activation by amyloid precursor protein: a novel excitoprotective mechanism involving modulation of tau phosphorylation. *J. Neurosci.* 25, 11542–11552.
- Hardy, J., and Selkoe, D.J. (2002). The amyloid hypothesis of Alzheimer's disease: progress and problems on the road to therapeutics. *Science* 297, 353–356.
- Hartl, D., Klatt, S., Roch, M., Konthur, Z., Klose, J., Willnow, T.E., and Rohe, M. (2013). Soluble alpha-APP (sAPPalpha) regulates CDK5 expression and activity in neurons. *PLoS ONE* 8, e65920.
- Hatch, R.J., Reid, C.A., and Petrou, S. (2014). Enhanced in vitro CA1 network activity in a sodium channel $\beta 1$ (C121W) subunit model of genetic epilepsy. *Epilepsia* 55, 601–608.

- Hay, N., and Sonenberg, N. (2004). Upstream and downstream of mTOR. *Genes Dev.* *18*, 1926–1945.
- Heber, S., Herms, J., Gajic, V., Hainfellner, J., Aguzzi, A., Rüdliche, T., von Kretschmar, H., von Koch, C., Sisodia, S., Tremml, P., et al. (2000). Mice with combined gene knock-outs reveal essential and partially redundant functions of amyloid precursor protein family members. *J. Neurosci.* *20*, 7951–7963.
- Hernandez, F., Lucas, J.J., and Avila, J. (2013). GSK3 and tau: two convergence points in Alzheimer's disease. *J. Alzheimers Dis.* *33 Suppl 1*, S141–S144.
- Hers, I., Vincent, E.E., and Tavaré, J.M. (2011). Akt signalling in health and disease. *Cell. Signal.* *23*, 1515–1527.
- Van den Heuvel, C., Blumbergs, P.C., Finnie, J.W., Manavis, J., Jones, N.R., Reilly, P.L., and Pereira, R.A. (1999). Upregulation of amyloid precursor protein messenger RNA in response to traumatic brain injury: an ovine head impact model. *Exp. Neurol.* *159*, 441–450.
- Ho, A., and Südhof, T.C. (2004). Binding of F-spondin to amyloid-beta precursor protein: a candidate amyloid-beta precursor protein ligand that modulates amyloid-beta precursor protein cleavage. *Proc. Natl. Acad. Sci. U.S.A.* *101*, 2548–2553.
- Hoe, H.-S., Lee, H.-K., and Pak, D.T.S. (2012). The upside of APP at synapses. *CNS Neurosci Ther* *18*, 47–56.
- Hoggl, S., Kuhn, P.-H., Colombo, A., and Lichtenthaler, S.F. (2011). Determination of the proteolytic cleavage sites of the amyloid precursor-like protein 2 by the proteases ADAM10, BACE1 and γ -secretase. *PLoS ONE* *6*, e21337.
- Horgan, A.M., Lagrange, M.T., and Copenhaver, P.F. (1995). A developmental role for the heterotrimeric G protein Go alpha in a migratory population of embryonic neurons. *Dev. Biol.* *172*, 640–653.
- Huang, Y., and Mucke, L. (2012). Alzheimer mechanisms and therapeutic strategies. *Cell* *148*, 1204–1222.
- Hutton, M., Lendon, C.L., Rizzu, P., Baker, M., Froelich, S., Houlden, H., Pickering-Brown, S., Chakraverty, S., Isaacs, A., Grover, A., et al. (1998). Association of missense and 5'-splice-site mutations in tau with the inherited dementia FTDP-17. *Nature* *393*, 702–705.
- Hyman, B.T., and Yuan, J. (2012). Apoptotic and non-apoptotic roles of caspases in neuronal physiology and pathophysiology. *Nat. Rev. Neurosci.* *13*, 395–406.
- Iijima-Ando, K., Sekiya, M., Maruko-Otake, A., Ohtake, Y., Suzuki, E., Lu, B., and Iijima, K.M. (2012). Loss of axonal mitochondria promotes tau-mediated neurodegeneration and Alzheimer's disease-related tau phosphorylation via PAR-1. *PLoS Genet.* *8*, e1002918.
- Intlekofer, K.A., and Cotman, C.W. (2013). Exercise counteracts declining hippocampal function in aging and Alzheimer's disease. *Neurobiology of Disease* *57*, 47–55.
- Ivanusic, D., Madela, K., Laue, M., and Denner, J. (2014). Visualization of HIV-1 Budding Structures. *AIDS Res. Hum. Retroviruses*.
- Jimenez, S., Torres, M., Vizuite, M., Sanchez-Varo, R., Sanchez-Mejias, E., Trujillo-Estrada, L., Carmona-Cuenca, I., Caballero, C., Ruano, D., Gutierrez, A., et al. (2011). Age-dependent accumulation of soluble amyloid beta (A β) oligomers reverses the neuroprotective

- effect of soluble amyloid precursor protein- α (sAPP(α)) by modulating phosphatidylinositol 3-kinase (PI3K)/Akt-GSK-3 β pathway in Alzheimer mouse model. *J. Biol. Chem.* **286**, 18414–18425.
- Jonsson, T., Atwal, J.K., Steinberg, S., Snaedal, J., Jonsson, P.V., Bjornsson, S., Stefansson, H., Sulem, P., Gudbjartsson, D., Maloney, J., et al. (2012). A mutation in APP protects against Alzheimer's disease and age-related cognitive decline. *Nature* **488**, 96–99.
- Jope, R.S., and Johnson, G.V.W. (2004). The glamour and gloom of glycogen synthase kinase-3. *Trends Biochem. Sci.* **29**, 95–102.
- Jope, R.S., Yuskaitis, C.J., and Beurel, E. (2007). Glycogen synthase kinase-3 (GSK3): inflammation, diseases, and therapeutics. *Neurochem. Res.* **32**, 577–595.
- Kaczmarek, A., Vandenabeele, P., and Krysko, D.V. (2013). Necroptosis: the release of damage-associated molecular patterns and its physiological relevance. *Immunity* **38**, 209–223.
- Kaden, D., Munter, L.M., Reif, B., and Multhaup, G. (2012). The amyloid precursor protein and its homologues: structural and functional aspects of native and pathogenic oligomerization. *Eur. J. Cell Biol.* **91**, 234–239.
- Kamboh, M.I. (2004). Molecular genetics of late-onset Alzheimer's disease. *Ann. Hum. Genet.* **68**, 381–404.
- Karran, E., Mercken, M., and De Strooper, B. (2011). The amyloid cascade hypothesis for Alzheimer's disease: an appraisal for the development of therapeutics. *Nat Rev Drug Discov* **10**, 698–712.
- Kawahara, M. (2010). Neurotoxicity of β -Amyloid Protein: Oligomerization, Channel Formation and Calcium Dyshomeostasis. *Current Pharmaceutical Design* **16**, 2779–2789.
- Kern, A., Roempp, B., Prager, K., Walter, J., and Behl, C. (2006). Down-regulation of endogenous amyloid precursor protein processing due to cellular aging. *J. Biol. Chem.* **281**, 2405–2413.
- Kerr, J.F., Wyllie, A.H., and Currie, A.R. (1972). Apoptosis: a basic biological phenomenon with wide-ranging implications in tissue kinetics. *Br. J. Cancer* **26**, 239–257.
- Khandelwal, P.J., Herman, A.M., and Moussa, C.E.-H. (2011). Inflammation in the early stages of neurodegenerative pathology. *J. Neuroimmunol.* **238**, 1–11.
- Kim, D., and Tsai, L.-H. (2009). Bridging physiology and pathology in AD. *Cell* **137**, 997–1000.
- Kim, N., Kim, J.Y., and Yenari, M.A. (2012). Anti-inflammatory properties and pharmacological induction of Hsp70 after brain injury. *Inflammopharmacology* **20**, 177–185.
- Kim, R., Emi, M., and Tanabe, K. (2006). Role of mitochondria as the gardens of cell death. *Cancer Chemother. Pharmacol.* **57**, 545–553.
- Kögel, D., Schomburg, R., Schürmann, T., Reimertz, C., König, H.-G., Poppe, M., Eckert, A., Müller, W.E., and Prehn, J.H.M. (2003). The amyloid precursor protein protects PC12 cells against endoplasmic reticulum stress-induced apoptosis. *J. Neurochem.* **87**, 248–256.
- Kögel, D., Schomburg, R., Copanaki, E., and Prehn, J.H.M. (2005). Regulation of gene expression by the amyloid precursor protein: inhibition of the JNK/c-Jun pathway. *Cell Death Differ.* **12**, 1–9.

- Kögel, D., Fulda, S., and Mittelbronn, M. (2010). Therapeutic exploitation of apoptosis and autophagy for glioblastoma. *Anticancer Agents Med Chem* 10, 438–449.
- Kögel, D., Concannon, C.G., Müller, T., König, H., Bonner, C., Poeschel, S., Chang, S., Egensperger, R., and Prehn, J.H.M. (2012a). The APP intracellular domain (AICD) potentiates ER stress-induced apoptosis. *Neurobiol. Aging* 33, 2200–2209.
- Kögel, D., Deller, T., and Behl, C. (2012b). Roles of amyloid precursor protein family members in neuroprotection, stress signaling and aging. *Exp Brain Res* 217, 471–479.
- Kohli, B.M., Pflieger, D., Mueller, L.N., Carbonetti, G., Aebersold, R., Nitsch, R.M., and Konietzko, U. (2012). Interactome of the amyloid precursor protein APP in brain reveals a protein network involved in synaptic vesicle turnover and a close association with Synaptotagmin-1. *J. Proteome Res.* 11, 4075–4090.
- Koo, E.H., and Squazzo, S.L. (1994). Evidence that production and release of amyloid beta-protein involves the endocytic pathway. *J. Biol. Chem.* 269, 17386–17389.
- Korolchuk, V.I., Mansilla, A., Menzies, F.M., and Rubinsztein, D.C. (2009). Autophagy inhibition compromises degradation of ubiquitin-proteasome pathway substrates. *Mol. Cell* 33, 517–527.
- Korte, M., Herrmann, U., Zhang, X., and Draguhn, A. (2012). The role of APP and APLP for synaptic transmission, plasticity, and network function: lessons from genetic mouse models. *Exp Brain Res* 217, 435–440.
- Kroemer, G., El-Deiry, W.S., Golstein, P., Peter, M.E., Vaux, D., Vandenabeele, P., Zhivotovsky, B., Blagosklonny, M.V., Malorni, W., Knight, R.A., et al. (2005). Classification of cell death: recommendations of the Nomenclature Committee on Cell Death. *Cell Death Differ* 12, 1463–1467.
- Krstic, D., and Knuesel, I. (2013). Deciphering the mechanism underlying late-onset Alzheimer disease. *Nat Rev Neurol* 9, 25–34.
- Krstic, D., Madhusudan, A., Doehner, J., Vogel, P., Notter, T., Imhof, C., Manalastas, A., Hilfiker, M., Pfister, S., Schwerdel, C., et al. (2012). Systemic immune challenges trigger and drive Alzheimer-like neuropathology in mice. *J Neuroinflammation* 9, 151.
- Kudo, T., Iqbal, K., Ravid, R., Swaab, D.F., and Grundke-Iqbal, I. (1994). Alzheimer disease: correlation of cerebro-spinal fluid and brain ubiquitin levels. *Brain Res.* 639, 1–7.
- Lacor, P.N., Buniel, M.C., Furlow, P.W., Clemente, A.S., Velasco, P.T., Wood, M., Viola, K.L., and Klein, W.L. (2007). Abeta oligomer-induced aberrations in synapse composition, shape, and density provide a molecular basis for loss of connectivity in Alzheimer's disease. *J. Neurosci.* 27, 796–807.
- Laemmli, U.K. (1970). Cleavage of structural proteins during the assembly of the head of bacteriophage T4. *Nature* 227, 680–685.
- LaFerla, F.M. (2002). Calcium dyshomeostasis and intracellular signalling in Alzheimer's disease. *Nat. Rev. Neurosci.* 3, 862–872.
- Lassmann, H., Bancher, C., Breitschopf, H., Wegiel, J., Bobinski, M., Jellinger, K., and Wisniewski, H.M. (1995). Cell death in Alzheimer's disease evaluated by DNA fragmentation in situ. *Acta Neuropathol.* 89, 35–41.

- Lavrik, I., Golks, A., and Krammer, P.H. (2005a). Death receptor signaling. *J. Cell. Sci.* *118*, 265–267.
- Lavrik, I.N., Golks, A., and Krammer, P.H. (2005b). Caspases: pharmacological manipulation of cell death. *J. Clin. Invest.* *115*, 2665–2672.
- Lee, C.H., Ahn, J.H., and Won, M.-H. (2014). New expression of 5-HT_{1A} receptor in astrocytes in the gerbil hippocampal CA1 region following transient global cerebral ischemia. *Neurol. Sci.*
- Lee, M.J., Lee, J.H., and Rubinsztein, D.C. (2013). Tau degradation: the ubiquitin-proteasome system versus the autophagy-lysosome system. *Prog. Neurobiol.* *105*, 49–59.
- Li, H., Wang, B., Wang, Z., Guo, Q., Tabuchi, K., Hammer, R.E., Südhof, T.C., and Zheng, H. (2010). Soluble amyloid precursor protein (APP) regulates transthyretin and Klotho gene expression without rescuing the essential function of APP. *Proc. Natl. Acad. Sci. U.S.A.* *107*, 17362–17367.
- Lin, N.-Y., Beyer, C., Gießl, A., Kireva, T., Scholtysek, C., Uderhardt, S., Munoz, L.E., Dees, C., Distler, A., Wirtz, S., et al. (2013). Autophagy regulates TNF α -mediated joint destruction in experimental arthritis. *Ann Rheum Dis* *72*, 761–768.
- Lipinski, M.M., Zheng, B., Lu, T., Yan, Z., Py, B.F., Ng, A., Xavier, R.J., Li, C., Yankner, B.A., Scherzer, C.R., et al. (2010). Genome-wide analysis reveals mechanisms modulating autophagy in normal brain aging and in Alzheimer's disease. *PNAS* *107*, 14164–14169.
- Loo, D.T., Copani, A., Pike, C.J., Whittemore, E.R., Walencewicz, A.J., and Cotman, C.W. (1993). Apoptosis is induced by beta-amyloid in cultured central nervous system neurons. *Proc Natl Acad Sci U S A* *90*, 7951–7955.
- Lorent, K., Overbergh, L., Moechars, D., De Strooper, B., Van Leuven, F., and Van den Berghe, H. (1995). Expression in mouse embryos and in adult mouse brain of three members of the amyloid precursor protein family, of the alpha-2-macroglobulin receptor/low density lipoprotein receptor-related protein and of its ligands apolipoprotein E, lipoprotein lipase, alpha-2-macroglobulin and the 40,000 molecular weight receptor-associated protein. *Neuroscience* *65*, 1009–1025.
- Lourenço, F.C., Galvan, V., Fombonne, J., Corset, V., Llambi, F., Müller, U., Bredesen, D.E., and Mehlen, P. (2009). Netrin-1 interacts with amyloid precursor protein and regulates amyloid-beta production. *Cell Death Differ.* *16*, 655–663.
- De Luca, A., Maiello, M.R., D'Alessio, A., Pergameno, M., and Normanno, N. (2012). The RAS/RAF/MEK/ERK and the PI3K/AKT signalling pathways: role in cancer pathogenesis and implications for therapeutic approaches. *Expert Opin. Ther. Targets* *16 Suppl 2*, S17–S27.
- Manczak, M., Anekonda, T.S., Henson, E., Park, B.S., Quinn, J., and Reddy, P.H. (2006). Mitochondria are a direct site of A β accumulation in Alzheimer's disease neurons: implications for free radical generation and oxidative damage in disease progression. *Hum. Mol. Genet.* *15*, 1437–1449.
- Mandelkow, E. (1999). Alzheimer's disease. The tangled tale of tau. *Nature* *402*, 588–589.
- Mandelkow, E.-M., and Mandelkow, E. (2012). Biochemistry and Cell Biology of Tau Protein in Neurofibrillary Degeneration. *Cold Spring Harb Perspect Med* *2*, a006247.

- Manning, B.D., and Cantley, L.C. (2007). AKT/PKB signaling: navigating downstream. *Cell* 129, 1261–1274.
- Marksteiner, J., Hinterhuber, H., and Humpel, C. (2007). Cerebrospinal fluid biomarkers for diagnosis of Alzheimer's disease: beta-amyloid(1-42), tau, phospho-tau-181 and total protein. *Drugs Today* 43, 423–431.
- Martin-Morris, L.E., and White, K. (1990). The *Drosophila* transcript encoded by the beta-amyloid protein precursor-like gene is restricted to the nervous system. *Development* 110, 185–195.
- Maslah, E., Westland, C.E., Rockenstein, E.M., Abraham, C.R., Mallory, M., Veinberg, I., Sheldon, E., and Mucke, L. (1997). Amyloid precursor proteins protect neurons of transgenic mice against acute and chronic excitotoxic injuries in vivo. *Neuroscience* 78, 135–146.
- Mattson, M.P., Cheng, B., Culwell, A.R., Esch, F.S., Lieberburg, I., and Rydel, R.E. (1993). Evidence for excitoprotective and intraneuronal calcium-regulating roles for secreted forms of the beta-amyloid precursor protein. *Neuron* 10, 243–254.
- Mattson, M.P., Mark, R.J., Furukawa, K., and Bruce, A.J. (1997). Disruption of brain cell ion homeostasis in Alzheimer's disease by oxy radicals, and signaling pathways that protect therefrom. *Chem. Res. Toxicol.* 10, 507–517.
- Maurer, U., Preiss, F., Brauns-Schubert, P., Schlicher, L., and Charvet, C. (2014). GSK-3 - at the crossroads of cell death and survival. *J. Cell. Sci.* 127, 1369–1378.
- Meng, L., Mohan, R., Kwok, B.H., Elofsson, M., Sin, N., and Crews, C.M. (1999). Epoxomicin, a potent and selective proteasome inhibitor, exhibits in vivo antiinflammatory activity. *Proc. Natl. Acad. Sci. U.S.A.* 96, 10403–10408.
- Merdes, G., Soba, P., Loewer, A., Bilic, M.V., Beyreuther, K., and Paro, R. (2004). Interference of human and *Drosophila* APP and APP-like proteins with PNS development in *Drosophila*. *EMBO J.* 23, 4082–4095.
- Midthune, B., Tyan, S.-H., Walsh, J.J., Sarsoza, F., Eggert, S., Hof, P.R., Dickstein, D.L., and Koo, E.H. (2012). Deletion of the amyloid precursor-like protein 2 (APLP2) does not affect hippocampal neuron morphology or function. *Mol. Cell. Neurosci.* 49, 448–455.
- Mielke, K., and Herdegen, T. (2000). JNK and p38 stresskinases--degenerative effectors of signal-transduction-cascades in the nervous system. *Prog. Neurobiol.* 61, 45–60.
- Minogue, A.M., Stubbs, A.K., Frigerio, C.S., Boland, B., Fadeeva, J.V., Tang, J., Selkoe, D.J., and Walsh, D.M. (2009). gamma-secretase processing of APLP1 leads to the production of a p3-like peptide that does not aggregate and is not toxic to neurons. *Brain Res.* 1262, 89–99.
- Moffat, J., Grueneberg, D.A., Yang, X., Kim, S.Y., Kloepfer, A.M., Hinkle, G., Piqani, B., Eisenhaure, T.M., Luo, B., Grenier, J.K., et al. (2006). A lentiviral RNAi library for human and mouse genes applied to an arrayed viral high-content screen. *Cell* 124, 1283–1298.
- Moriguchi, T., Toyoshima, F., Masuyama, N., Hanafusa, H., Gotoh, Y., and Nishida, E. (1997). A novel SAPK/JNK kinase, MKK7, stimulated by TNFalpha and cellular stresses. *EMBO J.* 16, 7045–7053.
- Morris, M., Maeda, S., Vossel, K., and Mucke, L. (2011). The Many Faces of Tau. *Neuron* 70, 410–426.

- Mudher, A., and Lovestone, S. (2002). Alzheimer's disease-do tauists and baptists finally shake hands? *Trends Neurosci.* 25, 22–26.
- Muller, U.C., and Zheng, H. (2012). Physiological Functions of APP Family Proteins. *Cold Spring Harb Perspect Med* 2.
- Müller, U.C., and Zheng, H. (2012). Physiological functions of APP family proteins. *Cold Spring Harb Perspect Med* 2, a006288.
- Müller, T., Meyer, H.E., Egensperger, R., and Marcus, K. (2008). The amyloid precursor protein intracellular domain (AICD) as modulator of gene expression, apoptosis, and cytoskeletal dynamics-relevance for Alzheimer's disease. *Prog. Neurobiol.* 85, 393–406.
- Müller, U.C., Pietrzik, C.U., and Deller, T. (2012). The physiological functions of the β -amyloid precursor protein APP. *Exp Brain Res* 217, 325–329.
- Murakami, N., Yamaki, T., Iwamoto, Y., Sakakibara, T., Kobori, N., Fushiki, S., and Ueda, S. (1998). Experimental brain injury induces expression of amyloid precursor protein, which may be related to neuronal loss in the hippocampus. *J. Neurotrauma* 15, 993–1003.
- Murga, C., Laguinge, L., Wetzker, R., Cuadrado, A., and Gutkind, J.S. (1998). Activation of Akt/protein kinase B by G protein-coupled receptors. A role for alpha and beta gamma subunits of heterotrimeric G proteins acting through phosphatidylinositol-3-OH kinasegamma. *J. Biol. Chem.* 273, 19080–19085.
- Murga, C., Fukuhara, S., and Gutkind, J.S. (2000). A novel role for phosphatidylinositol 3-kinase beta in signaling from G protein-coupled receptors to Akt. *J. Biol. Chem.* 275, 12069–12073.
- Nagele, E., Han, M., DeMarshall, C., Belinka, B., and Nagele, R. (2011). Diagnosis of Alzheimer's Disease Based on Disease-Specific Autoantibody Profiles in Human Sera. *PLoS ONE* 6, e23112.
- Nhan, H.S., Chiang, K., and Koo, E.H. (2014). The multifaceted nature of amyloid precursor protein and its proteolytic fragments: friends and foes. *Acta Neuropathol* 1–19.
- Nicolas, M., and Hassan, B.A. (2014). Amyloid precursor protein and neural development. *Development* 141, 2543–2548.
- Nikolaev, A., McLaughlin, T., O'Leary, D.D.M., and Tessier-Lavigne, M. (2009). APP binds DR6 to trigger axon pruning and neuron death via distinct caspases. *Nature* 457, 981–989.
- Nishimoto, I., Okamoto, T., Matsuura, Y., Takahashi, S., Okamoto, T., Murayama, Y., and Ogata, E. (1993). Alzheimer amyloid protein precursor complexes with brain GTP-binding protein G(o). *Nature* 362, 75–79.
- Nistor, M., Don, M., Parekh, M., Sarsoza, F., Goodus, M., Lopez, G.E., Kawas, C., Leverenz, J., Doran, E., Lott, I.T., et al. (2007). Alpha- and beta-secretase activity as a function of age and beta-amyloid in Down syndrome and normal brain. *Neurobiol. Aging* 28, 1493–1506.
- Nizzari, M., Venezia, V., Repetto, E., Caorsi, V., Magrassi, R., Gagliani, M.C., Carlo, P., Florio, T., Schettini, G., Tacchetti, C., et al. (2007). Amyloid precursor protein and Presenilin1 interact with the adaptor GRB2 and modulate ERK 1,2 signaling. *J. Biol. Chem.* 282, 13833–13844.

- Noda, Y., Asada, M., Kubota, M., Maesako, M., Watanabe, K., Uemura, M., Kihara, T., Shimohama, S., Takahashi, R., Kinoshita, A., et al. (2013). Copper enhances APP dimerization and promotes A β production. *Neurosci. Lett.* 547, 10–15.
- Ohta, K., Mizuno, A., Ueda, M., Li, S., Suzuki, Y., Hida, Y., Hayakawa-Yano, Y., Itoh, M., Ohta, E., Kobori, M., et al. (2010). Autophagy impairment stimulates PS1 expression and γ -secretase activity. *Autophagy* 6, 345–352.
- Orrenius, S., Nicotera, P., and Zhivotovsky, B. (2011). Cell death mechanisms and their implications in toxicology. *Toxicol. Sci.* 119, 3–19.
- Ozaki, T., Li, Y., Kikuchi, H., Tomita, T., Iwatsubo, T., and Nakagawara, A. (2006). The intracellular domain of the amyloid precursor protein (AICD) enhances the p53-mediated apoptosis. *Biochem. Biophys. Res. Commun.* 351, 57–63.
- Park, J.H., Gimbel, D.A., GrandPre, T., Lee, J.-K., Kim, J.-E., Li, W., Lee, D.H.S., and Strittmatter, S.M. (2006). Alzheimer precursor protein interaction with the Nogo-66 receptor reduces amyloid-beta plaque deposition. *J. Neurosci.* 26, 1386–1395.
- Patel, A.S., Lin, L., Geyer, A., Haspel, J.A., An, C.H., Cao, J., Rosas, I.O., and Morse, D. (2012). Autophagy in Idiopathic Pulmonary Fibrosis. *PLoS ONE* 7, e41394.
- Peter, M.E. (2011). Programmed cell death: Apoptosis meets necrosis. *Nature* 471, 310–312.
- Pinto, M., Morange, M., and Bensaude, O. (1991). Denaturation of proteins during heat shock. In vivo recovery of solubility and activity of reporter enzymes. *J. Biol. Chem.* 266, 13941–13946.
- Plotnikov, A., Zehorai, E., Procaccia, S., and Seger, R. (2011). The MAPK cascades: signaling components, nuclear roles and mechanisms of nuclear translocation. *Biochim. Biophys. Acta* 1813, 1619–1633.
- Pluta, R., Jabłoński, M., Ułamek-Kozioł, M., Kocki, J., Brzozowska, J., Januszewski, S., Furmaga-Jabłońska, W., Bogucka-Kocka, A., Maciejewski, R., and Czuczwar, S.J. (2013). Sporadic Alzheimer's disease begins as episodes of brain ischemia and ischemically dysregulated Alzheimer's disease genes. *Mol. Neurobiol.* 48, 500–515.
- Pohanka, M. (2011). Cholinesterases, a target of pharmacology and toxicology. *Biomed Pap Med Fac Univ Palacky Olomouc Czech Repub* 155, 219–229.
- Postina, R. (2008). A closer look at alpha-secretase. *Curr Alzheimer Res* 5, 179–186.
- Proskuryakov, S.Y., Konoplyannikov, A.G., and Gabai, V.L. (2003). Necrosis: a specific form of programmed cell death? *Exp. Cell Res.* 283, 1–16.
- Püntener, U., Booth, S.G., Perry, V.H., and Teeling, J.L. (2012). Long-term impact of systemic bacterial infection on the cerebral vasculature and microglia. *J Neuroinflammation* 9, 146.
- Putcha, G.V., Le, S., Frank, S., Besirli, C.G., Clark, K., Chu, B., Alix, S., Youle, R.J., LaMarche, A., Maroney, A.C., et al. (2003). JNK-mediated BIM phosphorylation potentiates BAX-dependent apoptosis. *Neuron* 38, 899–914.
- Reinhard, C., Hébert, S.S., and De Strooper, B. (2005). The amyloid-beta precursor protein: integrating structure with biological function. *EMBO J.* 24, 3996–4006.

- Reinhard, C., Borgers, M., David, G., and De Strooper, B. (2013). Soluble amyloid- β precursor protein binds its cell surface receptor in a cooperative fashion with glypican and syndecan proteoglycans. *J. Cell. Sci.* 126, 4856–4861.
- Ring, S., Weyer, S.W., Kilian, S.B., Waldron, E., Pietrzik, C.U., Filippov, M.A., Herms, J., Buchholz, C., Eckman, C.B., Korte, M., et al. (2007). The secreted beta-amyloid precursor protein ectodomain APPs alpha is sufficient to rescue the anatomical, behavioral, and electrophysiological abnormalities of APP-deficient mice. *J. Neurosci.* 27, 7817–7826.
- Roberson, E.D., Scarce-Levie, K., Palop, J.J., Yan, F., Cheng, I.H., Wu, T., Gerstein, H., Yu, G.-Q., and Mucke, L. (2007). Reducing endogenous tau ameliorates amyloid beta-induced deficits in an Alzheimer's disease mouse model. *Science* 316, 750–754.
- Rohn, T.T., Ivins, K.J., Bahr, B.A., Cotman, C.W., and Cribbs, D.H. (2000). A monoclonal antibody to amyloid precursor protein induces neuronal apoptosis. *J. Neurochem.* 74, 2331–2342.
- Roses, A.D. (1996). Apolipoprotein E and Alzheimer's disease. A rapidly expanding field with medical and epidemiological consequences. *Ann. N. Y. Acad. Sci.* 802, 50–57.
- Sandbrink, R., Masters, C.L., and Beyreuther, K. (1994). APP gene family: unique age-associated changes in splicing of Alzheimer's betaA4-amyloid protein precursor. *Neurobiol. Dis.* 1, 13–24.
- SantaCruz, K.S., Sonnen, J.A., Pezough, M.K., Desrosiers, M.F., Nelson, P.T., and Tyas, S.L. (2011). Alzheimer disease pathology in subjects without dementia in 2 studies of aging: the Nun Study and the Adult Changes in Thought Study. *J. Neuropathol. Exp. Neurol.* 70, 832–840.
- Satpute-Krishnan, P., DeGiorgis, J.A., Conley, M.P., Jang, M., and Bearer, E.L. (2006). A peptide zipcode sufficient for anterograde transport within amyloid precursor protein. *Proc. Natl. Acad. Sci. U.S.A.* 103, 16532–16537.
- Schmitz, C., Rutten, B.P.F., Pielen, A., Schäfer, S., Wirths, O., Tremp, G., Czech, C., Blanchard, V., Multhaup, G., Rezaie, P., et al. (2004). Hippocampal neuron loss exceeds amyloid plaque load in a transgenic mouse model of Alzheimer's disease. *Am. J. Pathol.* 164, 1495–1502.
- Schneider, L.S., Mangialasche, F., Andreasen, N., Feldman, H., Giacobini, E., Jones, R., Mantua, V., Mecocci, P., Pani, L., Winblad, B., et al. (2014). Clinical trials and late-stage drug development for Alzheimer's disease: an appraisal from 1984 to 2014. *J. Intern. Med.* 275, 251–283.
- Schroeter, M.L., Stein, T., Maslowski, N., and Neumann, J. (2009). Neural correlates of Alzheimer's disease and mild cognitive impairment: a systematic and quantitative meta-analysis involving 1351 patients. *Neuroimage* 47, 1196–1206.
- Schulte-Herbrüggen, O., Jockers-Scherübl, M.C., and Hellweg, R. (2008). Neurotrophins: from pathophysiology to treatment in Alzheimer's disease. *Curr Alzheimer Res* 5, 38–44.
- Sergeant, N., Bombois, S., Ghestem, A., Drobecq, H., Kostanjevecki, V., Missiaen, C., Wattez, A., David, J.-P., Vanmechelen, E., Sergheraert, C., et al. (2003). Truncated beta-amyloid peptide species in pre-clinical Alzheimer's disease as new targets for the vaccination approach. *J. Neurochem.* 85, 1581–1591.
- Shahani, N., Seshadri, S., Jaaro-Peled, H., Ishizuka, K., Hirota-Tsuyada, Y., Wang, Q., Koga, M., Sedlak, T.W., Korth, C., Brandon, N.J., et al. (2014). DISC1 regulates trafficking and processing of APP and A β generation. *Mol. Psychiatry*.

- Shaked, G.M., Chauv, S., Ubhi, K., Hansen, L.A., and Masliah, E. (2009). Interactions between the amyloid precursor protein C-terminal domain and G proteins mediate calcium dysregulation and amyloid beta toxicity in Alzheimer's disease. *FEBS J.* 276, 2736–2751.
- Shankar, G.M., and Walsh, D.M. (2009). Alzheimer's disease: synaptic dysfunction and Abeta. *Mol Neurodegener* 4, 48.
- Shankar, G.M., Li, S., Mehta, T.H., Garcia-Munoz, A., Shepardson, N.E., Smith, I., Brett, F.M., Farrell, M.A., Rowan, M.J., Lemere, C.A., et al. (2008). Amyloid-beta protein dimers isolated directly from Alzheimer's brains impair synaptic plasticity and memory. *Nat. Med.* 14, 837–842.
- Sherrington, R., Rogaev, E.I., Liang, Y., Rogaeva, E.A., Levesque, G., Ikeda, M., Chi, H., Lin, C., Li, G., Holman, K., et al. (1995). Cloning of a gene bearing missense mutations in early-onset familial Alzheimer's disease. *Nature* 375, 754–760.
- Shi, H., Kang, B., and Lee, J.Y. (2014). Zn(2+) effect on structure and residual hydrophobicity of amyloid β -peptide monomers. *J Phys Chem B* 118, 10355–10361.
- Skulachev, V.P. (2006). Bioenergetic aspects of apoptosis, necrosis and mitoptosis. *Apoptosis* 11, 473–485.
- Small, D.H., Nurcombe, V., Reed, G., Clarris, H., Moir, R., Beyreuther, K., and Masters, C.L. (1994). A heparin-binding domain in the amyloid protein precursor of Alzheimer's disease is involved in the regulation of neurite outgrowth. *J. Neurosci.* 14, 2117–2127.
- Smith-Swintosky, V.L., Pettigrew, L.C., Craddock, S.D., Culwell, A.R., Rydel, R.E., and Mattson, M.P. (1994). Secreted forms of beta-amyloid precursor protein protect against ischemic brain injury. *J. Neurochem.* 63, 781–784.
- Snowdon, D.A., and Nun Study (2003). Healthy aging and dementia: findings from the Nun Study. *Ann. Intern. Med.* 139, 450–454.
- Soba, P., Eggert, S., Wagner, K., Zentgraf, H., Siehl, K., Kreger, S., Löwer, A., Langer, A., Merdes, G., Paro, R., et al. (2005). Homo- and heterodimerization of APP family members promotes intercellular adhesion. *EMBO J.* 24, 3624–3634.
- Solfrizzi, V., Panza, F., Frisardi, V., Seripa, D., Logroscino, G., Imbimbo, B.P., and Pilotto, A. (2011). Diet and Alzheimer's disease risk factors or prevention: the current evidence. *Expert Rev Neurother* 11, 677–708.
- Song, S., and Jung, Y.-K. (2004). Alzheimer's disease meets the ubiquitin-proteasome system. *Trends Mol Med* 10, 565–570.
- Song, G., Ouyang, G., and Bao, S. (2005). The activation of Akt/PKB signaling pathway and cell survival. *J. Cell. Mol. Med.* 9, 59–71.
- Soriano, S., Lu, D.C., Chandra, S., Pietrzik, C.U., and Koo, E.H. (2001). The amyloidogenic pathway of amyloid precursor protein (APP) is independent of its cleavage by caspases. *J. Biol. Chem.* 276, 29045–29050.
- Stein, T.D., Anders, N.J., DeCarli, C., Chan, S.L., Mattson, M.P., and Johnson, J.A. (2004). Neutralization of transthyretin reverses the neuroprotective effects of secreted amyloid precursor protein (APP) in APPSW mice resulting in tau phosphorylation and loss of hippocampal neurons: support for the amyloid hypothesis. *J. Neurosci.* 24, 7707–7717.

- Steiner, H., Capell, A., Leimer, U., and Haass, C. (1999). Genes and mechanisms involved in beta-amyloid generation and Alzheimer's disease. *Eur Arch Psychiatry Clin Neurosci* 249, 266–270.
- Stoppini, L., Buchs, P.A., and Muller, D. (1991). A simple method for organotypic cultures of nervous tissue. *J. Neurosci. Methods* 37, 173–182.
- De Strooper, B., and Annaert, W. (2000). Proteolytic processing and cell biological functions of the amyloid precursor protein. *J. Cell. Sci.* 113 (Pt 11), 1857–1870.
- Surova, O., and Zhivotovsky, B. (2013). Various modes of cell death induced by DNA damage. *Oncogene* 32, 3789–3797.
- Sussman, M.A., Völkers, M., Fischer, K., Bailey, B., Cottage, C.T., Din, S., Gude, N., Avitabile, D., Alvarez, R., Sundararaman, B., et al. (2011). Myocardial AKT: the omnipresent nexus. *Physiol. Rev.* 91, 1023–1070.
- Swardfager, W., Lanctôt, K., Rothenburg, L., Wong, A., Cappell, J., and Herrmann, N. (2010). A meta-analysis of cytokines in Alzheimer's disease. *Biol. Psychiatry* 68, 930–941.
- Swomley, A.M., Förster, S., Keeney, J.T., Triplett, J., Zhang, Z., Sultana, R., and Butterfield, D.A. (2014). Abeta, oxidative stress in Alzheimer disease: Evidence based on proteomics studies. *Biochimica et Biophysica Acta (BBA) - Molecular Basis of Disease* 1842, 1248–1257.
- Talbot, K., Wang, H.-Y., Kazi, H., Han, L.-Y., Bakshi, K.P., Stucky, A., Fuino, R.L., Kawaguchi, K.R., Samoyedny, A.J., Wilson, R.S., et al. (2012). Demonstrated brain insulin resistance in Alzheimer's disease patients is associated with IGF-1 resistance, IRS-1 dysregulation, and cognitive decline. *J. Clin. Invest.* 122, 1316–1338.
- Thathiah, A., and De Strooper, B. (2011). The role of G protein-coupled receptors in the pathology of Alzheimer's disease. *Nat. Rev. Neurosci.* 12, 73–87.
- Thornberry, N.A., and Lazebnik, Y. (1998). Caspases: enemies within. *Science* 281, 1312–1316.
- Thornton, E., Vink, R., Blumbergs, P.C., and Van Den Heuvel, C. (2006). Soluble amyloid precursor protein alpha reduces neuronal injury and improves functional outcome following diffuse traumatic brain injury in rats. *Brain Res.* 1094, 38–46.
- Tian, B., Lessan, K., Kahm, J., Kleidon, J., and Henke, C. (2002). beta 1 integrin regulates fibroblast viability during collagen matrix contraction through a phosphatidylinositol 3-kinase/Akt/protein kinase B signaling pathway. *J. Biol. Chem.* 277, 24667–24675.
- Toro, P., Schönknecht, P., and Schröder, J. (2009). Type II diabetes in mild cognitive impairment and Alzheimer's disease: results from a prospective population-based study in Germany. *J. Alzheimers Dis.* 16, 687–691.
- Trazzi, S., Fuchs, C., De Franceschi, M., Mitrugno, V.M., Bartesaghi, R., and Ciani, E. (2014). APP-dependent alteration of GSK3 β activity impairs neurogenesis in the Ts65Dn mouse model of Down syndrome. *Neurobiol. Dis.* 67, 24–36.
- Troncoso, J.C., Sukhov, R.R., Kawas, C.H., and Koliatsos, V.E. (1996). In situ labeling of dying cortical neurons in normal aging and in Alzheimer's disease: correlations with senile plaques and disease progression. *J. Neuropathol. Exp. Neurol.* 55, 1134–1142.

- Del Turco, D., Schlaudraff, J., Bonin, M., and Deller, T. (2014). Upregulation of APP, ADAM10 and ADAM17 in the denervated mouse dentate gyrus. *PLoS ONE* 9, e84962.
- Vakkila, J., and Lotze, M.T. (2004). Inflammation and necrosis promote tumour growth. *Nat. Rev. Immunol.* 4, 641–648.
- Vandenabeele, P., Galluzzi, L., Vanden Berghe, T., and Kroemer, G. (2010). Molecular mechanisms of necroptosis: an ordered cellular explosion. *Nat. Rev. Mol. Cell Biol.* 11, 700–714.
- Vanden Berghe, T., Vanlangenakker, N., Parthoens, E., Deckers, W., Devos, M., Festjens, N., Guerin, C.J., Brunk, U.T., Declercq, W., and Vandenabeele, P. (2010). Necroptosis, necrosis and secondary necrosis converge on similar cellular disintegration features. *Cell Death Differ.* 17, 922–930.
- Vassar, R., Kuhn, P.-H., Haass, C., Kennedy, M.E., Rajendran, L., Wong, P.C., and Lichtenthaler, S.F. (2014). Function, therapeutic potential and cell biology of BACE proteases: current status and future prospects. *J. Neurochem.* 130, 4–28.
- Venezia, V., Nizzari, M., Repetto, E., Violani, E., Corsaro, A., Thellung, S., Villa, V., Carlo, P., Schettini, G., Florio, T., et al. (2006). Amyloid precursor protein modulates ERK-1 and -2 signaling. *Ann. N. Y. Acad. Sci.* 1090, 455–465.
- Verhoven, B., Schlegel, R.A., and Williamson, P. (1995). Mechanisms of phosphatidylserine exposure, a phagocyte recognition signal, on apoptotic T lymphocytes. *J. Exp. Med.* 182, 1597–1601.
- Vlahos, C.J., Matter, W.F., Hui, K.Y., and Brown, R.F. (1994). A specific inhibitor of phosphatidylinositol 3-kinase, 2-(4-morpholinyl)-8-phenyl-4H-1-benzopyran-4-one (LY294002). *J. Biol. Chem.* 269, 5241–5248.
- Waetzig, V., and Herdegen, T. (2005). Context-specific inhibition of JNKs: overcoming the dilemma of protection and damage. *Trends Pharmacol. Sci.* 26, 455–461.
- Wagner, S.L., Zhang, C., Cheng, S., Nguyen, P., Zhang, X., Rynearson, K.D., Wang, R., Li, Y., Sisodia, S.S., Mobley, W.C., et al. (2014). Soluble γ -Secretase Modulators Selectively Inhibit the Production of the 42-Amino Acid Amyloid β Peptide Variant and Augment the Production of Multiple Carboxy-Truncated Amyloid β Species. *Biochemistry* 53, 702–713.
- Walsh, D.M., and Selkoe, D.J. (2004). Oligomers on the brain: the emerging role of soluble protein aggregates in neurodegeneration. *Protein Pept. Lett.* 11, 213–228.
- Weingarten, M.D., Lockwood, A.H., Hwo, S.Y., and Kirschner, M.W. (1975). A protein factor essential for microtubule assembly. *Proc. Natl. Acad. Sci. U.S.A.* 72, 1858–1862.
- Wen, Y., Yang, S., Liu, R., and Simpkins, J.W. (2004). Transient cerebral ischemia induces site-specific hyperphosphorylation of tau protein. *Brain Res.* 1022, 30–38.
- Wentzell, J.S., Bolkan, B.J., Carmine-Simmen, K., Swanson, T.L., Musashe, D.T., and Kretschmar, D. (2012). Amyloid precursor proteins are protective in *Drosophila* models of progressive neurodegeneration. *Neurobiol. Dis.* 46, 78–87.
- Weyer, S.W., Klevanski, M., Delekate, A., Voikar, V., Aydin, D., Hick, M., Filippov, M., Drost, N., Schaller, K.L., Saar, M., et al. (2011). APP and APLP2 are essential at PNS and CNS synapses for transmission, spatial learning and LTP. *EMBO J.* 30, 2266–2280.

- Weyer, S.W., Zagrebelsky, M., Herrmann, U., Hick, M., Ganss, L., Gobbert, J., Gruber, M., Altmann, C., Korte, M., Deller, T., et al. (2014). Comparative analysis of single and combined APP/APLP knockouts reveals reduced spine density in APP-KO mice that is prevented by APP α expression. *Acta Neuropathol Commun* 2, 36.
- Williams, D.R. (2006). Tauopathies: classification and clinical update on neurodegenerative diseases associated with microtubule-associated protein tau. *Intern Med J* 36, 652–660.
- Winkler, E., Kamp, F., Scheuring, J., Ebke, A., Fukumori, A., and Steiner, H. (2012). Generation of Alzheimer disease-associated A β 42/43 by γ -secretase can directly be inhibited by modulation of membrane thickness. *J. Biol. Chem. jbc.M112.356659*.
- Würstle, M.L., Laussmann, M.A., and Rehm, M. (2012). The central role of initiator caspase-9 in apoptosis signal transduction and the regulation of its activation and activity on the apoptosome. *Exp. Cell Res.* 318, 1213–1220.
- Xiao, A.-W., He, J., Wang, Q., Luo, Y., Sun, Y., Zhou, Y.-P., Guan, Y., Lucassen, P.J., and Dai, J.-P. (2011). The origin and development of plaques and phosphorylated tau are associated with axonopathy in Alzheimer's disease. *Neurosci Bull* 27, 287–299.
- Yaar, M., Zhai, S., Pilch, P.F., Doyle, S.M., Eisenhauer, P.B., Fine, R.E., and Gilchrest, B.A. (1997). Binding of beta-amyloid to the p75 neurotrophin receptor induces apoptosis. A possible mechanism for Alzheimer's disease. *J. Clin. Invest.* 100, 2333–2340.
- Yankner, B.A., Duffy, L.K., and Kirschner, D.A. (1990). Neurotrophic and neurotoxic effects of amyloid beta protein: reversal by tachykinin neuropeptides. *Science* 250, 279–282.
- Yokokura, M., Mori, N., Yagi, S., Yoshikawa, E., Kikuchi, M., Yoshihara, Y., Wakuda, T., Sugihara, G., Takebayashi, K., Suda, S., et al. (2011). In vivo changes in microglial activation and amyloid deposits in brain regions with hypometabolism in Alzheimer's disease. *Eur. J. Nucl. Med. Mol. Imaging* 38, 343–351.
- Young-Pearse, T.L., Chen, A.C., Chang, R., Marquez, C., and Selkoe, D.J. (2008). Secreted APP regulates the function of full-length APP in neurite outgrowth through interaction with integrin beta1. *Neural Dev* 3, 15.
- Young-Pearse, T.L., Suth, S., Luth, E.S., Sawa, A., and Selkoe, D.J. (2010). Biochemical and functional interaction of disrupted-in-schizophrenia 1 and amyloid precursor protein regulates neuronal migration during mammalian cortical development. *J. Neurosci.* 30, 10431–10440.
- Yu, W.H., Cuervo, A.M., Kumar, A., Peterhoff, C.M., Schmidt, S.D., Lee, J.-H., Mohan, P.S., Mercken, M., Farmery, M.R., Tjernberg, L.O., et al. (2005). Macroautophagy—a novel β -amyloid peptide-generating pathway activated in Alzheimer's disease. *J Cell Biol* 171, 87–98.
- Yuan, J., and Yankner, B.A. (2000). Apoptosis in the nervous system. *Nature* 407, 802–809.
- Zheng, H., and Koo, E.H. (2006). The amyloid precursor protein: beyond amyloid. *Mol Neurodegener* 1, 5.
- Zheng, H., and Koo, E.H. (2011). Biology and pathophysiology of the amyloid precursor protein. *Mol Neurodegener* 6, 27.
- Zheng, W., Niu, L., Zhang, C., Zhu, C., Xie, F., Cao, C., and Li, G. (2014). Brain edema and protein expression of c-Fos and c-Jun in the brain after diffused brain injury. *Int J Clin Exp Pathol* 7, 2809–2817.

Zhu, X., Raina, A.K., Perry, G., and Smith, M.A. (2006). Apoptosis in Alzheimer disease: a mathematical improbability. *Curr Alzheimer Res* 3, 393–396.

Zymny, Andreas (2010). Untersuchungen zur Rolle von APP und APLPs bei der Zellalterung. Johann-Wolfgang-Goethe-Universität. *Diploma thesis*.

7 Appendix

7.1 Abbreviations

% (v/v)	volume percent
% (w/v)	weight percent
$\times g$	gravitation constant
°C	degree Celsius
aa	amino acids
Ab	antibody
AD	Alzheimer's disease
ADAM10	a disintegrin and metalloproteinase domain-containing protein 10
AICD	APP intracellular domain
APLP1	APP-like protein 1
APLP2	APP-like protein 2
APOE4	apolipoprotein allele E4
APP	amyloid precursor protein
APS	ammoniumpersulfate
ATP	adenosine triphosphate
A β	amyloid beta
BME	Basal Medium Eagle
BSA	bovine serum albumin
CA1	cornu ammonis (region) 1
cDNA	complementary DNA
CMV	cytomegalovirus
CNS	central nervous system
C-terminal	carboxyterminal
CTF	(APP) C-terminal fraction
DAPI	4'-6-diamino-2-phenylindol
DG	dentate gyrus
DMEM	Dulbecco's Modified Eagle Medium
DMSO	dimethylsulfoxide
DNA	desoxyribonucleic acid
<i>E. coli</i>	Escherichia coli
E1/E2	subdomains of sAPP α , the soluble ectodomain of APP
ECL	enhanced chemoluminescence
EOAD	early-onset AD
ex/em	extinction/emission
FACS	fluorescence-activated cell sorting
FAD	familial AD
FCS	fetal calf serum
FELASA	Federation of European Laboratory Animal Science Associations
G418	geneticine 418
GAPDH	glyceraldehyde 3-phosphate dehydrogenase
GFLD	growth factor-like domain
GFP	green fluorescent protein
Gluc	glucose
GSK3 β	glycogen synthase kinase 3 beta

HEK	human embryonic kidney (cells)
HPLC	high-performance liquid chromatography
HRP	horseradish peroxidase
HS	horse serum
IGF1	insulin-like growth factor 1
IGF1-R	insulin-like growth factor 1 receptor
IP	immunoprecipitation
I-R	insulin receptor
JNK	c-Jun N-terminal kinase
KD	knockdown
kD	kilo Dalton
KI	knockin
KO	knockout
LB	Luria Bertani
LOAD	late-onset AD
MAP	microtubule-associated protein
MEFs	mouse embryonic fibroblasts
MEM	Minimum Essential Medium
MLK3	mixed lineage kinase 3
MnSOD	manganese superoxide dismutase
mRNA	messenger RNA
MW	molecular weight
NB	neurobasal
NFT(s)	neurofibrillary tangle(s)
NGF	nerve growth factor
NMDA	N-methyl-D-aspartic acid
N-terminal	aminoterminal
OTCs	organotypic (hippocampal) slice cultures
P4-6	postnatal day 4-6
PAGE	polyacrylamide gel electrophoresis
PBS	phosphate buffered saline
PC12	pheochromocytoma cells
PDGF	platelet-derived growth factor
pen/strep	penicillin/streptomycin
pGSK3 α/β	phosphorylated glycogen synthase kinase 3 alpha/beta
PI	propidium iodide
PI3K	phosphatidylinositol 3-kinase
PS	presenilin
PTBD	phosphotyrosine-binding domain
PTX	Pertussis toxin
PVDF	polyvinylidene difluoride
RNA	ribonucleic acid
rpm	revolutions per minute
RT	room temperature
S, Ser	serine
sAPP α/β	soluble APP alpha/beta
SDS	sodium dodecyl sulfate
SEM	standard error of the mean
SH2	Src homology 2
shRNA	small hairpin ribonucleic acid

T, Thr	threonine
TBS	Tris-buffer solution
TEMED	N,N,N',N'-tetramethylethylenediamine
TM	transmembrane (region)
Tris	hydroxymethylaminoethane
Tween	polyoxyethylensorbitane monolaurate
UV	ultraviolet radiation
V	Volt
wt	wildtype
Δ CT15	delta carboxyterminal 15 (amino acids)

7.2 Tables

Table 1. Buffers and Solutions	23
Table 2. Media.....	26
Table 3. Cell Lines	27
Table 4. Animals	27
Table 5. Kits	28
Table 6. Primary Antibodies.....	28
Table 7. Secondary Antibodies	29
Table 8. Viral Vectors and Plasmids.....	29
Table 9. Bacterial Strain	30
Table 10. Software.....	30
Table 11. Equipment and Other Instruments.....	31
Table 12. Mechanisms of APP/sAPP α -mediated neuroprotection.....	76

7.3 Images

Figure 1. Hallmarks of Alzheimer's Disease.....	8
Figure 2. APP family members.	11
Figure 3. APP processing.....	12
Figure 4. Intrinsic and extrinsic pathway of apoptosis	16
Figure 5. Modulation of survival/stress signaling by APP and its putative interactors	21
Figure 6. Preparation of hippocampal slices	37
Figure 7. Vector maps of APP ectodomain constructs expressed in <i>Pichia pastoris</i>	48
Figure 8. Purified APP cleavage products from <i>Pichia pastoris</i>	52
Figure 9. Yeast-derived sAPP α and APP-E1 antagonize stress-triggered cell death.	53
Figure 10. Knockdown of APP in SH-SY5Y cells	
Figure 11. Recombinant sAPP α antagonizes cell death induced by proteasomal stress only in the presence of endogenous APP	56
Figure 12. Cell survival promoted by recombinant sAPP α /E1 depends on the presence of endogenous holo-APP	56
Figure 13. sAPP α -mediated suppression of cell death depends on the presence of holo-APP.....	56
Figure 14. sAPP α induces neuroprotection in organotypic hippocampal slices from wt mice but not from APP deficient mice	57

Figure 15. The absence of endogenous sAPP α exacerbates cell death in hippocampal slices under nutrient deprivation, which is rescued by exogenously applied recombinant sAPP α	58
Figure 16. sAPP α reduces neuronal death in the CA1 region of the hippocampus from wt mice but not in an APP-deficient background, while ADAM10 inhibitor treatment further exacerbates cell death.....	59
Figure 17. Recombinant sAPP α /E1 activate the PI3K/Akt survival pathway which requires the expression of holo-APP.....	61
Figure 18. Heat-inactivated recombinant yeast-derived sAPP α does not activate the PI3K/Akt survival pathway.....	62
Figure 19. sAPP α /E1-mediated PI3K/Akt signaling is restored in APP-retransfected APP-KD cells and can be detected in hippocampal neurons from wt mice	63
Figure 20. Knockdown of APP family members APLP1 and APLP2.....	64
Figure 21. Akt pathway activation and neuroprotection by sAPP α /E1 does not require APLP1 or APLP2.....	65
Figure 22. Mutant APP constructs utilized in this work.....	66
Figure 23. Akt survival signaling requires the APP intracellular C-terminal domain (AICD)	67
Figure 24. AICD-dependent PI3K/Akt signaling does not require the YENPTY motif of APP.....	68
Figure 25. Transfection efficiency and cell surface expression of AICD mutant constructs in comparison to wt control cells	69
Figure 26. Significant sAPP α -dependent induction of Akt activity in MEF cells.....	69
Figure 27. Akt pathway activation depends on the expression of the G-protein interaction motif	70
Figure 28. sAPP α -dependent activation of the PI3K/Akt is mediated by G-protein signaling	71
Figure 29. sAPP α -mediated cell survival is induced by G-protein-dependent activation of the PI3K/Akt pathway.....	72
Figure 30. IGF1 receptor expression is not required for sAPP α -mediated PI3K/Akt pathway activation.....	73
Figure 31. The GFLD of APP activated Akt signaling, but not the mutant GFLD incapable of binding copper.	74
Figure 32. Interaction partners of APP at the AICD.....	83
Figure 33. Hypothetical model of sAPP α -mediated Akt activation and survival signaling.....	87

8 Declaration/Erklärung

I hereby declare that I wrote the dissertation submitted without any unauthorized external assistance and used only sources acknowledged in the work. All textual passages which are appropriated verbatim or paraphrased from published and unpublished texts as well as all information obtained from oral sources are duly indicated and listed in accordance with bibliographical rules. In carrying out this research, I complied with the rules of standard scientific practice as formulated in the statutes of Johannes-Gutenberg-University Mainz.

Hiermit erkläre ich an Eides statt, dass ich die vorliegende Dissertation ohne unautorisierte externe Hilfe angefertigt und nur die angegebenen Quellen genutzt habe. Alle Textpassagen, die wörtlich oder paraphrasiert von publizierten wie unpublizierten Texten übernommen wurden sowie alle Informationen, die aus mündlichen Quellen stammen, wurden ordnungsgemäß belegt und nach bibliografischen Regeln aufgelistet. Während der Durchführung dieser Forschungsarbeit habe ich nach den Regeln der standardisierten wissenschaftlichen Praxis gearbeitet, wie sie in den Statuten der Johannes-Gutenberg-Universität zu Mainz formuliert ist.

Mainz, 2014

Nelli Milosch

9 Acknowledgments

[Personenbezogene Daten in der Danksagung sind gelöscht.]

10 Curriculum Vitae

Nelli Milosch née Röhner

* 26 July 1985 in Berlin, Germany

Education and Work Experience

[Personenbezogene Daten im Lebenslauf sind gelöscht.]

Internships and International Experience

[Personenbezogene Daten im Lebenslauf sind gelöscht.]

Activities and Honors

[Personenbezogene Daten im Lebenslauf sind gelöscht.]

Publications, Talks and Posters

Milosch N, ..., Weyer S, Buchholz C, Kins S, Behl C, Müller UC, Kögel D *et al.* Membrane-tethered APP and G protein-mediated signaling are required for sAPP α -induced activation of the Akt survival pathway. *Cell Death & Disease*, published online 28 August 2014.

Nensa F, ..., **Röhner N**, Kögel D, Theiss C, Marcus K, Müller T *et al.* FE65 interactomics revealed SV2A and SERCA2 as new binding proteins in the human brain. *Molecular and Cellular Proteomics* 2014; 13: 475-488.

Afshordel S, Hagl S, Werner D, **Röhner N**, Bazan NG, Kögel D, Eckert G *et al.* Omega-3 Polyunsaturated Fatty Acids improve mitochondrial function in a mouse model of brain aging - impact of Bcl-2 and NPD-1. *Prostaglandins, Leukotrienes & Essential Fatty Acids*, published online 9 June 2014.

Kundu A, **Milosch N**, Hajieva P, Behl C, Kögel D *et al.* Soluble Amyloid Precursor Protein modulates cellular BAG3-dependent proteasomal activity independent of holo-APP expression. *In preparation*.

Kiprianova I, **Milosch N**, Mohrenz IV, Seifert V, Kögel D *et al.* Sorafenib sensitizes glioma cells to the BH3 mimetic ABT-737 by targeting MCL-1 in an ATF5-independent manner. *In preparation*.

[Personenbezogene Daten im Lebenslauf sind gelöscht.]